[redacted]

ARR No. L5I04

NATIONAL ADVISORY COMMITTEE FOR AERONAUTICS

WARTIME REPORT

ORIGINALLY ISSUED
March 1946 as
Advance Restricted Report L5I04

ANALYSIS OF EFFECT OF ROLLING PULL-OUTS ON WING AND AILERON LOADS OF A FIGHTER AIRPLANE

By Henry A. Pearson and William S. Aiken, Jr.

Langley Memorial Aeronautical Laboratory
Langley Field, Va.

NACA

WASHINGTON

L - 270

NATIONAL ADVISORY COMMITTEE FOR AERONAUTICS

ADVANCE RESTRICTED REPORT

ANALYSIS OF EFFECT OF ROLLING PULL-OUTS ON WING AND AILERON LOADS OF A FIGHTER AIRPLANE

By Henry A. Pearson and William S. Aiken, Jr.

SUMMARY

An analysis was made to determine the effect of rolling pull-outs on the wing and aileron loads of a typical fighter airplane. The origin and magnitudes of the loads, shears, bending moments, and torques were determined for rolling pull-outs at six selected points on the V-n diagram. The results obtained indicated that higher loads are imposed upon the wings and ailerons by the rolling pull-out than would be imposed by application of the loading requirements for which the airplane was designed.

An increase in wing weight of 102 pounds, or about 15 percent, was found to be required if the wing were designed for a rolling pull-out instead of the usual symmetrical maneuver.

The analysis of the aileron loads indicated that although the aileron was structurally able to carry the maximum computed loads, the requirements for which the aileron was originally designed were found to be inadequate.

INTRODUCTION

One of the common combat maneuvers used by fighter pilots involves the use of ailerons in combination with either positive or negative load factors. Some pilots believe that the use of this maneuver would be desirable at all speeds within the flight range and with all normal accelerations within the V-n envelope.

Because neither angular acceleration nor angular velocity causes physiological effects so severe as those encountered with normal accelerations, pilots have less hesitancy in moving the ailerons than they do in moving the elevators. As a result, larger loads and torques may be placed on the wings and tail surfaces than those for which these surfaces would normally be designed.

The two extremes of the rolling pull-out would be (1) a steady angular velocity combined with a high normal acceleration, and (2) an angular acceleration combined with high normal acceleration either with or without rolling velocity. The first extreme was usually associated with a single fairly rapid movement of the ailerons, whereas the second was associated with either an extremely rapid reverse movement of the stick at a time when maximum rolling velocity exists or an extremely rapid single throw of the controls.

Although the old structural design requirements listed an unsymmetrical load condition for the wings, the rolling pull-out is not specifically considered; also, separate requirements are given for the wing and the aileron. The strength of the wing is determined by loads that are assumed to occur at selected points on the V-n diagram and to be distributed symmetrically over the wing span. The strength of the ailerons and wing hinge fittings are then determined by separate design specifications. Application of the unsymmetrical load requirements (100 to 70 percent) to a fighter airplane usually produces a critical condition only for the fuselage bulkheads to which the wings are attached, because no change is involved from the symmetrical case in either the span loading or torque distribution. In the combined rolling and normal-acceleration maneuver, both the spanwise load and torque distributions are considerably changed from the symmetrical condition.

At the time the present analysis was started, small difficulties, which were thought might be associated with a rolling pull-out, had been experienced with the ailerons on early versions of the P-47 airplane. Because this airplane was of conventional design and representative of modern fighter airplanes, it was chosen as the typical airplane for purposes of analysis. The results obtained, although not specifically applicable to other fighter airplanes, should be of significance and general interest.

The present analysis was made to show the origin of the loads occurring on the wing and ailerons in the rolling pull-out, to indicate the order of magnitude of these loads on a modern fighter airplane of conventional configuration, and to estimate the increase in structural weight that would result if the wings and ailerons were designed for these loads. The analysis included not only the use of experimental data obtained from flight, wind-tunnel, and static tests but also several steps and load distributions usually neglected in structural computations of this nature. The details of analysis therefore are also given.

SYMBOLS

ρ air density, slugs per cubic foot; with subscript 0 denotes value at sea level

V true airspeed, feet per second

V_e equivalent airspeed, feet per second $\left(V\sigma^{1/2}\right)$

$\sigma = \frac{\rho}{\rho_0}$

a velocity of sound, feet per second

M Mach number (V/a)

q dynamic pressure $\left(\frac{1}{2}\rho V^2\right)$

n wing load factor

W airplane weight, pounds

D airplane drag, pounds

S gross wing area, square feet

b wing span, feet

c wing chord at any station, feet

c_a aileron chord at any station, feet

c_a/c aileron chord ratio

α angle of attack, degrees

δ aileron angle, degrees; positive downward

δ_d component of aileron angle due to differential motion of ailerons, degrees

δ_a equal and opposite component of aileron angle, degrees

F empirical factor for modifying aileron angle for effects of compressibility (see fig. 10)

p angular velocity in roll, radians per second

$\dot{p}$ angular acceleration in roll, radians per second per second

g gravitational constant, feet per second per second

pb/2V helix angle described by wing tip, radians

l running load at any spanwise station, pounds per foot: with subscript a denotes aileron running load

c_l wing section lift coefficient (l/qc)

c_{l_b} wing section lift coefficient at zero wing lift with ailerons neutral (M = 0): nomenclature from reference 2

$c_{l_{a_1}}$ rate of change of wing section lift coefficient with wing lift coefficient (dc_l/dC_L) ; nomenclature from reference 2

$c_{l_{\delta_a}}$ rate of change of wing section lift coefficient with equal and opposite aileron deflection (M = 0)

$c_{l_{\delta_d}}$ rate of change of wing section lift coefficient with ailerons deflected together as flaps when ailerons are operated differentially (M = 0)

c_{l_p} rate of change of wing section lift coefficient with helix angle pb/2V (M = 0)

c_{l_t} rate of change of wing section lift coefficient with wing-twist parameter $\left(\frac{dc_l}{d\left(\frac{\theta}{F\frac{\delta_a q}{\sqrt{1-M^2}}}\right)}\right)$

c_n wing section normal-force coefficient

c_{n_a} aileron section normal-force coefficient $\left(l_a/qc_a\right)$

$c_{n_{a_o}}$ aileron section normal-force coefficient at zero lift with aileron undeflected

c_m wing section pitching-moment coefficient

c_{m_o} wing section pitching-moment coefficient about aerodynamic center $(M = 0)$

Δc_m increment in wing section pitching-moment coefficient due to aileron deflection; with subscript d denotes part due to flap-type deflection (droop) and with subscript a denotes part due to equal and opposite aileron deflection

C_L wing lift coefficient (nW/qS)

C_D airplane drag coefficient (D/qS)

e distance from section elastic center to section aerodynamic center, feet; positive when elastic center is behind aerodynamic center

y distance along wing span from plane of symmetry, feet

y' a particular distance along wing span, feet

t local or distributed torque at any section about elastic axis, pound-feet per foot

T accumulated torque at any station $\int_{b/2}^{y'} t\,dy$, pound-feet

S_h vertical shear, pounds

B.M. vertical bending moment, foot-pounds

C_l rolling-moment coefficient

C_{l_p} rate of change of rolling-moment coefficient with helix angle per radian $\left(dC_l/d\frac{pb}{2V}\right)$ (see equation (23) for definition)

C_{l_δ} rate of change of rolling-moment coefficient with aileron angle per degree $(dC_l/dF\delta)$ (see equation (21) for definition)

C_{l_t} rate of change of rolling-moment-loss coefficient due to wing twist $\left(\frac{dC_l}{d\left(\frac{qF\delta}{\sqrt{1 - M^2}}\right)}\right)$ (see equation (25) for definition)

m_θ torsional modulus of rigidity of wing at a given station, foot-pounds per degree

θ angle of twist at any section due to torque, degrees

w distributed wing weight, pounds per foot

w_1 weight of concentrated load items, pounds

k_X radius of gyration about X-axis, feet

BASIC DATA

In order to accomplish the objectives of the present analysis, data from several sources were used. In addition to information on the geometry of the wing, aileron, and aileron linkage, use was made of data from flight tests on the attainable aileron angles, static tests on the wing torsional stiffness, and wind-tunnel tests on some of the wing-aileron section characteristics. Some of this information ordinarily would not be available at the design stage; however, established engineering procedures exist for estimating the required quantities.

Geometric characteristics of wing and aileron.- The characteristics of the wing, including the plan form, the chord distribution, the ratio of aileron chord to wing chord, the quarter-chord line, the elastic-axis location, and the line through the center of gravity of each section, are shown in figure 1. These data were obtained from the manufacturer for the analysis of the wing.

The variation of right and left aileron angles measured on an early version of the airplane is shown in figure 2. For the analysis this motion was considered as the sum of two motions: an equal and opposite motion of the right and left ailerons and a simultaneous upward motion of both ailerons. The deflection δ_a produced by the equal and opposite motion is plotted as the abscissa in figure 3 and is numerically one half of the angle between the right and left ailerons. When an aileron moves downward δ_a is positive; when it moves upward δ_a is negative. The deflection δ_d produced by the simultaneous upward motion of both ailerons is plotted as the ordinate in figure 3 and in this case is negative for both ailerons. This deflection is herein referred to as either the "equivalent flap effect" or the "aileron droop." The actual deflection of an aileron δ is the algebraic sum of δ_a and δ_d.

Torsional stiffness of wing.- The torsional-stiffness distribution of the wing that was used in the analysis (short-dash curve in fig. 4) was obtained from static tests made by the Air Technical Service Command, Army Air Forces, Wright Field, Ohio of a P-47B wing. The ordinate in figure 4 is the torque in pound-feet that would have to be applied at a given station in order to produce 1° of twist at the station relative to the wing center line. The short-dash curve was selected because it was believed to represent most nearly the wing torsional stiffness of the airplane as flown.

As an indication, however, of the amount of variation that might be expected if a similar analysis were contemplated for another airplane, two additional curves are shown in figure 4; the long-short-dash curve is an experimental curve that applies to an airplane with loosely fitted ammunition doors or with doors either entirely removed or open. The solid curve represents results obtained from computations that were made by the manufacturer; in these computations the torque was considered to be resisted by the action of two main torque boxes and by two-spar action of the main spars. Also in the calculations a number of conservative assumptions were used; for example, the ammunition doors and all the structure behind the 70-percent-chord point were assumed to be completely ineffective in carrying torque.

Limit V-n diagram for normal gross-weight condition.- The limit V-n diagram at sea level for the airplane, which was the diagram used in the design of the wing as well as in the present analysis, is shown in figure 5. The critical points A, B, C, and D, for which the wing was designed, represent maneuver conditions. The diagram given applies to a normal airplane gross weight W of 12,000 pounds and a gross wing area S of 300 square feet. The wing lift coefficients at the corners of the diagram were listed by the manufacturer as 1.75, 0.419, -0.206, and -0.800 at the points A, B, C, and D, respectively. The equivalent airspeed V_e at points B and C is 553, at point A, 271, and at point D, 281 miles per hour.

Wind-tunnel data.- The section characteristics of the aileron that were used in the analysis were obtained from tests made in the Langley 8-foot high-speed tunnel on a model representing the wing section located 171 inches from the airplane center line. (See fig. 1.) In these tests the pressure distribution was measured at various aileron angles and angles of attack at Mach numbers varying from 0.2 to 0.75. Some of the results obtained in the tests, which have not been previously published, are shown in figures 6 to 9, which give the variation of aileron section normal-force coefficient c_{n_a} with wing section normal-force coefficient c_n for various aileron angles. Results are shown only for Mach numbers of 0.25, 0.475, 0.60, and 0.725. These results represent the values of the tunnel tests closest to the sea-level Mach number at points A to D on the V-n diagram.

The tunnel data could not be obtained at high Mach numbers in combination with either large angles of attack or large aileron deflections; in order to investigate high angle-of-attack conditions (upper and lower left-hand corners on the V-n diagram), therefore, extensive extrapolation of the tunnel data was necessary. The extrapolations are shown by the dashed lines in figures 6 to 9. The extrapolations shown are straight and parallel in accordance with thin airfoil theory.

For the P-47B aileron, the ratio of aileron chord to wing chord is not constant along the aileron span, and because the wind-tunnel tests had been made at a value of $c_a/c = 0.269$, extension of the experimental data to other values of c_a/c was necessary. In order to accomplish this extrapolation the data for $c_a/c = 0.269$ were analyzed to obtain values of $dc_m/d\delta$, $dc_l/d\alpha$, and $dc_l/d\delta$, and their variation with Mach number. Below the critical Mach number $dc_m/d\delta$ and $dc_l/d\alpha$ were found to increase in the usual manner, that is, approximately according to the factor $1/\sqrt{1 - M^2}$. The ratio $dc_l/d\delta$, however, did not vary in this manner, with the result that the aileron effectiveness factor $d\alpha/d\delta$ derived from $dc_l/d\alpha$ and $dc_l/d\delta$ decreased with an increase in Mach number. Comparison of the tunnel results for the P-47B aileron at $c_a/c = 0.269$ with the experimental variation of $d\alpha/d\delta$ with c_a/c for unsealed ailerons given in figure 11 of reference 1 indicated that at a Mach number of 0.585 the values of $d\alpha/d\delta$ would coincide. The curve in figure 11 of reference 1 was therefore assumed to apply to the P-47B aileron at $M = 0.585$ over the range of c_a/c required. The determination of the empirical correction factor F to account for other Mach numbers was the final step in the procedure. Figure 11 of reference 1 and values of the empirical factor F required to modify the basic curve for Mach number are given in figure 10 of the present paper. In this determination the implicit assumption is that the geometry of the aileron gap remains the same.

Because $dc_l/d\delta$ and $dc_m/d\delta$ were found to increase with Mach number in approximately the same manner, the following convenient ratio was formed:

$$f(c_a/c) = \frac{(dc_l/d\alpha)(d\alpha/d\delta)}{dc_m/d\delta}$$

A curve $f(c_a/c)$ (fig. 10) was then passed through the experimental tunnel point at $c_a/c = 0.269$ and proportioned in accordance with the theoretical curve obtained from the wing section theory as shown by the dashed line in figure 10.

Flight data.- In addition to the wind-tunnel data given in figures 1 to 9, use was made of flight-test results giving the measured relation between aileron control force, aileron angle, and the parameter $pb/2V$ at the time of maximum rolling velocity in abrupt aileron rolls from straight flight. For use in the present analysis the original flight data were converted, cross-plotted, and extrapolated to obtain stick force and aileron angles for each of a number of values of the factor $q/\sqrt{1 - M^2}$ varying from 100 to 1600 pounds per square foot. These results are shown in figure 11. The flight data included values of aileron stick forces ranging from about 20 to 60 pounds and values of $q/\sqrt{1 - M^2}$ of less than 700 pounds per square foot. Values beyond these limits were based upon an average of a number of independent extrapolations.

Flight data on the hinge moments have been used in preference to wind-tunnel data because the flight results were believed to be more nearly indicative of the actual case. The data given in figure 11, however, could have been computed from wind-tunnel-test results if the geometry of the wing and ailerons and the torsional stiffness of the wing were known.

OUTLINE OF METHOD OF ANALYSIS

In the present analysis the basic data were employed in the following manner to determine the effect of a rolling normal-acceleration maneuver on the wing and aileron loads:

(1) The wind-tunnel results were used to obtain section data concerning the slope of the lift curve $dc_l/d\alpha$ and the aileron flap effectiveness $d\alpha/d\delta$ for each station along the span.

(2) By use of the results from step (1), six separate aerodynamic spanwise load distributions (in this case c_l components only) were computed.

(3) The variation along the wing of the vertical shear, wing bending moment, and torques about the elastic axis caused by unit values of the various aerodynamic-load components of step (2), were obtained.

(4) The load distributions due to wing weight and concentrated weights were established and integrated to give the shear, wing bending moments, and torques about the elastic axis due to both normal and angular inertia.

(5) The rolling-moment coefficients associated with the spanwise loadings of step (2) were used to establish values of maximum rate of roll that could be obtained at various equivalent airspeeds and aileron deflections when wing twist due to aileron deflection was taken into account.

(6) Results of flight-test data, in which the stick-force variation with aileron deflection and the airspeed were measured during steady rolls, were then used to establish limit lines corresponding to several values of the aileron stick force for the results obtained in step (5).

(7) The values of the rolling-velocity parameter pb/2V, associated with the aileron deflection as established in step (6) for maximum aileron stick force, were assumed to exist simultaneously with the load factors occurring at each of the selected points of the V-n diagram.

(8) From the aerodynamic-load distributions occurring at each selected point on the V-n diagram, the variation of wing section normal-force coefficient along the span was obtained. By use of the high-speed wind-tunnel data of figures 6 to 9 the aileron normal-force coefficient along the aileron span was determined.

(9) The aileron load distributions from step (8) were integrated across the aileron span to obtain the total load corresponding to each selected point on the V-n diagram.

LOAD DISTRIBUTIONS

Aerodynamic

When experimental spanwise load distributions are not available, designers usually obtain the distributions required in step (2) of the preceding section by an application of the lifting-line theory. In the usual application of this theory the distribution of lift over the span is assumed to be a linear function of the angle of attack at each point of the span. This assumption makes it possible to superimpose various types of zero lift distributions on a distribution due to angle of attack of the wing as a whole. The procedure followed in the present paper for the computation of spanwise aerodynamic-load distributions is given in both references 2 and 3. The methods outlined in these references have been followed with only slight modifications in the determination of the aerodynamic-load distributions that follow.

The aerodynamic-load distribution on the wing was considered to consist of six component distributions as follows: an additional aerodynamic load, a built-in-twist aerodynamic load, an aileron-droop aerodynamic load, an equal and opposite aileron-deflection aerodynamic load, a damping-in-roll aerodynamic load, and an aerodynamic-load distribution due to wing flexibility. For each of these aerodynamic-load distributions, the running load, the shear, the bending moment, and the torque were first calculated in a general form so that the curves could be used in evaluating loads, shears, and so forth at several points on the V-n diagram.

In general, the running load in any one of the foregoing component distributions may be written as

$$l = Kc_{l_x}c \qquad (1)$$

where the constant K might include combinations of factors such as dynamic pressure, compressibility correction, aileron angle, helix angle, wing load factor, and wing loading. The wing section lift coefficient c_{l_x} depends on the type of load distribution considered.

With this definition of load per foot as a basis, the shear, bending moment, distributed torque, and accumulated torque at a particular section y' become, respectively,

$$S_h = K \int_{b/2}^{y'} c_{l_x} c \, dy \qquad (2)$$

$$B.M. = K \int_{b/2}^{y'} \int_{b/2}^{y'} c_{l_x} c \, dy \, dy \qquad (3)$$

$$t = K c_{l_x} ce \qquad (4)$$

$$T = K \int_{b/2}^{y'} c_{l_x} ce \, dy \qquad (5)$$

The integrations required in equations (2) to (5) were performed mechanically. The quantities K and c_{l_x} are determined for each of the various load distributions in the following paragraphs.

Additional aerodynamic-load distribution.- As part of the structural load requirements the load distribution due to an untwisted rigid wing is determined. This distribution is termed the "additional aerodynamic-load distribution" and is assumed to retain the same shape at all angles of attack and at all airspeeds; the ordinates of the distribution are simply proportional to the lift coefficient of the wing. The load l at any point is given by

$$l = C_L c_{l_{a1}} qc$$

Since

$$C_L = \frac{n\frac{W}{S}}{q}$$

then

$$l = n\frac{W}{S} c_{l_{a_1}} c \qquad (6)$$

and therefore for the additional aerodynamic-load distribution $K = n\frac{W}{S}$ and $c_{l_x} = c_{l_{a_1}}$. Figure 12 gives the results for the load per foot, vertical shear, bending moment, and accumulated torque caused by the additional aerodynamic load in terms of $K = n\frac{W}{S}$. By use of the customary assumption that the shape of the aerodynamic-load distribution and the location of the section aerodynamic centers do not change with Mach number, the results of figure 12 will apply at all airspeeds.

Aerodynamic-load distribution due to built-in twist.- As constructed, the wing had 4° of washout, which started from the spanwise station located at 100 inches. The aerodynamic load due to the built-in twist may be written as $l = qc_{l_b}c$ where c_{l_b} is a section lift coefficient at zero wing lift computed by the method of reference 2.

Because the section angles of attack due to built-in twist remain constant and the slopes of the section lift curves tend to vary with the factor $1/\sqrt{1 - M^2}$, as a first approximation the section-lift-coefficient variation along the span for any given zero-lift type of aerodynamic-load distribution was assumed to increase with Mach number in the same manner. The load equation (equation (1)) may then be written as

$$l = \frac{q}{\sqrt{1 - M^2}} c_{l_b} c \qquad (7)$$

For the built-in-twist aerodynamic-load distribution, therefore, $K = q/\sqrt{1 - M^2}$ and $c_{l_x} = c_{l_b}$. Figure 13 gives the distributions of the load, shear, bending moment, and accumulated torque in terms of K.

The method used for including the effect of compressibility is based on an assumption that is either commonly used or implicitly assumed in applying conventional methods for the computation of spanwise aerodynamic-load distribution.

Aerodynamic-load distribution due to ailerons deflected as flaps.- Although the two preceding aerodynamic-load distributions are usually computed in the course of a wing analysis, the four aerodynamic-load distributions that follow are not usually computed.

As noted previously, when ailerons are deflected differentially, a part of the deflection can be considered as a deflection of the ailerons together as flaps (fig. 3) and a part as an equal and opposite deflection of the right and left ailerons. A zero-lift distribution due to the flap deflection of the ailerons (droop) was computed by the method of reference 2 and by the use of the aileron-effectiveness factors given in figure 10 in combination with the aileron flap-chord-ratio variation (leading edge to trailing edge) shown in figure 1. The slopes of the section lift curves $dc_l/d\alpha$ were the same as those used in the additional and built-in-twist aerodynamic-load distributions. The zero-lift distribution was therefore obtained with the load at any point given by

$$l = F\delta_d \frac{q}{\sqrt{1 - M^2}} c_{l_{\delta_d}} c \qquad (8)$$

where $c_{l_{\delta_d}}$ is the section lift coefficient for a unit deflection and F is the factor required to modify the effective camber for a given deflection. The factor F varies with Mach number as noted in figure 10. As before, the factor $1/\sqrt{1 - M^2}$ was used to modify the local loads for an increase due to Mach number; therefore $K = F\delta_d \frac{q}{\sqrt{1 - M^2}}$. The results given in figure 14 are for a deflection or droop δ_d, in degrees, and the proper angle of droop for a given equal and opposite aileron deflection must be obtained from figure 3.

Aerodynamic-load distribution due to equal and opposite aileron deflection.- By use of the foregoing procedure the aerodynamic-load distribution for the wing, due to the equal and opposite deflection of the ailerons, was computed for a unit aileron angle. Such a computation yields a zero-lift distribution directly but with a resultant rolling moment.

The load at any point along the span may be given in a form similar to equation (8) as

$$l = F\delta_a \frac{q}{\sqrt{1 - M^2}} c_{l_{\delta_a}} c \qquad (9)$$

For the aerodynamic-load distribution due to the equal and opposite aileron deflection, therefore, $K = F\delta_a \frac{q}{\sqrt{1 - M^2}}$ and $c_{l_x} = c_{l_{\delta_a}}$. The distributions for load, shear, bending moment, and accumulated torque in terms of $K = F\delta_a \frac{q}{\sqrt{1 - M^2}}$ are given in figure 15.

Aerodynamic-load distribution due to damping in roll.- As a result of the rolling velocity that is caused by the equal and opposite part of the aileron deflection, a damping moment occurs. The load distribution due to the damping moment was computed as though the wing had a linear antisymmetrical twist increasing from zero at the airplane center line to a unit value at the tip.

The load at any point along the span may be given by the equation

$$l = \frac{pb}{2V} \frac{q}{\sqrt{1 - M^2}} c_{l_p} c \qquad (10)$$

For the aerodynamic-load distribution due to damping in roll equation (10) shows that $K = \frac{pb}{2V} \frac{q}{\sqrt{1 - M^2}}$ and $c_{l_x} = c_{l_p}$. Figure 16 gives the distributions for load, shear, bending moment, and accumulated torque in terms of $K = \frac{pb}{2V} \frac{q}{\sqrt{1 - M^2}}$.

<u>Aerodynamic-load distribution due to wing flexibility</u>.- For a rigid wing the previous distributions are all that would be required. In the case of a nonrigid wing, however, a twist exists that is caused by the torque contributed by the loads (when the elastic axis and line of aerodynamic centers do not coincide) and by the section pitching moments. The torque may cause an appreciable wing twist when the airspeed is high or when the torque caused either by the sections or the ailerons is large.

The twist caused by the various torques on the wing induces a load distribution upon the wing. The total primary wing twist at any section may be divided into the following four parts:

(1) Twist caused by the distributed wing weight as well as that contributed by large weight items. (Such a twist occurs when the centroids of the weights are displaced from the elastic axis. See fig. 1.)

(2) Twist caused by aerodynamic loads that act at the line of aerodynamic centers. (Such a twist occurs when the aerodynamic center line does not coincide with the elastic axis. See fig. 1.)

(3) Twist caused by section pitching moments (ailerons undeflected).

(4) Twist caused by deflecting the ailerons either together as flaps (δ_d) or equally and oppositely as ailerons (δ_a).

The aerodynamic torque giving rise to the twist may be represented by the equation

$$t = c_l qce + \frac{qc^2}{\sqrt{1 - M^2}}\left(c_{m_o} + \Delta c_{m_d} + \Delta c_{m_a}\right) \qquad (11)$$

The breakdown of the torque distributions contributed by the various lift distributions is presented in figures 12 to 16.

The local torque acting about the elastic axis due to the section moment c_{m_o} in equation (11) is given by

$$t = \frac{q}{\sqrt{1 - M^2}} c_{m_o} c^2 \qquad (12)$$

The local torque contributed by aileron deflection δ_a is

$$t = \Delta c_{m_a} q c^2$$

$$= \frac{dc_m}{d\delta} \delta_a q c^2 \qquad (13)$$

The factor $dc_m/d\delta$ was obtained from

$$\frac{dc_m}{d\delta} = \frac{(dc_l/d\alpha)(d\alpha/d\delta)}{f(c_a/c)} \qquad (14)$$

Numerical values of $d\alpha/d\delta$ and $f(c_a/c)$ are available from figure 10. When equation (14) is substituted in equation (13), the factor $1/\sqrt{1 - M^2}$ is introduced to account for increased section lift-curve slopes and the factor F is introduced to modify the value of $d\alpha/d\delta$, the following equation for the distributed torque across the aileron span is obtained:

$$t = \frac{F\delta_a q}{\sqrt{1 - M^2}\ f(c_a/c)} \frac{dc_l}{d\alpha} \frac{d\alpha}{d\delta} c^2 \qquad (15)$$

Figure 17 shows the distributed torque for the P-47B wing as computed from equations (12) and (15) and the curves given in figures 1 and 10. The accumulated torque at each station caused by the foregoing torque distributions is also given in figure 17.

If the wing torsional stiffness is defined as the torque required at a particular spanwise station y' to give a deflection of 1° at that station (see fig. 4 for variation), the twist θ at any station resulting from the section pitching moments (ailerons undeflected) is given by

$$\frac{\theta}{q/\sqrt{1 - M^2}} = \frac{1}{m_{\theta_{y'}}} \int_{b/2}^{y'} c_{m_o} c^2\, dy + \int_{y'}^{0} \frac{c_{m_o} c^2\, dy}{m_\theta} \qquad (16)$$

where $m_{\theta_{y'}}$ is the stiffness at the particular section and m_θ is the variable stiffness at sections inboard of y'. If c_{m_o} is a constant, equation (16) can be rearranged as follows:

$$\frac{\theta}{c_{m_o} q/\sqrt{1 - M^2}} = \frac{1}{m_{\theta_{y'}}} \int_{b/2}^{y'} c^2 \, dy + \int_{y'}^{0} \frac{c^2}{m_\theta} \, dy \qquad (17)$$

The twist caused by deflected ailerons is given by

$$\frac{\theta}{F\delta_a q/\sqrt{1 - M^2}} = \frac{1}{m_{\theta_{y'}}} \int_{b/2}^{y'} \frac{\frac{dc_l}{d\alpha} \frac{d\alpha}{d\delta} c^2 \, dy}{f(c_a/c)} + \int_{y'}^{0} \frac{\frac{dc_l}{d\alpha} \frac{d\alpha}{d\delta} c^2 \, dy}{m_\theta f(c_a/c)} \qquad (18)$$

The twist curves computed from equations (17) and (18) are shown in figure 18. These curves were obtained by use of figures 1, 4, and 10, together with the values of $dc_l/d\alpha$ used in obtaining the aerodynamic-load distributions. Figure 18 shows that the twist curves due to section pitching moment c_{m_o} and aileron deflection δ_a are quite similar in shape in spite of the fact that the twist curve due to c_{m_o} arises as a result of an integration over the complete span, whereas the twist curve due to aileron deflection results from an integration of torques acting over the aileron span.

Although separate zero-lift load distributions can be computed for either of the twist curves given in figure 18, the distribution associated with the twist due to the section pitching moment c_{m_o} is of less importance than that associated with the twist due to deflected ailerons Δc_{m_a}. The effects associated with the distribution due to Δc_{m_a} are more important in the determination of the reduction of the rolling ability of the airplane than in the change produced in the shears and bending moments along the span. The changes in the load distributions due to the twists resulting from c_{m_o} and Δc_{m_d} are such that no change in the rolling characteristics of the airplane results because the loadings produced are symmetrical about the center line. The results of figure 18 indicate that approximately 1.4° of aileron deflection would cause the same twist at the wing tip as would the section pitching moments when c_{m_0} is taken as -0.008, which was the low-speed value of the section pitching-moment coefficient used in the design of the wing. For a wing with a high pitching-moment coefficient the twist due to the sections becomes more important and may not be omitted.

Because the zero-lift loads produced by the elastic deformation of the wing are in general of secondary importance compared with other loads, a load curve was computed only for the twist distribution caused by equal and opposite deflection of the ailerons. By the method used in computing the loading for a rigid wing with equal and opposite deflection of the ailerons and for the load distribution due to damping in roll, the lift at any point along the span due to the twist distribution can be defined by

$$l = \frac{F\delta_a q}{\sqrt{1 - M^2}} c_{l_t} \frac{q}{\sqrt{1 - M^2}} c \qquad (19)$$

In equation (19) c_{l_t} is the local lift coefficient that would be associated with the antisymmetrical-twist curve given by the solid line in figure 18. The factor F for the load distribution due to the wing flexibility considered is then equal to $F\delta_a \frac{q^2}{1 - M^2}$.

The load, shear, bending moment, and accumulated-torque distributions are shown in figure 19.

Summary of the aerodynamic-load coefficients.- For convenience the coefficients in equations (1) to (5) that were used with the distributions shown in figures 12 to 16 and 19 are summarized in the following table:

Type of distribution	F	c_{l_x}
Additional	$n\frac{W}{S}$	$c_{l_{a_1}}$
Built-in twist	$\frac{q}{\sqrt{1 - M^2}}$	c_{l_b}
Drooped ailerons	$F\delta_d \frac{q}{\sqrt{1 - M^2}}$	$c_{l_{\delta_d}}$
Equal and opposite aileron deflection	$F\delta_a \frac{q}{\sqrt{1 - M^2}}$	c_{l_δ}
Damping in roll	$\frac{pb}{2V} \frac{q}{\sqrt{1 - M^2}}$	c_{l_p}
Wing twist	$F\delta_a \frac{q^2}{1 - M^2}$	c_{l_t}

Weight and Inertia

Normal-inertia distribution.- The wing weight distribution used in the analysis, exclusive of large concentrated loads, is given in figure 20. This distribution was furnished by the manufacturer for the structural analysis of the wing. In addition to the distributed weight, a number of large concentrated weight items, such as the landing gear, machine guns, and ammunition boxes were housed in the wing. The locations of these items along the span relative to the elastic axis are given in figure 1.

The running-load curves, including the effects of the concentrated loads, were integrated to give the shear and bending-moment variations along the span. In addition the torque distribution of the running load and the concentrated weights about the elastic axis were integrated to give the accumulated torque at each spanwise station. The ordinates of the curves shown in figure 20 are proportional to the load factor n.

Angular-inertia distribution.- The angular-inertia distribution for the distributed wing weight was evaluated from the results given in figure 20 for the running load. The equivalent wing weight at each station with an angular acceleration present is equal to $w\dot{p}y'/g$ and the equivalent weight of each of the concentrated loads is $w_1\dot{p}y'/g$. The running-load curves for the angular inertia were integrated to give the shear, bending-moment, and accumulated-torque curves resulting from the wing weight. These curves are shown in figure 21.

VALUES OF PARAMETERS USED FOR LOAD COMPUTATIONS

Although the previous sections have been devoted to the determination, in a general form, of the load, shear, bending moment, and torques of the various component loadings, the values of $pb/2V$, $\dot{p}$, $F\delta_a$, and $q/\sqrt{1 - M^2}$ that can be attained must be established in order that the results given in figures 15 to 21 can be applied at the various points on the V-n diagram.

Helix angle pb/2V.- The antisymmetrical spanwise aerodynamic-load distributions, that is, the distributions due to equal and opposite aileron deflection, damping in roll, and wing twist, must be used in the determination of the attainable value of the helix angle.

The applied rolling moment for a unit equal and opposite aileron deflection is

$$\text{Rolling moment} = 2F\delta_a \frac{q}{\sqrt{1 - M^2}} \int_{b/2}^{0} c_{l_\delta} cy \, dy \qquad (20)$$

The applied rolling moment can be redefined by the equation

$$\text{Rolling moment} = \frac{F\delta_a}{\sqrt{1 - M^2}} C_{l_\delta} qSb \qquad (21)$$

In the span-load computations, the value of C_{l_δ} was computed to be 0.00263 (δ_a in deg).

The damping moment due to roll from equation (10) is given by

$$\text{Damping moment} = \frac{pb}{2V} \frac{2q}{\sqrt{1 - M^2}} \int_{b/2}^{0} c_{l_p}\, cy\, dy \qquad (22)$$

The damping moment can be redefined by the equation

$$\text{Damping moment} = \frac{pb}{2V} \frac{q}{\sqrt{1 - M^2}} C_{l_p} Sb \qquad (23)$$

The value of C_{l_p} used in equation (23) was found from the span-load computations to be 0.44 when the helix angle $pb/2V$ was given in radians.

The loss in rolling moment due to twist resulting from equal and opposite aileron deflection can, from equation (19), be given by

$$\text{Rolling-moment loss} = \frac{F\delta_a q^2}{1 - M^2} \int_{b/2}^{0} c_{l_t} cy\, dy \qquad (24)$$

The rolling-moment loss can be redefined by the equation

$$\text{Rolling-moment loss} = \frac{F\delta_a q^2}{1 - M^2} C_{l_t} Sb \qquad (25)$$

where the value of C_{l_t} was computed to be 1.586×10^{-6} (δ_a in deg).

By the use of equations (21), (23), and (25), when the damping moment is equal to the applied rolling moment, the following relation between the attainable value of the parameter $pb/2V$, the aileron angle, and the airspeed is obtained:

$$\frac{F\delta_a q}{\sqrt{1 - M^2}} C_{l_\delta} Sb - \frac{F\delta_a q^2}{1 - M^2} C_{l_t} Sb = \frac{pb}{2V} \frac{q}{\sqrt{1 - M^2}} C_{l_p} Sb \qquad (26)$$

When equation (26) is simplified and solved for $pb/2V$ the following equation is obtained:

$$\frac{pb}{2V} = \frac{\left(C_{l_\delta} - \frac{qC_{l_t}}{\sqrt{1 - M^2}}\right)F\delta_a}{C_{l_p}} \qquad (27)$$

By the use of the values of C_{l_δ}, C_{l_p}, and C_{l_t} given in the preceding paragraphs the variation of $pb/2V$ with $F\delta_a$ is shown in figure 22 for a number of values of $q/\sqrt{1 - M^2}$. In figure 22 the aileron reversal speed may be seen to be reached at a value of $\frac{q}{\sqrt{1 - M^2}} = 1660$.

Angular acceleration $\dot{p}$.- Although the limiting values of $q/\sqrt{1 - M^2}$ and $F\delta_a$ to be used in the computations have not been established, the value of maximum angular acceleration in terms of $pb/2V$ for an abrupt aileron reversal from a steady roll can be determined. Examination of equation (26) indicates that if the stick movement were assumed to be made instantaneously and no lag in lift occurred, the angular acceleration would be theoretically twice that obtained in a single movement. Under these conditions the ratio of the maximum angular acceleration to the gravitational constant g is

$$\frac{\dot{p}}{g} = \frac{2\frac{pb}{2V} \frac{q}{\sqrt{1 - M^2}} C_{l_p} Sb}{k_X^2 W} \qquad (28)$$

When numerical values are assigned to the constant terms C_{l_p}, S, b, and W and $k_X^2 = (5.75)^2$, equation (28) becomes

$$\frac{\dot{p}}{g} = 0.02735\frac{pb}{2V}\frac{q}{\sqrt{1 - M^2}} \qquad (29)$$

Maximum value of $q/\sqrt{1 - M^2}$.- The maximum values of $q/\sqrt{1 - M^2}$ that can be obtained depend on the airplane drag coefficient, the wing loading, and the air density. When the airplane weight equals the drag the relation between the attainable Mach number M and these variables is

$$M = \sqrt{\frac{2}{\rho a^2}}\sqrt{\frac{W/S}{C_D}} \qquad (30)$$

The long-short-dash curves of figure 23 show the variation obtained from equation (30) for several standard pressure altitudes with a wing loading of $\frac{W}{S}$ = 40.0 pounds per square foot. The solid-line coefficient curves (curves A and B) in figure 23 are based on wind-tunnel results. The dashed continuation of these curves represents the extrapolation required in order to apply the tunnel results. Curve A represents the variation used by the manufacturer in the design, and curve B was obtained from a generalized curve furnished by the Langley 8-foot high-speed tunnel. The intersections of curves A and B with the curve computed by equation (30) represent the terminal Mach number that would be reached at each of the altitudes listed when the airplane was diving in a standard atmosphere of the density and temperature existing at that altitude.

A relation between $q/\sqrt{1 - M^2}$ and V_e is shown in figure 24 for a number of standard pressure altitudes. This figure also gives the relation between q and V_e. By use of the results shown in figure 23 limit lines can be drawn on figure 24 to indicate the maximum speeds that the airplane could attain at various altitudes. The limit lines A and B correspond to similar ones in figure 23. The part of the limit lines between 30,000 and 40,000 feet (approx. the ceiling of the airplane) has been arbitrarily faired to a point at 40,000 feet corresponding to V_e of 250 miles per hour. Figure 24 shows that the aileron reversal speed corresponding to $q/\sqrt{1 - M^2}$ of 1660 is about 620 miles per hour at sea level and only 330 miles per hour (true airspeed of 660 mph) at 40,000 feet. The actual or practical margin against aileron reversal, however, is greater at the higher altitudes than at the lower altitudes, as may be seen from the limit lines A and B. Without a compressibility correction, the reversal speed is 825 miles per hour at sea level.

Aileron angles.- In addition to establishing the limiting values of $q/\sqrt{1 - M^2}$ the values of the parameter $F\delta_a$ that can be reached must also be established. In the analysis these values were obtained by the use of the flight-test data given in figure 11. These data were used to establish the curves in figure 22 for 20, 40, 60, and 80 pounds change in force on the stick, the 80-pound change in stick force being considered a maximum that a pilot could exert although a lower value might be more reasonable.

In a similar analysis, wind-tunnel results could have been used to establish the limit lines. In the present case, however, the flight results are preferable because an integrated value is obtained.

SELECTION OF CONDITIONS FOR ANALYSIS

The preceding sections have been devoted to the presentation of the basic data that were used to show how the load-distribution curves were obtained in a general form, and to the determination of limiting values of various parameters that are needed to evaluate the loads. The next step is the selection of the conditions for investigation of the loads on the primary structure of the wing and aileron.

In the design of the primary wing structure the conditions requiring investigation are the usual ones in which the largest up or down load occurs in combination with a far-forward center-of-pressure position (points A and D on the V-n diagram) and also when the largest up or down loads occur in combination with a rearward center-of-pressure position (points B and C on the V-n diagram). Insofar as the front spar or spars are concerned in the rolling maneuver, the critical design load will occur near the highest value of $F\delta_a q/\sqrt{1 - M^2}$ that can be obtained for a given equivalent airspeed when the aileron is deflected upward, the airplane is rolling steadily, and the maximum allowable normal accelerating load is on the wing. In this condition the positive pitching-moment increment due to the upward-deflected aileron results in a forward movement of the center of pressure. The reduction in load due to the upward-deflected aileron, however, is approximately balanced by the increase in loading due to damping. Figures 22 and 24 show that this condition would occur at an altitude estimated to be above 30,000 feet with a value of $q/\sqrt{1 - M^2} = 275$ at $V_e = 271$ (point A on V-n diagram) with $F\delta_a = -11.0^\circ$ and $\frac{pb}{2V} = 0.0553$.

Similar reasonings show that in the rolling maneuver the critical design load for the rear spar would occur at the highest value of $F\delta_a q/\sqrt{1 - M^2}$ that can be obtained at the limiting equivalent airspeed ($V_e = 553$) with the aileron in the down position, the airplane rolling steadily, and the maximum accelerating load on the wing. Figures 22 and 24 also show that this condition would occur at an altitude of about 2000 feet for a value of $q/\sqrt{1 - M^2} = 1170$ at $V_e = 553$ with $F\delta_a = 3.78^\circ$ and $\frac{pb}{2V} = 0.0066$.

Insofar as the design of the aileron is concerned, the largest loads will occur when $F\delta_a$ has the largest value for a given equivalent airspeed and stick force. Figures 22 and 24 show that this large value of $F\delta_a$ occurs when $q/\sqrt{1 - M^2}$ has the smallest values - that is, at sea level - although at this stage in the present analysis it is not known whether the steady roll or the angularly accelerated condition is the more severe.

The analysis has revealed that a number of altitudes, as well as a number of equivalent airspeeds, would be involved in the selection of critical conditions for the wing and aileron. Most of the critical conditions for the wing and aileron design occur at relatively low altitudes; therefore, for simplicity and to keep the computations within reasonable bounds the analysis for the P-47B airplane has been confined to sea-level conditions.

Because the basic wind-tunnel and flight data require extensive extrapolation in the consideration of points A, B, C, and D on the V-n diagram in combination with a stick-force increment of 80 pounds, investigation of two intermediate points where the extrapolation of tunnel and flight data would not be so severe seemed desirable. An estimate of the loads thus would be obtained between points A and B on the V-n diagram in what might be considered a more common maneuver. Points E and F of the V-n diagram were therefore investigated for a 40-pound stick-force increment.

The values of the various parameters that would apply at sea level for each of the selected points on the V-n diagram are given in table I. The values for points E and F are listed for a 40-pound stick force, whereas the values for the other points correspond to an 80-pound stick force. Because general curves of the various loadings are given, other conditions could be chosen for investigation if desired.

COMPUTATION OF RESULTS AT SELECTED POINTS ON V-n DIAGRAM

Wings

The general load curves having been determined (figs. 12 to 21) and the conditions selected for the analysis (table I), the loads occurring on the wing and ailerons were computed.

The parameters used for the computation of load, shear, bending moment, and torque on the wing are given in table II. The values listed were obtained from figures 12 to 21 for several selected spanwise stations.

Span loading.- The net span-load distribution along the wing was computed from the values given in tables I and II for each of the selected points on the V-n diagram. The computations are made in table III in which the ordinates of the various load curves (table II) are multiplied by the appropriate constants (table I) to determine the load at a given spanwise station.

For each point on the V-n diagram, the loads are subdivided into three groups, each group consisting of one symmetrical and two antisymmetrical loadings. One of the two antisymmetrical groups refers to the loadings that occur in a steady roll, whereas the other refers to the loadings that occur in a roll at the maximum attainable $pb/2V$ with maximum angular acceleration (stick reversal).

The results given in figure 25 for the curves of symmetrical load were obtained from rows 5, 17, 29, 41, 53, and 65 of table III, from rows 9, 21, 33, 45, 57, and 69 for the curves of antisymmetrical load; and from rows 12, 24, 36, 48, 60, and 72 for the curves of stick-reversal load. The results shown apply to the right wing in a right roll. The results apply equally well to the left wing if the signs of the antisymmetrical parts are reversed.

Shear distribution.- The net shear distribution for each of the selected V-n diagram points is computed in table IV. A division is made in this table similar to the one employed in table III for the loads. In table III, loads acting upward are assumed to produce positive shear, and the two numbers that arise from the shear contributions of concentrated loads are braced together. The upper number in the brace refers to the shear just outboard of the location of the concentrated load, whereas the lower number refers to the shear just inboard of the concentrated load.

Figure 26 gives the results for the right wing in a right roll in such a manner that the effect of the antisymmetrical loads on the total shear at any spanwise station can be seen immediately.

Bending-moment distributions.- The bending-moment distributions are computed in table V and the variations obtained are given in figure 27. The notations in this table follow those of tables III and IV and, as before, the bending-moment distributions of the right wing in a right roll are divided into symmetrical and antisymmetrical parts.

Torque distributions.- The accumulated torque distributions about the elastic axis of the wing are computed in table VI. As in the other tables, the various torque distributions are divided into those that are symmetrical and those that are antisymmetrical about the airplane center line. The two numbers that occur in the braces arise from the contributions caused by concentrated loads. The upper number in the brace refers to the accumulated torque just outboard of the concentrated load, whereas the lower number refers to the torque just inboard of the concentrated load. Stalling moments result in positive torques. The results of torque distributions on the right wing in a right roll are given in figure 28.

Aileron Load Distribution

The load distributions across the ailerons were determined at each of the selected points on the V-n diagram as follows:

(1) From the aerodynamic-load distribution on the wing in way of the aileron (table III), the total wing section lift coefficient at the various spanwise stations was found from the equation

$$c_l = \frac{l}{qc}$$

(2) Reference was made to the wind-tunnel data (figs. 6 to 9) and cross plots of these data were made to determine the over-all values of c_{n_a} at the proper Mach numbers. The cross plots of the tunnel data consisted of a plot of the aileron normal-force coefficient at zero lift with flaps undeflected against Mach number, a plot of dc_{n_a}/dc_l against Mach number that includes the use of the slopes of the straight lines of figures 6 to 9, and a plot of c_{n_a} against δ at $c_n = 0$ for various Mach numbers from the straight dashed lines of figures 6 to 9.

(3) Because the aileron flap-chord ratio varied along the span and the wind-tunnel data applied only to a flap-chord ratio of 0.269, the results of step (2) were adjusted for chord ratio. This adjustment was accomplished by multiplying the results of step (2) by the ratio of the flap parameters obtained from the wing section theory at various flap-chord ratios with the corresponding flap parameters for a flap-chord ratio of 0.269.

(4) The over-all values of c_{n_a} obtained from step (3) were divided into several increments arising from the various spanwise distributions that were considered. These incremental values of Δc_{n_a} were substituted in the equation

$$\Delta l_a = \Delta c_{n_a} qc$$

in order to determine the aerodynamic load at any station. Because the data obtained from the tunnel had been evaluated in this manner for the different Mach numbers, it was desirable to employ the same definition rather than to correct low-speed results for Mach number by use of the factor $F/\sqrt{1 - M^2}$.

The component aerodynamic-load distributions obtained by the foregoing procedure are shown in figures 29 and 30. Figure 29 gives the component aerodynamic-load distribution obtained in the pull-out with steady roll, and figure 30 gives the corresponding aerodynamic-load distributions for the rolling pull-out with maximum angular acceleration (stick reversal). The only distributions shown in figures 29 and 30 are those due to the additional distribution on the wing, equal and opposite deflection of the ailerons, the total aerodynamic-load distribution, and a combined distribution composed of secondary aileron loadings resulting from rolling, wing twist, geometric twist, and aileron droop. The aerodynamic-load distributions given by figures 29 and 30 were integrated to obtain each component load as well as the total load on the aileron that occurs at each selected point on the V-n diagram. The results of the integrations are given in table VII in such form that the contribution of each of the component aerodynamic loads may readily be determined and the importance of the contribution estimated.

DISCUSSION

Wings

The results in figure 25 and table III indicate that larger antisymmetrical load differences occur along the span in the rolling and normal-acceleration maneuver in which the stick is reversed than in the steady-roll maneuver. In either maneuver the spanwise-load differences are not so large as might be expected from the severity of the conditions investigated. In the steady roll the aerodynamic-load distribution due to aileron deflection not only produces a rolling moment that is equal and opposite to the sum of the moments due to damping in roll and elastic twist, but the shape of the distribution curves is quite similar. In the angularly accelerated condition the accelerating aerodynamic-load and the angular-inertia-load distributions, in addition to being nearly equal and opposite with respect to total moment, are of approximately the same form. Reference 4 shows similar results and discusses the effect of various wing weight distributions and aileron sizes and positions.

The small spanwise-loading changes give rise to relatively small shear and bending-moment changes, as may be noted from figures 26 and 27 and tables IV and V. The large changes in the torque distribution shown in figure 28 indicate, however, that the more important changes occur in the chordwise loading rather than in the spanwise loading.

Figure 28 and table VI indicate that, with the exception of point B on the V-n diagram, the torque increment at the root due to deflected ailerons is almost as large as the symmetrical torque at the root. At the outboard wing stations, however, the torque increment due to the deflected ailerons is in some instances several times greater than the symmetrical torque. A comparison of the results in figure 28 shows that the angularly accelerated maneuver produces slightly larger torque increments than the steady rolling maneuver. The largest torques are seen to occur at point C on the V-n diagram. The results in table VI show that the torques contributed by the aerodynamic loads acting at the aerodynamic centers and the normal-inertia loads acting at the center of gravity of the section are large with respect to torques from the section pitching-moment coefficient.

The fact that the torque increment in the most severe case investigated is approximately twice that for which the wing was presumably designed is, in the present case, offset by the fact that the experimental stiffness was about twice the calculated stiffness. (See fig. 4.) The stresses in the beams and in the skin for the maneuvers considered would therefore be little more than those for which the wing was originally designed and, so far as the primary structure of the wing is concerned, the airplane probably could withstand the stresses imposed in the combined rolling pull-out.

The intermediate points E and F, which were investigated with the 40-pound stick force, in general show values that are intermediate between those for the 80-pound stick force at either points A and D or B and C. The loads at points E and F therefore are not so critical as they are at the other points. These loads are, however, more critical than those occurring in a symmetrical maneuver because the increase in torque is roughly 60 percent of the increase obtained with the 80-pound stick force.

Although the present analysis indicates that different components of the structure would have different critical design altitudes, altitude has little effect on the shear and bending moments because the extra shear and bending-moment components are small relative to the symmetrical components even though, roughly, a 20-percent difference in the attainable values of $F\delta_a q/\sqrt{1 - M^2}$ would exist between 0 and 30,000 feet. The torque values, however, will be increased by about 20 percent. Because of the extrapolation required in the present case, the magnitude of the increase cannot be stated very definitely. If, however, the percentage increase were of this magnitude, the various altitudes would have to be taken into account in the design of the primary structure of the wing.

An estimate can be made of the increase that would be required in the wing-structure weight if the wing had been designed for the rolling pull-out. In order to obtain this estimate the wing-weight running load along the span was divided into component running loads consisting of shear-carrying material, torsional-moment-carrying material, and miscellaneous material. The division was made in accordance with the assumptions used in the analysis of the wing - that the vertical shear was carried solely by the solid spar webs, the bending moment was carried by the spar flanges and certain adjacent stringers, and the torsional moment was carried by the outer skin and by bending action of the spars. The foregoing division of the running loads is shown in figure 31.

In order to determine the weight increase necessary with respect to shear-carrying material, the distribution for the shear-carrying material (fig. 31) was multiplied by the ratio of the largest antisymmetrical shear to the largest symmetrical shear occurring at that same station. Integration of the curve thus obtained indicated that a minimum of 5.2 pounds of shear-carrying material would have to be added to the spar webs of each wing in order to withstand the extra shears introduced by the maneuvers considered. The amount to be added would, in a practical case, probably be somewhat larger because of the impracticability of graduating the web thickness as required by the computations.

In order to determine the weight increase necessary with respect to the bending-moment-carrying material, the distribution for the bending-moment-carrying material (fig. 31) was multiplied by the ratio of the largest antisymmetrical bending moment to the largest symmetrical bending moment at the same station. The curve thus obtained was integrated across the span, and the amount of additional bending material was determined as $20\frac{1}{2}$ pounds per wing. This amount of weight would be distributed along the span either as additions to the spar flanges or in the form of larger or more numerous stringers.

In order to estimate the weight increase in the torque-carrying material the assumption was made that, for the type of construction used, the spar flanges and the adjacent stringers would carry some of the torque by differential bending, and the skin and the torque boxes would carry the rest of the torque. The extra material that was required could therefore be put either entirely in the skin or entirely in the spar caps, although an alternative procedure would be to proportion the extra material between both for most efficient use along the wing span. At the outer stations the greater part of the torque load is carried by the skin; therefore, the most efficient use of the material would be obtained if the extra weight were added in the form of skin material at the outboard stations and in the form of spar material at the inboard stations.

The estimate of the weight increase, when the skin material at the outboard stations and the spar material at the inboard stations are increased, was obtained by determining a new torsional-stiffness curve for the wing that would give the same twist variation along the span under the largest total torque (point C, fig. 28) as would be obtained with the largest symmetrical torque, also shown in figure 28 with the original computed torsional stiffness. Although this viewpoint is only one of several that could be taken in order to determine the weight increase, it had the advantage that the parts of the wing that are not stiffened would, to a first approximation at least, not be subject to greater stresses than in the symmetrical maneuver.

In the application of the foregoing estimate, the method outlined in reference 5 for the calculation of wing torsional stiffness proved useful. The detailed procedure for the computations was one of "cut and try" in which the upper and lower skin of the torque boxes and the spar webs, which formed a part of the torque boxes, were increased along the span until the desired torsional-stiffness curve was obtained.

The weight increase per wing in the torque-carrying material was determined as 77 pounds, of which 61 pounds were added to the skin and 16 pounds to the spar webs.

The weight increase for the entire wing would thus be about 102 pounds or 14.35 percent.

Ailerons

The aerodynamic-load distributions over the ailerons (figs. 29 and 30) are in general of the shape that would be expected from the aileron plan form. (See fig. 1.) Table VII shows that for these ailerons the loads due to droop, built-in twist, and elastic twist are generally small with respect to the loads due to equal and opposite deflection of the ailerons and also with respect to the aileron loads due to the additional aerodynamic load. The results given in table VII indicate that the highest loads occur at point C on the V-n diagram (fig. 5). The aerodynamic load occurring in the pull-out with steady roll differs very little from that occurring in the pull-out with aileron stick reversal. If, however, aileron inertia were taken into account (each aileron weighs 26.5 lb) the load for the steady roll with combined normal acceleration would be slightly larger.

The largest aileron loads given in table VII are downward-acting loads, whereas the requirements of reference 6 specify that the downward load need be only one-half the upward load. Aside from the difference in the direction of the critical load, the computed limit load, in accordance with the requirements of reference 6, would be 957 pounds per aileron, whereas the computed limit aerodynamic load with the rolling pull-out (8g and max. pb/2V) would be roughly 3300 pounds. Table VII also shows that the computed aileron loads at any of the points investigated, whether with 40-(points E and F) or 80-pound stick force, are larger than 957 pounds per aileron. Static tests of the aileron by the Republic Aviation Corporation are understood to have shown a breaking load of 3760 pounds when chordwise loadings similar to those obtained in the wind tunnel were used.

The large difference between the required loads and those of the present computations, together with the large margin of safety that exists between the breaking load and the design load, indicates that a large improvement in aileron design could be had by the improvement of both the load specifications and the method of application of the loads to the design.

CONCLUDING REMARKS

The analysis of the effect of the rolling pull-out on the wing and aileron loads of a typical fighter airplane indicated that available applicable aerodynamic data were deficient in the coverage of angle of attack, aileron deflection, and Mach number. Because of the limitations of the wind tunnels, any similar analysis will probably show the same results whether the aerodynamic data were obtained by specific tests or by an analysis of existing results that necessitates extrapolation of the data.

The following specific conclusions applying to the P-47B airplane may be drawn:

(1) The computations indicated that if the airplane were designed to take into account the rolling pull-out, an increase in wing weight of at least 102 pounds, or approximately 14.35 percent, would be necessary. The division of weight would be roughly as follows.

20 pounds extra material in the spar caps for extra bending

5 pounds extra material in the spar webs to take care of extra shear

61 pounds extra material in the upper and lower skins that form the torque boxes

16 pounds extra material in the webs of the torque boxes

(2) The computations indicated that the ailerons of the P-47B airplane could withstand the loads imposed in the rolling pull-out with either a 40- or an 80-pound stick force without exceeding the ultimate breaking loads, although the loads would be larger in either case than the specified limit loads for which the ailerons were designed.

(3) The results showed an aileron reversal speed of 620 miles per hour at sea level and 660 miles per hour at 40,000 feet. Even though terminal velocity for this airplane were taken as 553 miles per hour at sea level, the computed reversal speed would be only 12 percent greater than the terminal velocity.

A generalization of the results obtained in the analysis for the rolling pull-out indicated that:

(1) The maneuver that combines the maximum normal acceleration with maximum rolling velocity

and angular acceleration (that is, stick reversal from steady roll at maximum load factors) is likely to give rise to loadings on the primary wing structure that are slightly more severe than those that occur in the steady roll performed in combination with maximum load factors.

(2) The aerodynamic-load distribution due to deflected ailerons being similar in shape and opposite in magnitude to the distribution due to damping in roll results in only small changes in either the shear or bending moments that pass a given spanwise station. The angular-inertia distribution being similar in shape and approximately of the same magnitude, but opposite in direction, to the distribution due to deflected ailerons, the change in span loading on the wings in the angularly accelerated maneuver is due primarily to the damping in roll. A net loading that results in somewhat larger values of shear and bending-moment increments than are obtained in steady roll is produced.

(3) The shear and bending-moment increments in the rolling pull-out will be small; the torque increment will be large and may be double the initial symmetrical torque on the wing.

(4) Existing requirements for the loads on the ailerons not only give values of the load that are too small, but the direction of the largest load may be in an opposite direction to the load determined by present specifications.

Langley Memorial Aeronautical Laboratory
National Advisory Committee for Aeronautics
Langley Field, Va.

REFERENCES

1. Weick, Fred E., and Jones, Robert T.: Résumé and Analysis of N.A.C.A. Lateral Control Research. NACA Rep. No. 605, 1937.

2. Anon.: Spanwise Air-Load Distribution. ANC-1(1), Army-Navy-Commerce Committee on Aircraft Requirements. U.S. Govt. Printing Office, April 1938.

3. Pearson, H. A.: Span Load Distribution for Tapered Wings with Partial-Span Flaps. NACA Rep. No. 585, 1937.

4. Pearson, Henry A.: A Study of Unsymmetrical-Loading Conditions. NACA TN No. 757, 1940.

5. Boilschmidt, J. L.: Rigidity of Wing and Tail Surfaces. Aircraft Engineering, vol. XVI, no. 186, Aug. 1944, pp. 228-234.

6. Anon.: Stress Analysis Criteria. Air Corps Specification No. C-1803-A (formerly X-1803-A), Nov. 15, 1939, and Amendment No. 5, April 10, 1943.

TABLE I

VALUES OF PARAMETERS USED IN COMPUTATIONS

[Sea level; stick force, 80 lb]

Point on V-n diagram	Equivalent airspeed from fig. 5 (mph)	Mach number	$q/\sqrt{1 - M^2}$ from fig. 22	pb/2V from fig. 21	$F\delta_a$ from fig. 21 (deg)	F from fig. 11	Angular acceleration from equation (29) (rad/sec^2)
A	271	0.355	200	0.0673	12.75	1.106	11.82
B	553	.725	1120	.0078	3.96	.860	7.66
C	553	.725	1120	.0078	3.96	.860	7.66
D	281	.368	217	.0640	12.30	1.106	12.19
E	460	.603	679	[a].0125	[a]3.55	.982	[a]7.45
F	460	.603	679	[a].0125	[a]3.55	.982	[a]7.45

[a]Stick force, 40 pounds.

NATIONAL ADVISORY
COMMITTEE FOR AERONAUTICS

TABLE II

PARAMETERS USED IN COMPUTATION OF LOAD, SHEAR, BENDING MOMENT, AND TORQUE DISTRIBUTIONS

Row	Components \ Station (in.)	240	225	220	175	160	145	140	120	100	80	64	26	Fig.
	Load													
1	Additional	2.19	3.98	5.64	6.70	7.15	7.54	7.65	8.08	8.43	8.71	8.89	9.14	12
2	Built-in twist	-.327	-.490	-.418	-.217	-.102	0	.029	.129	.194	.233	.251	.270	13
3	Aileron droop	.0019	.0282	.0695	.0780	.0640	.0434	.0355	0	-.0333	-.0504	-.0560	-.0600	14
4	Aileron deflected	.0182	.0596	.1202	.1442	.1344	.1130	.1049	.0700	.0400	.0213	.0134	.0026	15
5	Twist × 10^4	.284	.532	.621	.651	.594	.515	.468	.382	.282	.194	.142	.051	19
6	Damping	7.60	12.60	15.71	16.29	15.98	15.29	14.99	13.52	11.76	9.75	7.99	3.40	16
7	Normal inertia	6.4	14.7	19.1	22.9	25.6	28.9	30.4	36.6	43.4	47.6	49.8	52.4	20
8	Angular inertia	130	275	315	336	345	355	358	365	359	321	266	113	21
	Shear													
9	Additional	1.0	4.5	14.5	27.5	36.5	45.6	49.0	61.6	75.5	90.0	101.5	130.0	12
10	Built-in twist	-.10	-.62	-1.60	-2.28	-2.47	-2.53	-2.52	-2.39	-2.11	-1.75	-1.43	-.59	13
11	Aileron droop	-.005	.018	.122	.287	.374	.440	.457	.496	.461	.387	.315	.132	14
12	Aileron deflected	.010	.062	.250	.534	.710	.870	.915	1.055	1.140	1.192	1.220	1.242	15
13	Twist × 10^4	.09	.60	1.91	3.28	4.05	4.77	4.97	5.70	6.25	6.65	6.86	7.16	19
14	Damping	1.6	15.0	45.0	78.5	98.5	118.0	124.6	146.5	169.5	187.0	198.0	216.0	16
[a]15	Normal inertia	2	13	50	{90 / 315	345	{382 / 608	620	{675 / 790	950	1025	{1090 / 1470	1630	20
[a]16	Angular inertia	70	300	950	{1600 / 4680	5300	{5800 / 8500	8590	{9200 / 11,400	12,000	12,550	{13,000 / 14,920	15,500	21
	Bending moment													
17	Additional	0	4	22	65	102	157	178	270	382	516	648	1011	12
18	Built-in twist	-.1	-.4	-2.9	-7.1	-10.1	-13.2	-14.3	-18.3	-22.1	-25.2	-27.4	-30.7	13
19	Aileron droop	-.005	.005	.14	.55	1.00	1.52	1.71	2.48	3.27	3.99	4.45	5.16	14
20	Aileron deflected	0	.04	.33	1.13	1.92	2.08	3.25	4.90	6.75	8.70	10.30	14.25	15
21	Twist × 10^4	0	.3	2.9	8.2	12.8	18.2	20.3	29.3	39.2	49.9	58.9	81.0	19
22	Damping	0	10	70	190	300	440	490	720	990	1290	1575	2200	16
23	Normal inertia	0	10	90	350	620	1080	1310	2500	3900	5560	7050	11,890	20
24	Angular inertia	100	300	1600	4500	10,600	17,200	20,100	36,000	55,000	75,200	93,100	140,500	21
	Torque													
25	Additional	0	0.60	2.45	4.45	5.60	6.50	7.05	8.15	9.30	11.00	12.90	20.15	12
26	Built-in twist	-.008	-.064	-.256	-.361	-.38	-.399	-.398	-.385	-.361	-.321	-.269	-.051	13
27	Aileron droop	-.0005	.0025	.0216	.0455	.0564	.0640	.0660	.0690	.0662	.0578	.0460	0	14
28	Aileron deflected	.0010	.0080	.0425	.0875	.1096	.1265	.1315	.1444	.1525	.1578	.1618	.1660	15
29	Twist × 10^4	.005	.082	.307	.530	.631	.709	.728	.787	.857	.883	.920	.986	19
30	Damping	.2	1.9	7.2	12.6	15.2	17.4	18.0	20.1	22.0	24.1	25.9	30.2	16
31	c_{m_0}	0	11	62	147	208	272	295	399	505	622	720	968	17
32	Δc_{m_a}	0	.035	.428	1.012	1.448	1.920	2.094	2.365	2.365	2.365	2.365	2.365	17
[a]33	Normal inertia	1	5	32	{83 / 70	107	{154 / 141	157	{239 / 254	350	468	{570 / 558	808	20
[a]34	Angular inertia	10	110	500	{1130 / 1020	1520	{2070 / 1910	2120	{2950 / 3560	4440	5300	{5910 / 5540	6470	21

[a]When two numbers are braced together, the upper number refers to a point just outboard of a concentrated load whereas the lower number refers to a point just inboard of the concentrated load.

NATIONAL ADVISORY
COMMITTEE FOR AERONAUTICS

TABLE III

COMPUTATION OF LOAD DISTRIBUTION IN RIGHT ROLL

[Loads given in lb/ft]

Row	Formula (a) \ Station (in.)	240	225	200	175	160	145	140	120	100	80	64	26	Distribution
	Point A; stick force, 80 pounds													
1	[1] × nW/S	701	1274	1805	2144	2288	2413	2448	2586	2698	2787	2845	2925	Symmetrical
2	[2] × $q/\sqrt{1 - M^2}$	-65	-98	-84	-43	-20	0	6	26	38	47	50	54	
3	[3] × $F\delta_d q/\sqrt{1 - M^2}$	-1	-9	-22	-25	-20	-14	-11	0	10	16	18	19	
4	[7] × n	-51	-118	-153	-183	-205	-231	-243	-293	-347	-381	-398	-419	
5	$\sum$(1) to (4)	584	1049	1546	1893	2043	2168	2200	2319	2399	2469	2515	2579	
6	[4] × $F\delta_a q/\sqrt{1 - M^2}$	-46	-152	-306	-367	-342	-288	-267	-176	-102	-54	-34	-7	Antisymmetrical (steady roll)
7	[5] × $F\delta_a q^2/1 - M^2$	14	27	32	33	30	26	25	20	14	10	7	3	
8	[6] × $\frac{pb}{2V}q/\sqrt{1 - M^2}$	102	170	211	219	215	206	202	182	159	131	108	46	
9	(6) + (7) + (8)	70	45	-63	-115	-97	-56	-40	24	71	87	81	42	
10	-(6) - (7) + (8)	134	295	485	553	327	468	444	340	247	175	135	50	Antisymmetrical (stick reversal)
11	[8] × $\dot{p}/g$	-48	-101	-116	-123	-127	-130	-131	-134	-132	-118	-98	-41	
12	(10) + (11)	86	194	369	430	200	338	313	206	115	57	37	9	
	Point B; stick force, 80 pounds													
13	[1] × nW/S	701	1274	1805	2144	2288	2413	2448	2586	2698	2787	2845	2925	Symmetrical
14	[2] × $q/\sqrt{1 - M^2}$	-366	-549	-468	-243	-114	0	32	144	217	261	281	302	
15	[3] × $F\delta_d q/\sqrt{1 - M^2}$	0	-4	-11	-12	-10	-7	-6	0	5	8	9	9	
16	[7] × n	-51	-118	-153	-183	-205	-231	-243	-293	-347	-381	-398	-419	
17	$\sum$(13) to (16)	284	603	1173	1706	1959	2175	2231	2437	2573	2675	2737	2817	
18	[4] × $F\delta_a q/\sqrt{1 - M^2}$	-81	-264	-533	-639	-596	-501	-465	-310	-177	-94	-59	-12	Antisymmetrical (steady roll)
19	[5] × $F\delta_a q^2/1 - M^2$	141	264	308	323	295	256	242	190	140	96	70	26	
20	[6] × $\frac{pb}{2V}q/\sqrt{1 - M^2}$	66	110	137	142	140	134	131	118	103	85	70	30	
21	(18) + (19) + (20)	126	110	-88	-174	-161	-111	-92	-2	66	87	81	44	
22	-(18) - (19) + (20)	6	110	362	458	441	379	354	238	140	83	59	16	Antisymmetrical (stick reversal)
23	[8] × $\dot{p}/g$	-31	-65	-75	-80	-82	-84	-85	-87	-85	-76	-63	-27	
24	(22) + (23)	-25	45	287	378	359	295	269	151	55	7	-4	-11	
	Point C; stick force, 80 pounds													
25	[1] × nW/S	-350	-637	-902	-1072	-1144	-1206	-1224	-1293	-1349	-1394	-1422	-1462	Symmetrical
26	[2] × $q/\sqrt{1 - M^2}$	-366	-549	-468	-243	-114	0	32	144	217	261	281	302	
27	[3] × $F\delta_d q/\sqrt{1 - M^2}$	0	-4	-11	-12	-10	-7	-6	0	5	8	9	9	
28	[7] × n	26	59	76	92	102	116	122	146	174	190	199	210	
29	$\sum$(25) to (28)	-690	-1131	-1305	-1235	-1166	-1097	-1076	-1003	-953	-935	-933	-941	
30	[4] × $F\delta_a q/\sqrt{1 - M^2}$	-81	-264	-533	-639	-596	-501	-465	-310	-177	-94	-59	-12	Antisymmetrical (steady roll)
31	[5] × $F\delta_a q^2/1 - M^2$	141	264	308	323	295	256	242	190	140	96	70	26	
32	[6] × $\frac{pb}{2V}q/\sqrt{1 - M^2}$	66	110	137	142	140	134	131	118	103	85	70	30	
33	(30) + (31) + (32)	126	110	-88	-174	-161	-111	-92	-2	66	87	81	44	
34	-(30) - (31) + (32)	6	110	362	458	441	379	354	238	140	83	59	16	Antisymmetrical (stick reversal)
35	[8] × $\dot{p}/g$	-31	-65	-75	-80	-82	-84	-85	-87	-85	-76	-63	-27	
36	(34) + (35)	-25	45	287	378	359	295	269	151	55	7	-4	-11	

[a]Numbers in brackets [ ] refer to rows in table II. Numbers in parentheses ( ) refer to rows in table III.

NATIONAL ADVISORY
COMMITTEE FOR AERONAUTICS

TABLE III - Concluded

COMPUTATION OF LOAD DISTRIBUTION IN RIGHT ROLL - Concluded

Row	Formula (a) \ Station (in.)	240	225	200	175	160	145	140	120	100	80	64	26	Distribution
	Point D; stick force, 80 pounds													
37	[1] × nW/S	-350	-637	-902	-1072	-1144	-1206	-1224	-1293	-1349	-1394	-1422	-1462	Symmetrical
38	[2] × $q/\sqrt{1-M^2}$	-71	-106	-91	-47	-22	0	6	28	42	51	54	59	
39	[3] × $F\delta_a q/\sqrt{1-M^2}$	-1	-9	-22	-24	-20	-14	-11	0	10	16	18	19	
40	[7] × n	26	59	76	92	102	116	122	146	174	190	199	210	
41	$\sum$(37) to (40)	-396	-693	-939	-1051	-1084	-1104	-1107	-1119	-1123	-1137	-1151	-1174	
42	[4] × $F\delta_a q/\sqrt{1-M^2}$	-49	-159	-321	-385	-359	-302	-280	-187	-107	-57	-36	-16	Antisymmetrical (steady roll)
43	[5] × $F\delta_a q^2/1-M^2$	16	31	36	38	34	30	28	22	16	11	8	3	
44	[6] × $\frac{pb}{2V}q/\sqrt{1-M^2}$	106	175	218	226	222	212	208	188	164	135	111	47	
45	(42) + (43) + (44)	73	47	-67	-121	-103	-60	-44	23	73	89	83	34	
46	-(42) - (43) + (44)	139	303	503	573	547	484	460	353	255	181	139	60	Antisymmetrical (stick reversal)
47	[8] × $\dot{p}/g$	-49	-104	-119	-127	-130	-134	-135	-138	-136	-121	-100	-43	
48	(46) + (47)	90	199	384	446	417	350	325	215	119	60	39	17	
	Point E; stick force, 40 pounds													
49	[1] × nW/S	701	1274	1805	2144	2288	2413	2448	2586	2698	2787	2845	2925	Symmetrical
50	[2] × $q/\sqrt{1-M^2}$	-222	-333	-284	-147	-69	0	20	88	132	158	170	183	
51	[3] × $F\delta_a q/\sqrt{1-M^2}$	0	-2	-4	-5	-4	-3	-2	0	2	3	3	4	
52	[7] × n	-51	-116	-153	-183	-205	-231	-243	-293	-347	-381	-398	-419	
53	$\sum$(49) to (52)	428	821	1364	1809	2010	2179	2223	2381	2485	2567	2620	2693	
54	[4] × $F\delta_a q/\sqrt{1-M^2}$	-44	-144	-290	-348	-324	-272	-253	-169	-96	-51	-32	-8	Antisymmetrical (steady roll)
55	[5] × $F\delta_a q^2/1-M^2$	46	87	102	106	97	84	80	62	46	32	23	7	
56	[6] × $\frac{pb}{2V}q/\sqrt{1-M^2}$	64	107	133	138	136	130	127	115	100	83	68	29	
57	(54) + (55) + (56)	66	50	-55	-104	-91	-58	-46	8	50	64	59	28	
58	-(54) - (55) + (56)	62	164	321	380	363	318	300	222	150	102	77	30	Antisymmetrical (stick reversal)
59	[8] × $\dot{p}/g$	-45	-95	-109	-117	-120	-123	-124	-127	-125	-111	-92	-39	
60	(58) + (59)	17	69	212	263	243	195	176	95	25	-9	-15	-9	
	Point F; stick force, 40 pounds													
61	[1] × nW/S	-350	-637	-902	-1072	-1144	-1206	-1224	-1293	-1349	-1394	-1422	-1462	Symmetrical
62	[2] × $q/\sqrt{1-M^2}$	-222	-333	-284	-147	-69	0	20	88	132	158	170	183	
63	[3] × $F\delta_a q/\sqrt{1-M^2}$	0	-2	-4	-5	-4	-3	-2	0	2	3	3	4	
64	[7] × n	26	59	76	92	102	116	122	146	174	190	199	210	
65	$\sum$(61) to (64)	-546	-913	-1114	-1132	-1115	-1093	-1084	-1059	-1041	-1043	-1050	-1065	
66	[4] × $F\delta_a q/\sqrt{1-M^2}$	-44	-144	-290	-348	-324	-272	-253	-169	-96	-51	-32	-8	Antisymmetrical (steady roll)
67	[5] × $F\delta_a q^2/1-M^2$	46	87	102	106	97	84	80	62	46	32	23	7	
68	[6] × $\frac{pb}{2V}q/\sqrt{1-M^2}$	64	107	133	138	136	130	127	115	100	83	68	29	
69	(66) + (67) + (68)	66	50	-55	-104	-91	-58	-46	8	50	64	59	28	
70	-(66) - (67) + (68)	62	164	321	380	363	318	300	222	150	102	77	30	Antisymmetrical (stick reversal)
71	[8] × $\dot{p}/g$	-45	-95	-109	-117	-120	-123	-124	-127	-125	-111	-92	-39	
72	(70) + (71)	17	69	212	263	243	195	176	95	25	-9	-15	-9	

[a]Numbers in brackets [ ] refer to rows in table II. Numbers in parentheses ( ) refer to rows in table III.

NATIONAL ADVISORY
COMMITTEE FOR AERONAUTICS

TABLE IV

COMPUTATION OF SHEAR DISTRIBUTION IN RIGHT ROLL

[Shears given in lb × 10^{-1}]

Row	Formula [a] \ Station (in.)	240	225	200	175	160	145	140	120	100	80	64	26	Distribution
Point A; stick force, 80 pounds														
1	[9] × nW/S	32	144	464	880	1168	1459	1568	1971	2616	2880	3248	4160	
2	[10] × $q/\sqrt{1-M^2}$	-2	-12	-32	-46	-49	-51	-50	-48	-42	-35	-29	-12	
3	[11] × $F\delta_a q/\sqrt{1-M^2}$	0	-1	-4	-9	-12	-14	-14	-16	-15	-12	-10	-4	Symmetrical
[b]4	[15] × n	-2	-10	-40	-72 / -252	-276	-306 / -486	-496	-540 / -632	-760	-820	-872 / -1176	-1304	
[b]5	$\sum$(1) to (4)	28	121	388	753 / 573	831	1088 / 908	1008	1367 / 1275	1799	2013	2337 / 2033	2840	
6	[12] × $F\delta_a q/\sqrt{1-M^2}$	-2	-16	-64	-136	-181	-222	-233	-269	-290	-304	-311	-316	
7	[13] × $F\delta_a q^2/1-M^2$	0	3	10	17	21	24	25	29	32	34	35	36	Antisymmetrical (steady roll)
8	[14] × $\frac{pb}{2V}q/\sqrt{1-M^2}$	2	20	61	106	133	159	168	200	228	252	266	291	
9	(6) + (7) + (8)	0	7	7	-13	-27	-39	-40	-40	-30	-18	-10	11	
10	-(6) - (7) + (8)	4	33	115	225	293	357	376	440	486	522	542	571	
[b]11	[16] × $\dot{p}/g$	-3	-11	-35	-59 / -179	-194	-213 / -312	-315	-338 / -418	-440	-461	-477 / -548	-569	Antisymmetrical (stick reversal)
[b]12	(10) + (11)	1	22	80	166 / 46	99	144 / 45	61	102 / 22	46	61	65 / -6	2	
Point B; stick force, 80 pounds														
13	[9] × nW/S	32	144	464	880	1168	1459	1568	1971	2416	2880	3248	4160	
14	[13] × $q/\sqrt{1-M^2}$	-11	-69	-179	-255	-277	-283	-282	-268	-236	-196	-160	-66	
15	[11] × $F\delta_a q/\sqrt{1-M^2}$	0	0	-2	-4	-6	-7	-7	-8	-7	-6	-5	-2	Symmetrical
[b]16	[15] × n	-2	-10	-40	-72 / -252	-276	-306 / -486	-496	-540 / -632	-760	-820	-870 / -1176	-1304	
[b]17	$\sum$(13) to (16)	19	65	243	549 / 369	609	863 / 683	783	1155 / 1063	1413	1858	2213 / 1907	2788	
18	[12] × $F\delta_a q/\sqrt{1-M^2}$	-4	-28	-111	-237	-315	-386	-405	-467	-505	-528	-540	-550	
19	[13] × $F\delta_a q^2/1-M^2$	4	30	95	163	201	237	247	283	310	330	340	355	Antisymmetrical (steady roll)
20	[14] × $\frac{pb}{2V}q/\sqrt{1-M^2}$	1	13	39	69	86	103	109	130	148	163	173	187	
21	(18) + (19) + (20)	1	15	23	-5	-28	-46	-49	-54	-47	-35	-27	-8	
22	-(18) - (19) + (20)	1	11	55	143	200	252	267	314	343	361	373	382	
[b]23	[16] × $\dot{p}/g$	-2	-7	-23	-38 / -116	-126	-138 / -202	-204	-219 / -271	-286	-299	-309 / -355	-369	Antisymmetrical (stick reversal)
[b]24	(22) + (23)	-1	4	32	105 / 27	74	114 / 50	63	95 / 43	57	62	64 / 18	13	
Point C; stick force, 80 pounds														
25	[9] × nW/S	-16	-72	-232	-440	-584	-730	-784	-986	-1208	-1440	-1624	-2080	
26	[10] × $q/\sqrt{1-M^2}$	-11	-69	-179	-255	-277	-283	-282	-268	-236	-196	-160	-66	
27	[11] × $F\delta_a q/\sqrt{1-M^2}$	0	0	-2	-4	-6	-7	-7	-8	-7	-6	-5	-2	Symmetrical
[b]28	[15] × n	1	5	20	56 / 126	138	153 / 243	248	270 / 316	380	410	436 / 588	652	
[b]29	$\sum$(25) to (28)	-26	-136	-393	-663 / -573	-729	-867 / -777	-825	-992 / -946	-1071	-1232	-1353 / -1201	-1496	
30	[12] × $F\delta_a q/\sqrt{1-M^2}$	-4	-28	-111	-237	-315	-386	-405	-467	-505	-528	-540	-550	
31	[13] × $F\delta_a q^2/1-M^2$	4	30	95	163	201	237	247	283	310	330	340	355	Antisymmetrical (steady roll)
32	[14] × $\frac{pb}{2V}q/\sqrt{1-M^2}$	1	13	39	69	86	103	109	130	148	163	173	187	
33	(30) + (31) + (32)	1	15	23	-5	-28	-46	-49	-54	-47	-35	-27	-8	
34	-(30) - (31) + (32)	1	11	55	143	200	252	267	314	343	361	373	382	
[b]35	[16] × $\dot{p}/g$	-2	-7	-23	-38 / -116	-126	-138 / -202	-204	-219 / -271	-286	-299	-309 / -355	-369	Antisymmetrical (stick reversal)
[b]36	(34) + (35)	-1	4	32	105 / 27	74	114 / 50	63	95 / 43	57	62	64 / 18	13	

[a]Numbers in brackets [] refer to rows in table II. Numbers in parentheses ( ) refer to rows in table IV.
[b]When two numbers are braced together the upper number refers to a point just outboard of a concentrated load whereas the lower number refers to a point just inboard of the concentrated load.

NATIONAL ADVISORY
COMMITTEE FOR AERONAUTICS

TABLE IV - Concluded

COMPUTATION OF SHEAR DISTRIBUTION IN RIGHT ROLL - Concluded

Row	Formula (a) \ Station (in.)	240	225	200	175	160	145	140	120	100	80	64	26	Distribution
	Point D; stick force, 80 pounds													
37	[9] × nW/S	-16	-72	-232	-440	-584	-730	-784	-986	-1208	-1440	-1624	-2080	Symmetrical
38	[10] × $q/\sqrt{1 - M^2}$	-2	-14	-35	-50	-54	-55	-55	-52	-46	-38	-31	-13	
39	[11] × $F\delta_d q/\sqrt{1 - M^2}$	0	-1	-4	-9	-12	-14	-14	-15	-14	-12	-10	-4	
b40	[15] × n	1	5	20	36 / 126	138	153 / 243	248	270 / 316	380	410	436 / 588	652	
b41	Σ(37) to (40)	-17	-82	-251	-463 / -373	-512	-646 / -556	-605	-783 / -737	-888	-1060	-1229 / -1077	-1445	
42	[12] × $F\delta_a q/\sqrt{1 - M^2}$	-3	-16	-67	-142	-190	-232	-244	-282	-304	-318	-326	-331	Antisymmetrical (steady roll)
43	[13] × $F\delta_a q^2/\overline{1 - M^2}$	1	4	11	19	24	28	29	33	36	38	40	41	
44	[14] × $\frac{pb}{2V} q/\sqrt{1 - M^2}$	2	21	62	109	137	164	173	206	235	260	275	300	
45	(42) + (43) + (44)	0	9	6	-14	-29	-40	-42	-43	-33	-20	-11	10	
46	-(42) - (43) + (44)	4	33	118	232	303	368	300	455	503	540	561	590	Antisymmetrical (stick reversal)
b47	[16] × $\dot{p}/g$	-3	-11	-36	-60 / -184	-200	-219 / -321	-325	-348 / -431	-454	-474	-491 / -564	-586	
b48	(46) + (47)	1	22	82	172 / 48	103	149 / 47	63	107 / 24	49	66	70 / -3	4	
	Point E; stick force, 40 pounds													
49	[9] × nW/S	32	144	464	880	1168	1459	1568	1971	2416	2880	3248	4160	Symmetrical
50	[10] × $q/\sqrt{1 - M^2}$	-7	-42	-109	-155	-168	-172	-171	-162	-143	-119	-97	-40	
51	[11] × $F\delta_d q/\sqrt{1 - M^2}$	0	0	-1	-2	-2	-3	-3	-3	-3	-2	-2	-1	
b52	[15] × n	-2	-10	-40	-72 / -252	-276	-306 / -486	-496	-540 / -632	-760	-820	-872 / -1176	-1304	
b53	Σ(49) to (52)	23	92	314	651 / 471	722	978 / 798	898	1266 / 1174	1510	1939	2277 / 1973	2815	
54	[12] × $F\delta_a q/\sqrt{1 - M^2}$	-2	-15	-60	-129	-171	-210	-221	-254	-275	-287	-294	-299	Antisymmetrical (steady roll)
55	[13] × $F\delta_a q^2/\overline{1 - M^2}$	2	10	31	54	66	78	81	93	102	109	112	117	
56	[14] × $\frac{pb}{2V} q/\sqrt{1 - M^2}$	1	13	38	67	84	100	106	126	144	159	168	183	
57	(54) + (55) + (56)	1	8	9	-8	-21	-32	-34	-35	-29	-19	-14	1	
58	-(54) - (55) + (56)	1	18	67	142	189	232	246	287	317	337	350	365	Antisymmetrical (stick reversal)
b59	[16] × $\dot{p}/g$	-2	-10	-33	-56 / -169	-184	-201 / -295	-298	-319 / -396	-416	-436	-451 / -518	-538	
b60	(58) + (59)	-1	8	34	86 / -27	5	31 / -63	-52	-32 / -109	-99	-99	-101 / -168	-173	
	Point F; stick force, 40 pounds													
61	[9] × nW/S	-16	-72	-232	-440	-584	-730	-784	-986	-1208	-1440	-1624	-2080	Symmetrical
62	[10] × $q/\sqrt{1 - M^2}$	-7	-42	-109	-155	-168	-172	-171	-162	-143	-119	-97	-40	
63	[11] × $F\delta_d q/\sqrt{1 - M^2}$	0	0	-1	-2	-2	-3	-3	-3	-3	-2	-2	-1	
b64	[15] × n	1	5	20	36 / 126	138	153 / 245	248	270 / 316	380	410	436 / 568	652	
b65	Σ(61) to (64)	-22	-139	-322	-561 / -471	-616	-752 / -662	-710	-681 / -835	-974	-1151	-1287 / -1135	-1469	
66	[12] × $F\delta_a q/\sqrt{1 - M^2}$	-2	-15	-60	-129	-171	-210	-221	-254	-275	-287	-294	-299	Antisymmetrical (steady roll)
67	[13] × $F\delta_a q^2/\overline{1 - M^2}$	2	10	31	54	66	78	81	93	102	109	112	117	
68	[14] × $\frac{pb}{2V} q/\sqrt{1 - M^2}$	1	13	38	67	84	100	106	126	144	159	168	183	
69	(66) + (67) + (68)	1	8	9	-8	-21	-32	-34	-35	-29	-19	-14	1	
70	-(66) - (67) + (68)	1	18	67	142	189	232	246	287	317	337	350	365	Antisymmetrical (stick reversal)
b71	[16] × $\dot{p}/g$	-2	-10	-33	-56 / -169	-184	-201 / -295	-298	-319 / -396	-416	-436	-451 / -518	-538	
b72	(70) + (71)	-1	8	34	86 / -27	5	31 / -63	-52	-32 / -109	-99	-99	-101 / -168	-173	

[a]Numbers in brackets [ ] refer to rows in table II. Numbers in parentheses ( ) refer to rows in table IV.

[b]When two numbers are braced together, the upper number refers to a point just outboard of a concentrated load whereas the lower number refers to a point just inboard of the concentrated load.

NATIONAL ADVISORY
COMMITTEE FOR AERONAUTICS

TABLE V

COMPUTATION OF BENDING-MOMENT DISTRIBUTION IN RIGHT ROLL

[Bending moments given in ft-lb × 10^{-2}]

Row	Formula (a) \ Station (in.)	240	225	200	175	160	145	140	120	100	80	64	26	Distribution
	Point A; stick force, 80 pounds													
1	[17] × nW/S	0	13	70	208	326	502	570	864	1222	1651	2074	3235	Symmetrical
2	[18] × $q/\sqrt{1 - M^2}$	0	-1	-6	-14	-20	-26	-29	-37	-44	-50	-55	-61	
3	[19] × $F\delta_a q/\sqrt{1 - M^2}$	0	0	0	-2	-3	-5	-5	-8	-10	-13	-14	-16	
4	[23] × n	0	-1	-7	-28	-50	-86	-105	-200	-312	-446	-564	-951	
5	Σ(1) to (4)	0	11	57	164	255	385	431	619	856	1142	1441	2207	
6	[20] × $F\delta_a q/\sqrt{1 - M^2}$	0	-1	-8	-29	-49	-73	-83	-125	-172	-222	-262	-363	Antisymmetrical (steady roll)
7	[21] × $F\delta_a q^2/1 - M^2$	0	0	2	4	7	9	10	15	20	25	30	41	
8	[22] × $\frac{pb}{2V}q/\sqrt{1 - M^2}$	0	1	9	26	40	59	66	97	133	174	212	296	
9	(6) + (7) + (8)	0	0	3	1	-2	-5	-7	-13	-19	-23	-20	-26	
10	-(6) - (7) + (8)	0	2	15	51	82	123	139	207	285	371	444	618	Antisymmetrical (stick reversal)
11	[24] × $\dot{p}/g$	0	-1	-6	-16	-39	-63	-74	-132	-202	-276	-342	-516	
12	(10) + (11)	0	1	9	35	43	60	65	75	83	95	102	102	
	Point B; stick force, 80 pounds													
13	[17] × nW/S	0	13	70	208	326	502	570	864	1222	1651	2074	3235	Symmetrical
14	[18] × $q/\sqrt{1 - M^2}$	-1	-4	-32	-80	-113	-148	-160	-205	-248	-282	-307	-344	
15	[19] × $F\delta_a q/\sqrt{1 - M^2}$	0	0	0	-1	-2	-2	-3	-4	-5	-6	-7	-8	
16	[23] × n	0	-1	-7	-28	-50	-86	-105	-200	-312	-446	-564	-951	
17	Σ(13) to (16)	-1	8	31	99	161	266	302	455	657	917	1196	1932	
18	[20] × $F\delta_a q/\sqrt{1 - M^2}$	0	-2	-15	-50	-85	-128	-144	-217	-299	-386	-456	-631	Antisymmetrical (steady roll)
19	[21] × $F\delta_a q^2/1 - M^2$	0	2	14	41	64	90	101	145	194	248	292	402	
20	[22] × $\frac{pb}{2V}q/\sqrt{1 - M^2}$	0	1	6	17	26	38	43	63	86	113	138	192	
21	(18) + (19) + (20)	0	1	5	8	5	0	0	-9	-19	-25	-26	-37	
22	-(18) - (19) + (20)	0	1	7	26	47	77	86	135	191	251	302	421	Antisymmetrical (stick reversal)
23	[24] × $\dot{p}/g$	0	-1	-4	-10	-25	-41	-48	-86	-131	-179	-222	-334	
24	(22) + (23)	0	0	3	16	22	36	38	49	60	72	80	87	
	Point C; stick force, 80 pounds													
25	[17] × nW/S	0	-6	-35	-104	-163	-251	-285	-432	-611	-826	-1037	-1618	Symmetrical
26	[18] × $q/\sqrt{1 - M^2}$	-1	-4	-32	-80	-113	-148	-160	-205	-248	-282	-307	-344	
27	[19] × $F\delta_a q/\sqrt{1 - M^2}$	0	0	0	-1	-2	-2	-3	-4	-5	-6	-7	-8	
28	[23] × n	0	0	4	14	25	43	52	100	156	223	282	476	
29	Σ(25) to (28)	-1	-10	-63	-171	-253	-358	-396	-541	-708	-891	-1069	-1494	
30	[20] × $F\delta_a q/\sqrt{1 - M^2}$	0	-2	-15	-50	-85	-128	-144	-217	-299	-386	-456	-631	Antisymmetrical (steady roll)
31	[21] × $F\delta_a q^2/1 - M^2$	0	2	14	41	64	90	101	145	194	248	292	402	
32	[22] × $\frac{pb}{2V}q/\sqrt{1 - M^2}$	0	1	6	17	26	38	43	63	86	113	138	192	
33	(30) + (31) + (32)	0	1	5	8	5	0	0	-9	-19	-25	-26	-37	
34	-(30) - (31) + (32)	0	1	7	26	47	77	86	135	191	251	302	421	Antisymmetrical (stick reversal)
35	[24] × $\dot{p}/g$	0	-1	-4	-10	-25	-41	-48	-86	-131	-179	-222	-334	
36	(34) + (35)	0	0	3	16	22	36	38	49	60	72	80	87	

[a]Numbers in brackets [ ] refer to rows in table II. Numbers in parentheses ( ) refer to rows in table V.

NATIONAL ADVISORY
COMMITTEE FOR AERONAUTICS

TABLE V - Concluded

COMPUTATION OF BENDING-MOMENT DISTRIBUTION IN RIGHT ROLL - Concluded

Row	Formula (a) \ Station (in.)	240	225	200	175	160	145	140	120	100	80	64	26	Distribution
	Point D; stick force, 80 pounds													
37	[17] × nW/S	0	-6	-35	-104	-163	-251	-285	-432	-611	-826	-1037	-1618	
38	[18] × $q/\sqrt{1 - M^2}$	0	-1	-6	-15	-22	-29	-31	-40	-48	-55	-60	-67	
39	[19] × $F\delta_d q/\sqrt{1 - M^2}$	0	0	0	-2	-3	-5	-5	-8	-10	-12	-14	-16	Symmetrical
40	[23] × n	0	0	4	14	25	43	52	100	156	223	282	476	
41	$\sum$(37) to (40)	0	-7	-37	-107	-163	-242	-269	-380	-513	-670	-829	-1225	
42	[20] × $F\delta_a q/\sqrt{1 - M^2}$	0	-1	-9	-30	-51	-77	-87	-131	-180	-232	-275	-380	
43	[21] × $F\delta_a q^2/1 - M^2$	0	0	2	5	7	10	12	17	23	29	34	47	Antisymmetrical (steady roll)
44	[22] × $\frac{pb}{2V}q/\sqrt{1 - M^2}$	0	1	10	26	42	61	68	100	138	179	219	305	
45	(42) + (43) + (44)	0	0	3	1	-2	-6	-7	-14	-19	-24	-22	-28	
46	-(42) - (43) + (44)	0	2	17	51	86	128	143	214	295	382	460	638	
47	[24] × $\dot{p}/g$	0	-1	-6	-16	-40	-65	-76	-136	-208	-284	-352	-531	Antisymmetrical (stick reversal)
48	(46) + (47)	0	1	11	35	46	63	67	78	87	98	108	107	
	Point E; stick force, 40 pounds													
49	[17] × nW/S	0	13	70	208	326	502	570	864	1222	1651	2074	3235	
50	[18] × $q/\sqrt{1 - M^2}$	-1	-3	-20	-48	-69	-90	-97	-124	-150	-171	-186	-208	
51	[19] × $F\delta_d q/\sqrt{1 - M^2}$	0	0	0	0	-1	-1	-1	-2	-2	-2	-3	-3	Symmetrical
52	[23] × n	0	-1	-7	-28	-50	-86	-105	-200	-312	-446	-564	-951	
53	$\sum$(49) to (52)	-1	9	43	132	206	325	367	538	758	1032	1321	2073	
54	[20] × $F\delta_a q/\sqrt{1 - M^2}$	0	-1	-8	-27	-46	-69	-78	-118	-163	-210	-248	-343	
55	[21] × $F\delta_a q^2/1 - M^2$	0	0	5	13	21	30	33	48	64	82	96	132	Antisymmetrical (steady roll)
56	[22] × $\frac{pb}{2V}q/\sqrt{1 - M^2}$	0	1	6	16	25	37	42	61	84	110	134	187	
57	(54) + (55) + (56)	0	0	3	2	0	-2	-3	-9	-15	-18	-18	-24	
58	-(54) - (55) + (56)	0	2	9	30	50	76	67	131	183	238	286	398	
59	[24] × $\dot{p}/g$	0	-1	-6	-15	-37	-60	-70	-125	-191	-261	-323	-488	Antisymmetrical (stick reversal)
60	(58) + (59)	0	1	3	15	13	16	17	6	-8	-23	-37	-90	
	Point F; stick force, 40 pounds													
61	[17] × nW/S	0	-6	-35	-104	-163	-251	-285	-432	-611	-826	-1037	-1618	
62	[18] × $q/\sqrt{1 - M^2}$	-1	-3	-20	-48	-69	-90	-97	-124	-150	-171	-186	-208	
63	[19] × $F\delta_d q/\sqrt{1 - M^2}$	0	0	0	0	-1	-1	-1	-2	-2	-2	-3	-3	Symmetrical
64	[23] × n	0	0	4	14	25	43	52	100	156	223	282	476	
65	$\sum$(61) to (64)	-1	-9	-51	-138	-208	-299	-331	-458	-607	-776	-944	-1353	
66	[20] × $F\delta_a q/\sqrt{1 - M^2}$	0	-1	-8	-27	-46	-69	-78	-118	-163	-210	-248	-343	
67	[21] × $F\delta_a q^2/1 - M^2$	0	0	5	13	21	30	33	48	64	82	96	132	Antisymmetrical (steady roll)
68	[22] × $\frac{pb}{2V}q/\sqrt{1 - M^2}$	0	1	6	16	25	37	42	61	84	110	134	187	
69	(66) + (67) + (68)	0	0	3	2	0	-2	-3	-9	-15	-18	-18	-24	
70	-(66) - (67) + (68)	0	2	9	30	50	76	87	131	183	238	286	398	
71	[24] × $\dot{p}/g$	0	-1	-6	-15	-37	-60	-70	-125	-191	-261	-323	-488	Antisymmetrical (stick reversal)
72	(70) + (71)	0	1	3	15	13	16	17	6	-8	-23	-37	-90	

[a] Numbers in brackets [ ] refer to rows in table II. Numbers in parentheses ( ) refer to rows in table V.

NATIONAL ADVISORY
COMMITTEE FOR AERONAUTICS

TABLE VI

COMPUTATION OF TORQUE DISTRIBUTION IN RIGHT ROLL

[Torques given in lb-ft × 10⁻³]

Row	Formula (a) \ Station (in.)	240	225	200	175	160	145	140	120	100	80	64	26	Distribution
	Point A; stick force, 80 pounds													
1	[23] × nW/S	0	19	78	142	179	208	226	261	298	352	413	645	Symmetrical
2	[26] × $q/\sqrt{1-M^2}$	0	-2	-5	-7	-8	-8	-8	-8	-7	-6	-5	-1	
3	[27] × $F\delta_d q/\sqrt{1-M^2}$	0	0	-1	-1	-2	-2	-2	-2	-2	-2	-2	0	
4	[31] × $C_{m_0} q/\sqrt{1-M^2}$	0	-2	-10	-24	-33	-44	-47	-64	-81	-100	-115	-155	
b5	[33] × n	1	4	26	66 56	86	123 113	126	191 203	280	374	456 446	646	
b6	$\sum$(1) to (5)	1	19	88	176 166	222	277 267	295	378 390	488	618	747 737	1135	
7	[28] × $F\delta_a q/\sqrt{1-M^2}$	0	-2	-11	-22	-28	-32	-34	-37	-39	-40	-41	-42	Antisymmetrical (steady roll)
8	[29] × $F\delta_a q^2/1-M^2$	0	0	2	3	3	4	4	4	4	4	5	5	
9	[30] × $\frac{pb}{2V}q/\sqrt{1-M^2}$	0	3	10	17	20	23	24	27	30	32	35	41	
10	[32] × $Fq/\sqrt{1-M^2}$	0	9	109	258	369	489	554	603	603	603	603	603	
11	(7) + (8) + (9) + (10)	0	10	110	256	364	484	528	597	598	599	602	607	
12	-(7) - (8) + (9) + (10)	0	-4	-90	-222	-324	-438	-460	-543	-558	-555	-532	-525	Antisymmetrical (stick reversal)
b13	[34] × $\dot{p}/g$	0	-4	-18	-42 -37	-56	-76 -70	-78	-108 -131	-163	-194	-217 -203	-237	
b14	(12) + (13)	0	-8	-108	-264 -259	-380	-514 -508	-558	-651 -674	-701	-729	-749 -735	-762	
	Point B; stick force, 80 pounds													
15	[23] × nW/S	0	19	78	142	179	208	226	261	298	352	413	645	Symmetrical
16	[26] × $q/\sqrt{1-M^2}$	-1	-9	-29	-40	-44	-45	-45	-43	-40	-36	-30	-6	
17	[27] × $F\delta_d q/\sqrt{1-M^2}$	0	0	0	-1	-1	-1	-1	-1	-1	-1	-1	0	
18	[31] × $C_{m_0} q/\sqrt{1-M^2}$	0	-10	-56	-137	-186	-244	-264	-358	-452	-557	-645	-883	
b19	[33] × n	1	4	26	66 56	86	123 113	126	191 203	280	374	456 446	646	
b20	$\sum$(15) to (19)	0	4	19	30 20	34	41 31	42	50 62	65	132	193 185	402	
21	[28] × $F\delta_a q/\sqrt{1-M^2}$	0	-4	-19	-39	-49	-56	-58	-64	-68	-70	-71	-74	Antisymmetrical (steady roll)
22	[29] × $F\delta_a q^2/1-M^2$	0	4	15	26	31	35	36	39	42	44	46	49	
23	[30] × $\frac{pb}{2V}q/\sqrt{1-M^2}$	0	2	6	11	13	15	16	18	19	21	23	26	
24	[32] × $Fq/\sqrt{1-M^2}$	0	16	190	448	642	851	928	1048	1048	1048	1048	1046	
25	(21) + (22) + (23) + (24)	0	18	192	446	637	845	922	1041	1041	1043	1046	1049	
26	-(21) - (22) + (23) + (24)	0	-14	-180	-424	-611	-815	-890	-1005	-1003	-1001	-1000	-997	Antisymmetrical (stick reversal)
b27	[34] × $\dot{p}/g$	0	-3	-12	-27 -24	-36	-49 -46	-50	-70 -85	-106	-126	-141 -132	-154	
b28	(26) + (27)	0	-17	-192	-451 -448	-647	-864 -861	-940	-1075 -1090	-1109	-1127	-1141 -1132	-1151	
	Point C; stick force, 80 pounds													
29	[25] × nW/S	0	-10	-39	-71	-90	-104	-113	-150	-149	-176	-206	-322	Symmetrical
30	[26] × $q/\sqrt{1-M^2}$	-1	-9	-29	-40	-44	-45	-45	-43	-40	-36	-30	-6	
31	[27] × $F\delta_d q/\sqrt{1-M^2}$	0	0	0	-1	-1	-1	-1	-1	-1	-1	-1	0	
32	[31] × $C_{m_0} q/\sqrt{1-M^2}$	0	-10	-56	-137	-186	-244	-264	-358	-452	-557	-645	-883	
b33	[33] × n	0	-2	-13	-33 -28	-43	-62 -56	-63	-96 -102	-140	-187	-228 -223	-323	
b34	$\sum$(29) to (33)	-1	-31	-137	-282 -277	-364	-456 -450	-486	-628 -654	-782	-957	-1110 -1105	-1554	
35	[28] × $F\delta_a q/\sqrt{1-M^2}$	0	-4	-19	-39	-49	-56	-58	-64	-68	-70	-71	-74	Antisymmetrical (steady roll)
36	[29] × $F\delta_a q^2/1-M^2$	0	4	13	26	31	35	36	39	42	44	46	49	
37	[30] × $\frac{pb}{2V}q/\sqrt{1-M^2}$	0	2	6	11	13	15	16	18	19	21	23	26	
38	[32] × $Fq/\sqrt{1-M^2}$	0	16	190	[illegible]	642	851	926	1048	1048	1048	1046	1048	
39	(35) + (36) + (37) + (38)	0	18	192	[illegible]	637	845	922	1041	1041	1043	1046	1049	
40	-(35) - (36) + (37) + (38)	0	-14	-180	-424	-611	-815	-890	-1005	-1003	-1001	-1000	-997	Antisymmetrical (stick reversal)
b41	[34] × $\dot{p}/g$	0	-3	-12	-27 -24	-36	-49 -46	-50	-70 -85	-106	-126	-141 -132	-154	
b42	(40) + (41)	0	-17	-192	-451 [illegible]	-647	-864 -861	-940	-1075 -1090	-1109	-1127	-1141 -1132	-1151	

[a]Numbers in brackets [] refer to rows in table II. Numbers in parentheses ( ) refer to rows in table VI.
[b]When two numbers are braced together, the upper number refers to a point just outboard of a concentrated load while the lower number refers to a point just inboard of the concentrated load.

NATIONAL ADVISORY
COMMITTEE FOR AERONAUTICS

TABLE VI - Concluded

COMPUTATION OF TORQUE DISTRIBUTION IN RIGHT ROLL - Concluded

Row	Formula (a) \ Station (in.)	240	225	200	175	160	145	140	120	100	80	64	26	Distribution
	Point D: stick force, 80 pounds													
43	[25] × nW/S	0	-10	-39	-71	-90	-104	-113	-130	-149	-176	-206	-322	Symmetrical
44	[26] × $q/\sqrt{1-M^2}$	0	-2	-6	-8	-8	-9	-9	-8	-8	-7	-6	-1	
45	[27] × $F\delta_d q/\sqrt{1-M^2}$	0	0	-1	-1	-2	-2	-2	-2	-2	-2	-1	0	
46	[31] × $C_{m_0} q/\sqrt{1-M^2}$	0	-2	-11	-26	-36	-47	-51	-69	-88	-108	-125	-168	
b47	[33] × n	0	-2	-13	-33 / -28	-43	-62 / -56	-63	-96 / -102	-140	-187	-228 / -223	-323	
b48	∑(43) to (47)	0	-16	-70	-139 / -134	-179	-224 / -218	-238	-305 / -311	-387	-480	-566 / -561	-814	
49	[28] × $F\delta_a q/\sqrt{1-M^2}$	0	-2	-11	-23	-29	-34	-35	-38	-41	-42	-43	-44	Antisymmetrical (steady roll)
50	[29] × $F\delta_a q^2/1-M^2$	0	0	2	3	4	4	4	5	5	5	5	6	
51	[30] × $\frac{pb}{2V}q/\sqrt{1-M^2}$	0	3	10	18	21	24	25	28	31	34	36	42	
52	[32] × $Fq/\sqrt{1-M^2}$	0	9	114	270	386	512	559	631	631	631	631	631	
53	(49) + (50) + (51) + (52)	0	10	115	268	382	506	553	626	626	628	629	635	
54	-(49) - (50) + (51) + (52)	0	-4	-95	-232	-340	-458	-503	-570	-564	-560	-557	-551	Antisymmetrical (stick reversal)
b55	[34] × δ/g	0	-4	-19	-43 / -39	-58	-78 / -72	-80	-112 / -135	-168	-200	-223 / -209	-244	
b56	(54) + (55)	0	-8	-114	-275 / -271	-398	-536 / -530	-583	-682 / -705	-732	-760	-780 / -766	-795	
	Point E; stick force, 40 pounds													
57	[25] × nW/S	0	19	78	142	179	208	226	261	298	352	413	645	Symmetrical
58	[26] × $q/\sqrt{1-M^2}$	0	-6	-18	-25	-26	-27	-27	-26	-25	-22	-18	-3	
59	[27] × $F\delta_d q/\sqrt{1-M^2}$	0	0	0	0	0	0	0	0	0	0	0	0	
60	[31] × $C_{m_0} q/\sqrt{1-M^2}$	0	-6	-34	-80	-113	-148	-160	-217	-274	-338	-391	-526	
b61	[33] × n	1	4	26	66 / 56	86	123 / 113	126	191 / 203	280	374	456 / 446	646	
b62	∑(57) to (61)	1	11	52	103 / 93	126	156 / 146	165	209 / 221	279	366	460 / 450	762	
63	[28] × $F\delta_a q/\sqrt{1-M^2}$	0	-2	-10	-21	-26	-30	-32	-35	-37	-38	-39	-40	Antisymmetrical (steady roll)
64	[29] × $F\delta_a q^2/1-M^2$	0	1	5	9	10	12	12	13	14	14	15	16	
65	[30] × $\frac{pb}{2V}q/\sqrt{1-M^2}$	0	2	6	11	13	15	15	17	19	20	22	26	
66	[32] × $Fq/\sqrt{1-M^2}$	0	8	103	244	349	463	505	570	570	570	570	570	
67	(63) + (64) + (65) + (66)	0	9	104	243	346	460	500	565	566	566	568	572	
68	-(63) - (64) + (65) + (66)	0	-5	-92	-221	-320	-430	-470	-531	-528	-526	-524	-520	Antisymmetrical (stick reversal)
b69	[34] × δ/g	0	-4	-17	-39 / -35	-53	-72 / -66	-74	-102 / -124	-154	-184	-205 / -192	-224	
b70	(68) + (69)	0	-9	-109	-260 / -256	-373	-502 / -496	-544	-633 / -655	-682	-710	-720 / -716	-744	
	Point F: stick force, 40 pounds													
71	[25] × nW/S	0	-10	-39	-71	-90	-104	-113	-130	-149	-176	-206	-322	Symmetrical
72	[26] × $q/\sqrt{1-M^2}$	0	-6	-18	-25	-26	-27	-27	-26	-25	-22	-18	-3	
73	[27] × $F\delta_d q/\sqrt{1-M^2}$	0	0	0	0	0	0	0	0	0	0	0	0	
74	[31] × $C_{m_0} q/\sqrt{1-M^2}$	0	-6	-34	-80	-113	-148	-160	-217	-274	-338	-391	-526	
b75	[33] × n	0	-2	-13	-33 / -28	-43	-62 / -56	-63	-96 / -102	-140	-187	-228 / -223	-323	
b76	∑(71) to (75)	0	-24	-104	-209 / -204	-272	-341 / -335	-363	-469 / -475	-588	-723	-843 / -838	-1174	
77	[28] × $F\delta_a q/\sqrt{1-M^2}$	0	-2	-10	-21	-26	-30	-32	-35	-37	-38	-39	-40	Antisymmetrical (steady roll)
78	[29] × $F\delta_a q^2/1-M^2$	0	1	5	9	10	12	12	13	14	14	15	16	
79	[30] × $\frac{pb}{2V}q/\sqrt{1-M^2}$	0	2	6	11	13	15	15	17	19	20	22	26	
80	[32] × $Fq/\sqrt{1-M^2}$	0	8	103	244	349	463	505	570	570	570	570	570	
81	(77) + (78) + (79) + (80)	0	9	104	243	346	460	500	565	566	566	568	572	
82	-(77) - (78) + (79) + (80)	0	-5	-92	-221	-320	-430	-470	-531	-528	-526	-524	-520	Antisymmetrical (stick reversal)
b83	[34] × δ/g	0	-4	-17	-39 / -35	-53	-72 / -66	-74	-102 / -124	-154	-184	-205 / -192	-224	
b84	(82) + (83)	0	-9	-109	-260 / -256	-373	-502 / -496	-544	-633 / -655	-682	-710	-729 / -716	-744	

[a] Numbers in brackets [ ] refer to rows in table II. Numbers in parentheses ( ) refer to rows in table VI.
[b] When two numbers are braced together, the upper number refers to a point just outboard of a concentrated load whereas the lower number refers to a point just inboard of the concentrated load.

NATIONAL ADVISORY
COMMITTEE FOR AERONAUTICS

TABLE VII

AERODYNAMIC LOADS ON AILERONS IN RIGHT ROLL

NATIONAL ADVISORY COMMITTEE FOR AERONAUTICS

Point on V-n diagram	Type of load	Steady roll		Stick reversal		Conditions
		Left	Right	Left	Right	
A	Additional	906	906	906	906	q = 187
	Built-in twist	-20	-20	-20	-20	$\frac{q}{\sqrt{1-M^2}} = 200$
	Aileron droop	-87	-140	-140	-87	
	Aileron deflection	846	-1248	-1248	846	$\delta_a = 11.52$
	Twist	-11	11	11	-11	$\delta_d = -1.43$
	Damping	-93	93	-93	93	$\frac{pb}{2V} = 0.0673$
	C_{n_o}	24	24	24	24	
	Total	1565	-374	-560	1751	$C_L = 1.75$
B	Additional	505	505	505	505	q = 771.5
	Built-in twist	-75	-75	-75	-75	$\frac{q}{\sqrt{1-M^2}} = 1120$
	Aileron droop	-66	-59	-59	-66	
	Aileron deflection	2110	-2735	-2735	2110	$\delta_a = 4.60$
	Twist	-50	50	50	-50	$\delta_d = -0.16$
	Damping	-33	33	-33	33	$\frac{pb}{2V} = 0.0078$
	C_{n_o}	-187	-187	-187	-187	
	Total	2204	-2468	-2534	2270	$C_L = 0.419$
C	Additional	-246	-246	-246	-246	q = 771.5
	Built-in twist	-75	-75	-75	-75	$\frac{q}{\sqrt{1-M^2}} = 1120$
	Aileron droop	-66	-59	-59	-66	
	Aileron deflection	2110	-2735	-2735	2110	$\delta_a = 4.60$
	Twist	-50	50	50	-50	$\delta_d = -0.16$
	Damping	-33	33	-33	33	$\frac{pb}{2V} = 0.0078$
	C_{n_o}	-187	-187	-187	-187	
	Total	1453	-3219	-3285	1519	$C_L = -0.206$
D	Additional	-460	-460	-460	-460	q = 201.8
	Built-in twist	-26	-26	-26	-26	$\frac{q}{\sqrt{1-M^2}} = 217$
	Aileron droop	-91	-132	-132	-91	
	Aileron deflection	907	-1308	-1308	907	$\delta_a = 11.12$
	Twist	-13	13	13	-13	$\delta_d = -1.30$
	Damping	-97	97	-97	97	$\frac{pb}{2V} = 0.0640$
	C_{n_o}	26	26	26	26	
	Total	246	-1790	-1984	440	$C_L = -0.80$
E	Additional	1188	1188	1188	1188	q = 541.6
	Built-in twist	-105	-105	-105	-105	$\frac{q}{\sqrt{1-M^2}} = 679$
	Aileron droop	-20	-35	-35	-20	
	Aileron deflection	1032	-1330	-1330	1032	$\delta_a = 3.615$
	Twist	-43	43	43	-43	$\delta_d = -0.09$
	Damping	-76	76	-76	76	$\frac{pb}{2V} = 0.0125$
	C_{n_o}	0	0	0	0	
	Total	1976	-163	-315	2128	$C_L = 0.60$
F	Additional	-588	-588	-588	-588	q = 541.6
	Built-in twist	-105	-105	-105	-105	$\frac{q}{\sqrt{1-M^2}} = 679$
	Aileron droop	-20	-35	-35	-20	
	Aileron deflection	1032	-1330	-1330	1032	$\delta_a = 3.615$
	Twist	-43	43	43	-43	$\delta_d = -0.09$
	Damping	-76	76	-76	76	$\frac{pb}{2V} = 0.0125$
	C_{n_o}	0	0	0	0	
	Total	200	-1939	-2091	352	$C_L = -0.296$

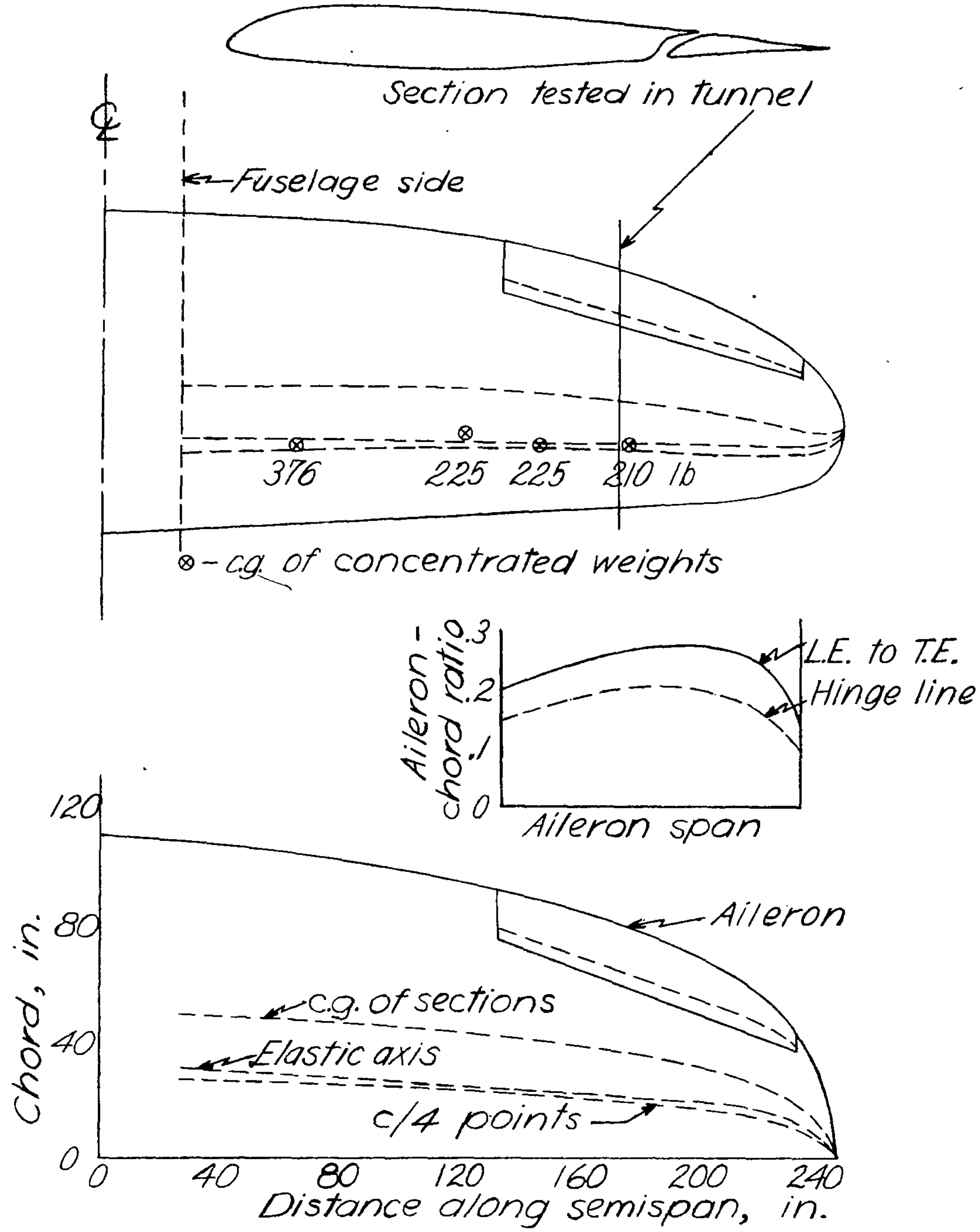

Figure 1.- Wing chord distribution and location of axes.

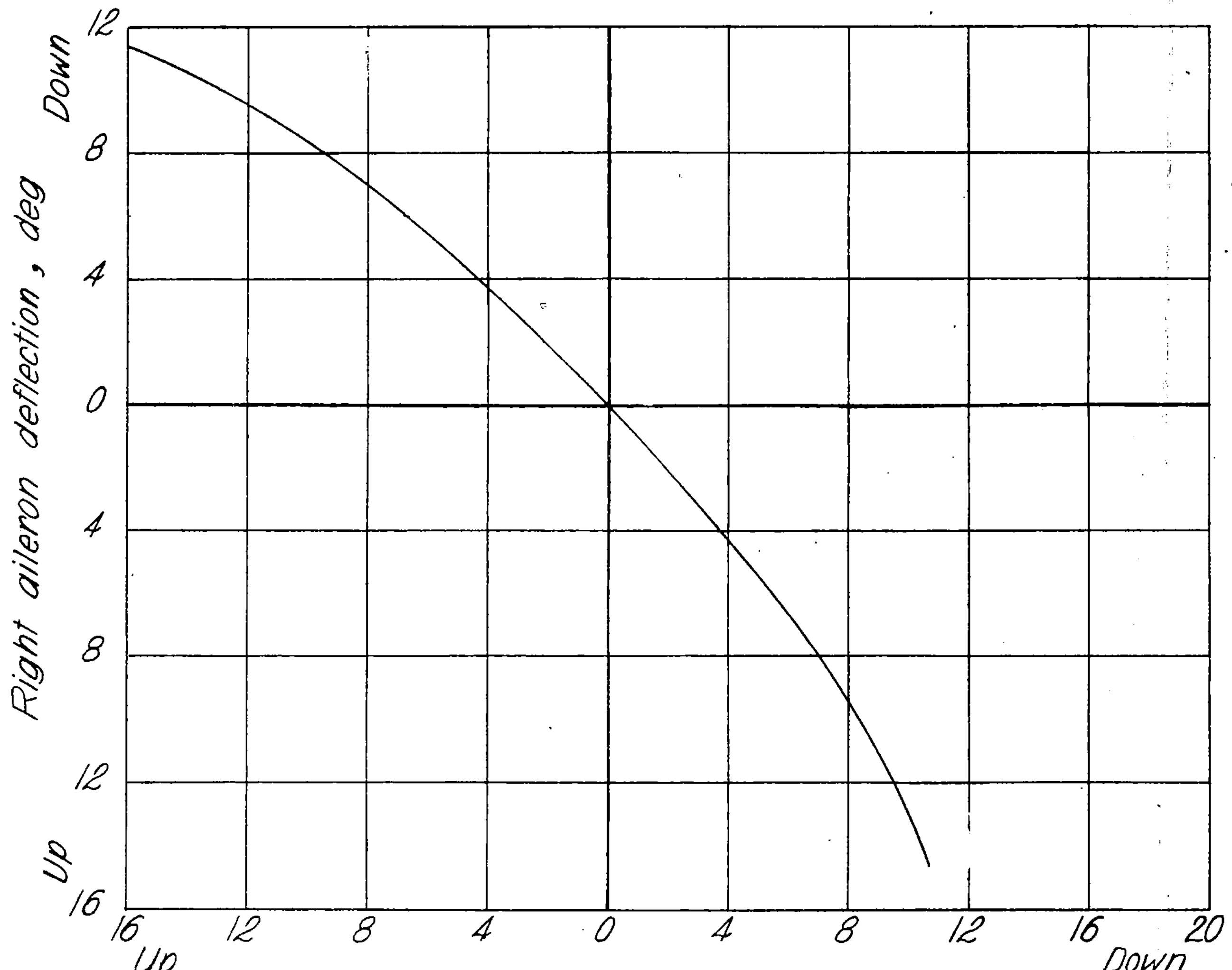

Figure 2.-Relation between left and right aileron deflections.

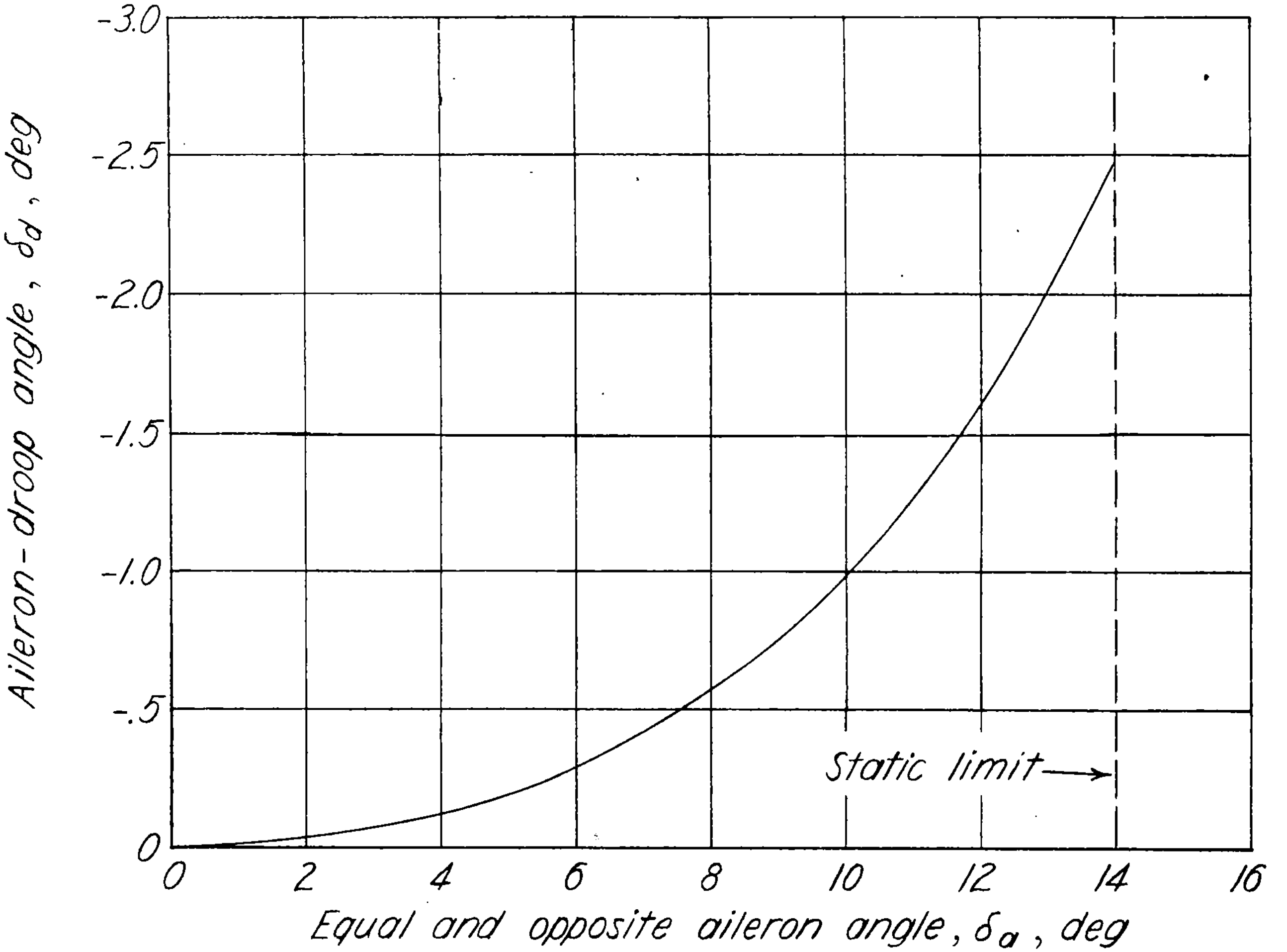

Figure 3.- Variation of aileron droop with equal and opposite aileron deflection. $\delta = \delta_a + \delta_d$

NATIONAL ADVISORY
COMMITTEE FOR AERONAUTICS

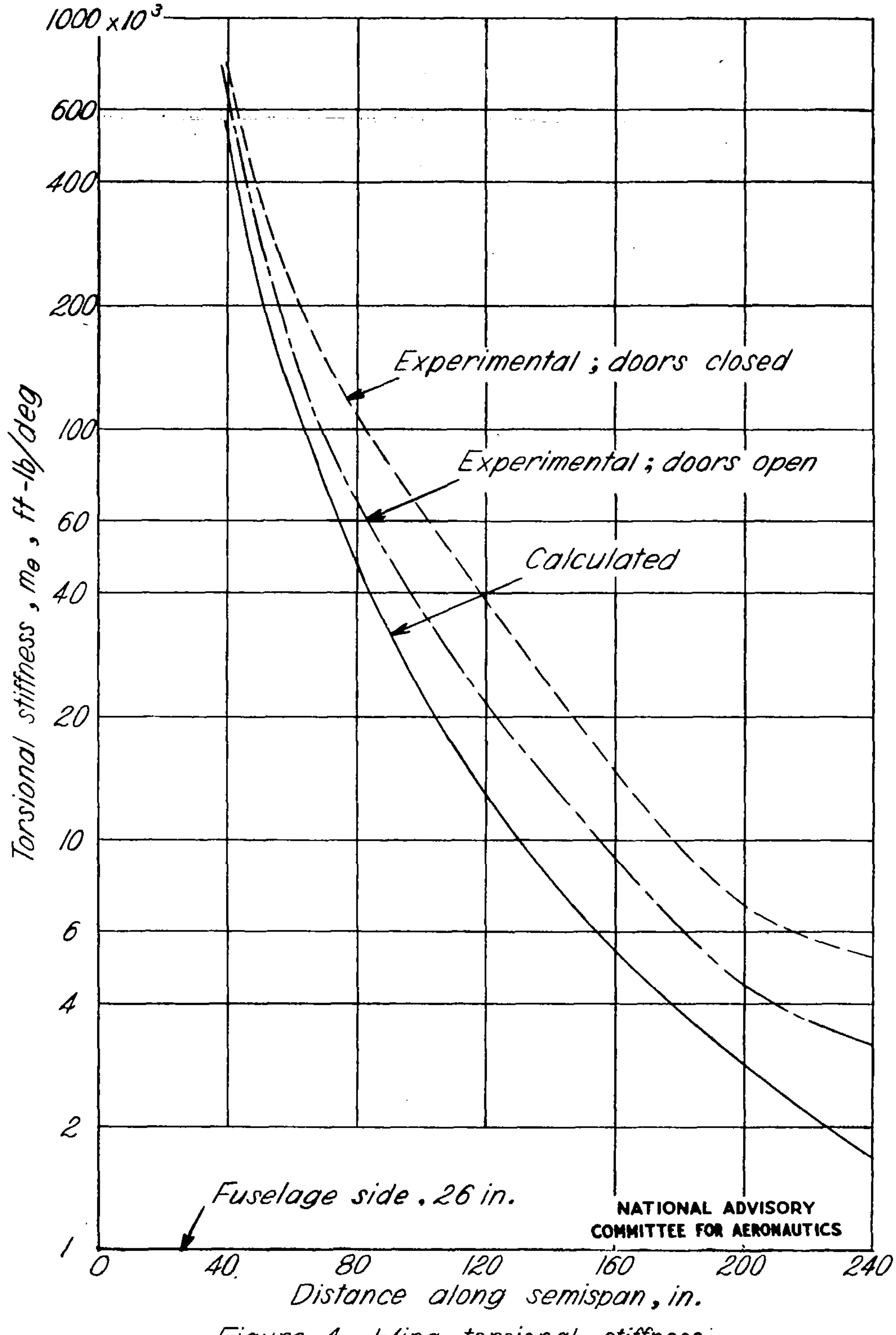

Figure 4.- Wing torsional stiffness.

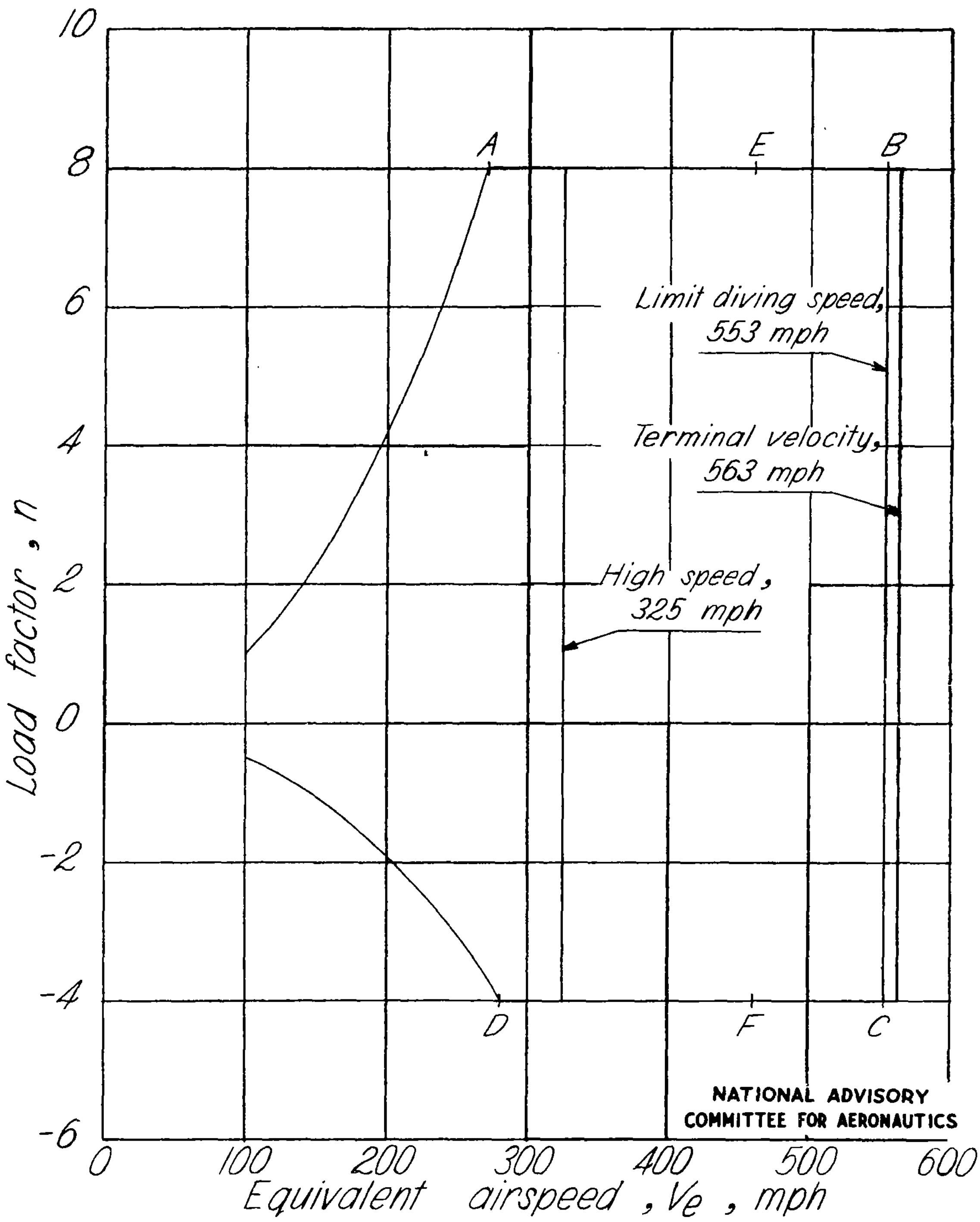

Figure 5.- Sea-level limit V-n diagram for airplane with a normal gross weight of 12,000 pounds. Gross wing area, 300 square feet.

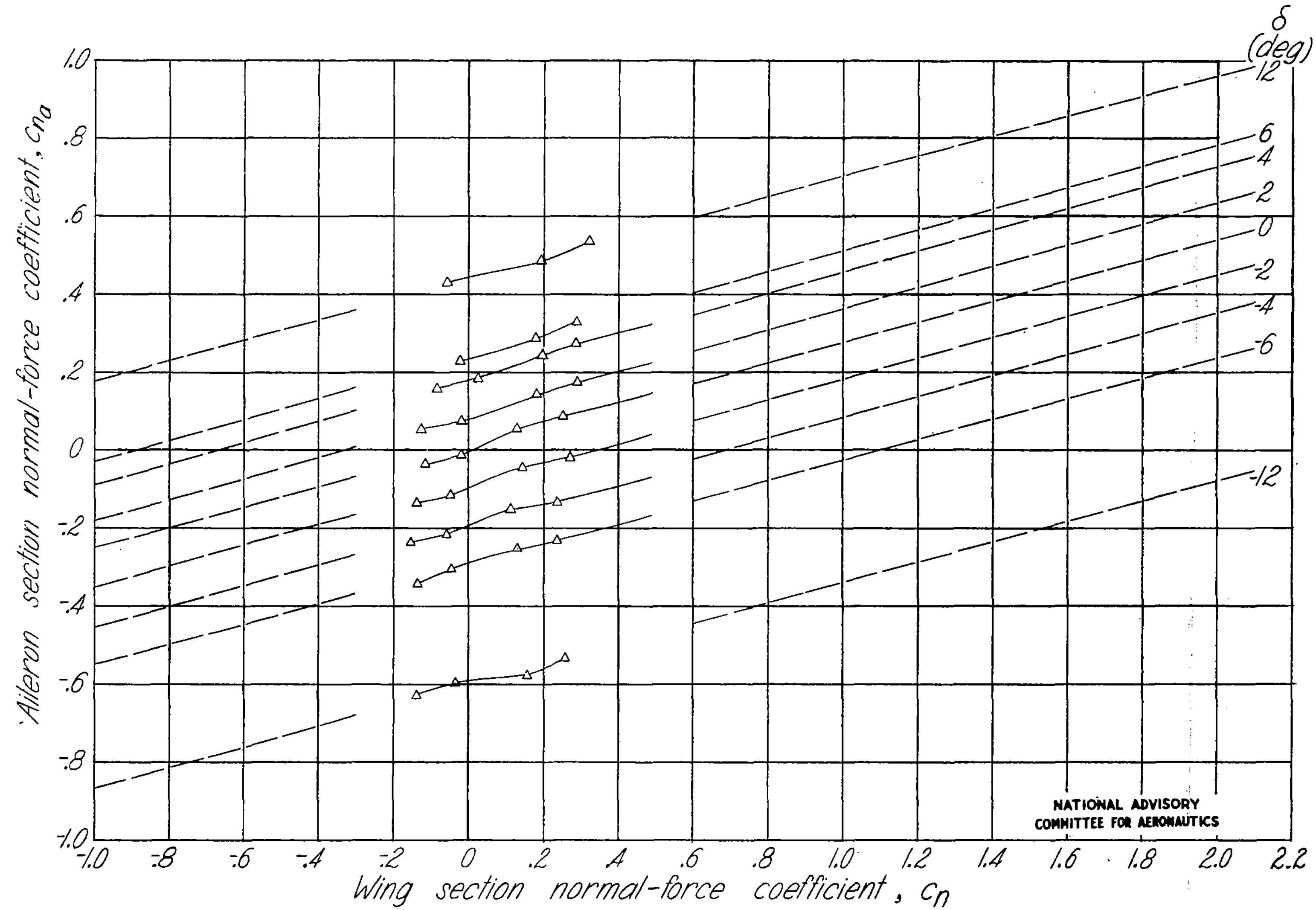

Figure 6.-Variation of c_{n_a} with c_n for various aileron deflections for M=0.25 . Dashed lines indicate extrapolations.

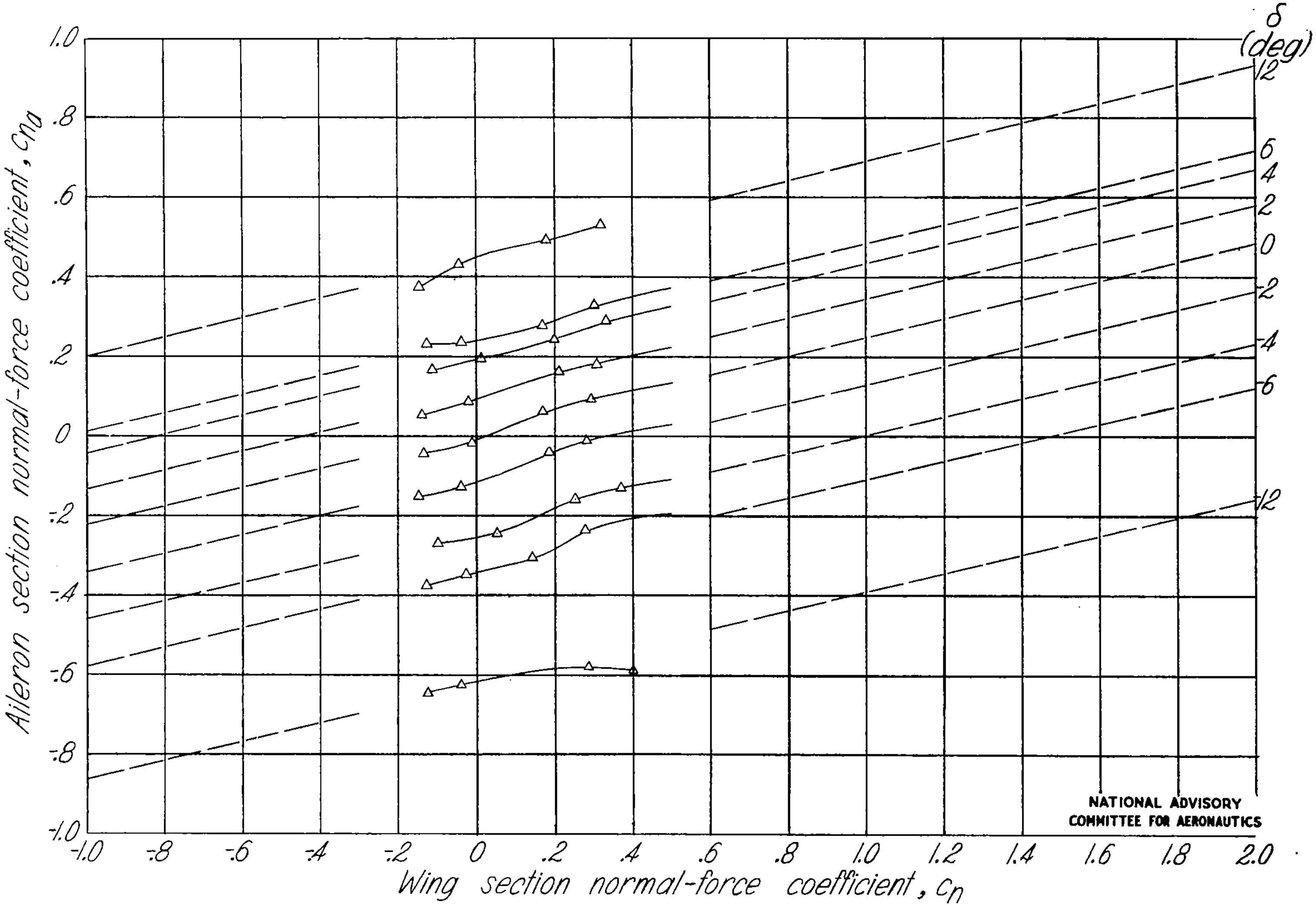

Figure 7.-Variation of c_{n_a} with c_n for various aileron deflections for M=0.475. Dashed lines indicate extrapolations.

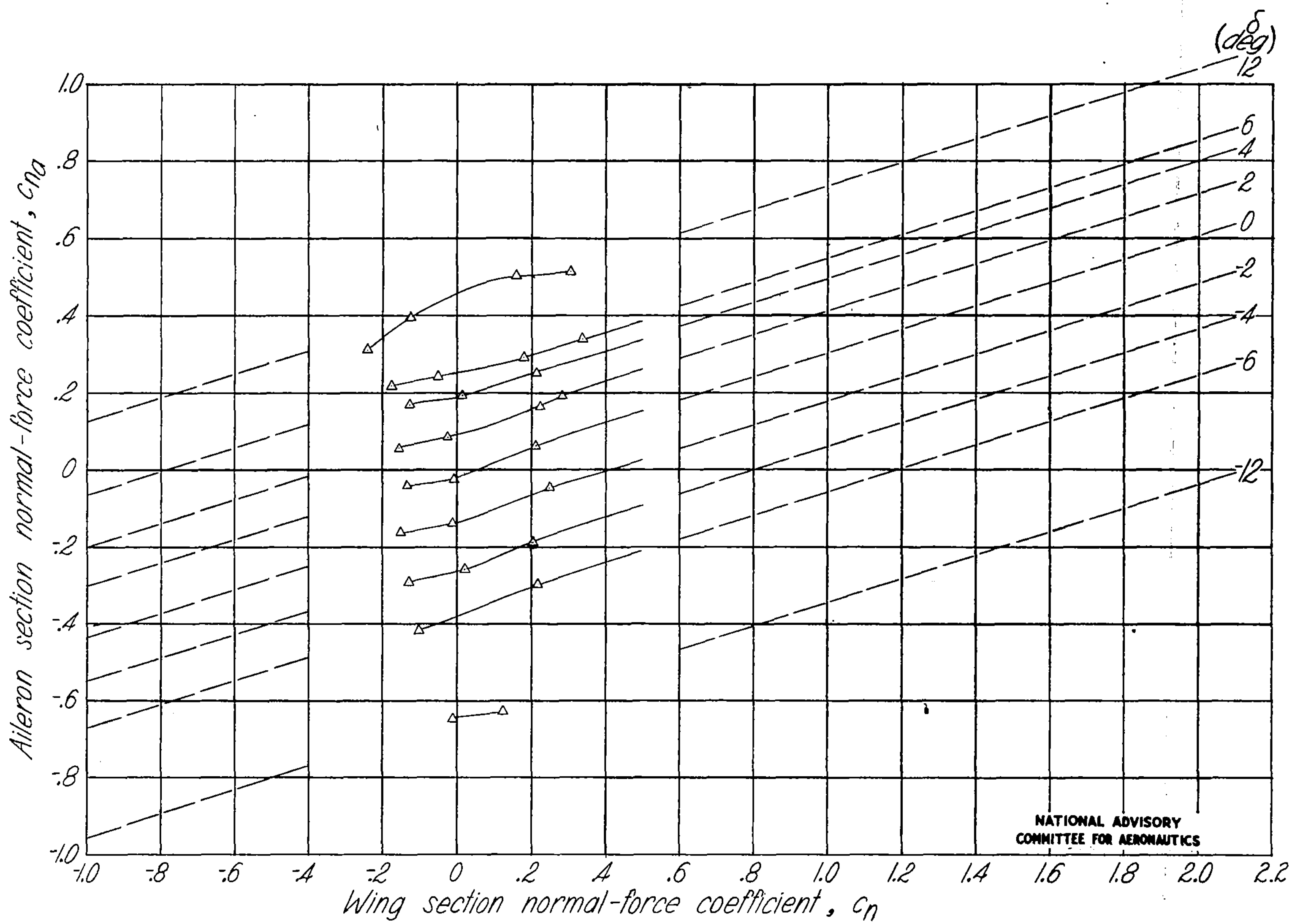

Figure 8.- Variation of c_{n_a} with c_n for various aileron deflections for M=0.60. Dashed lines indicate extrapolations.

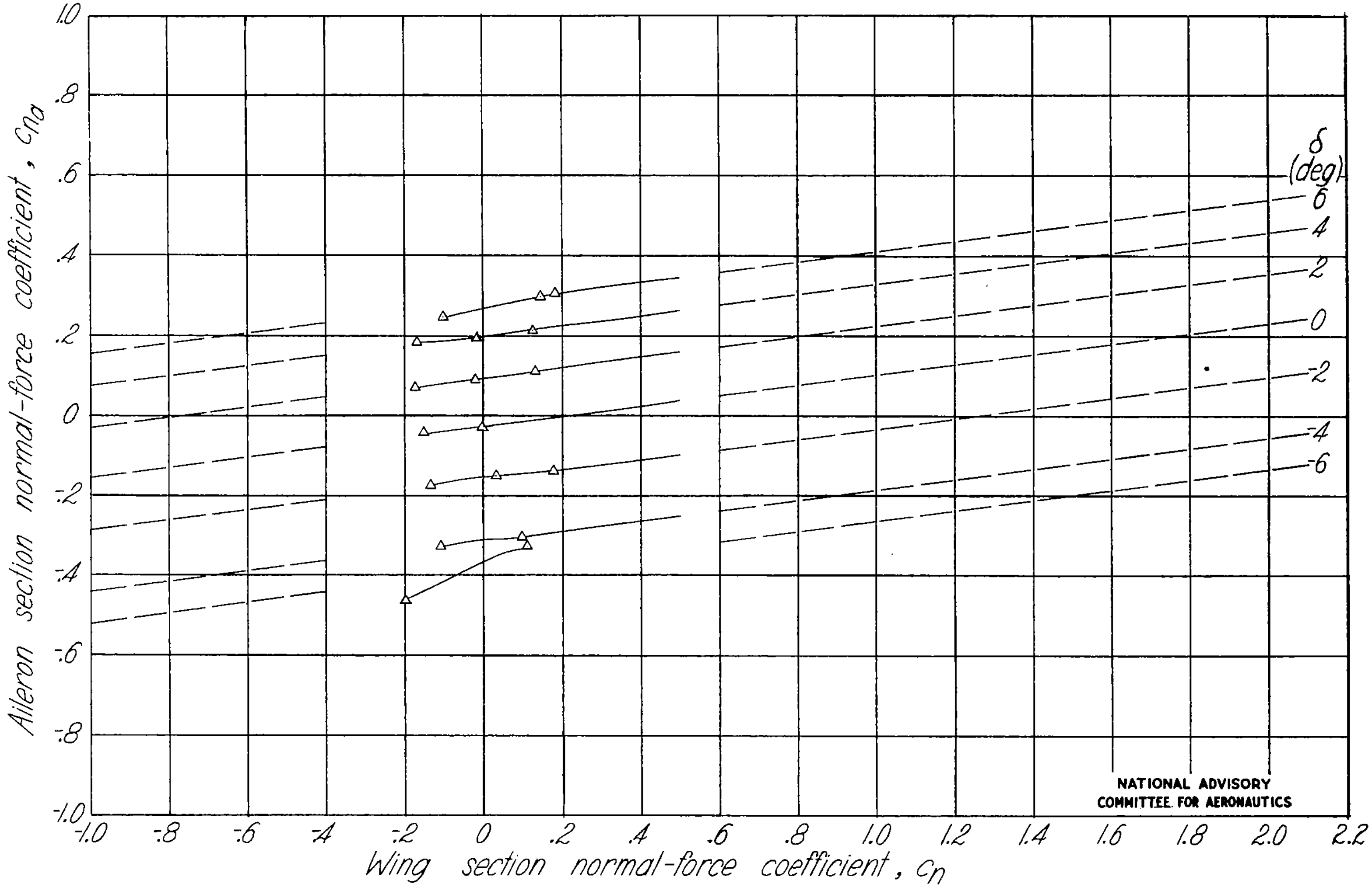

Figure 9.- Variation of c_{n_a} with c_n for various aileron deflections for $M = 0.725$. Dashed lines indicate extrapolations.

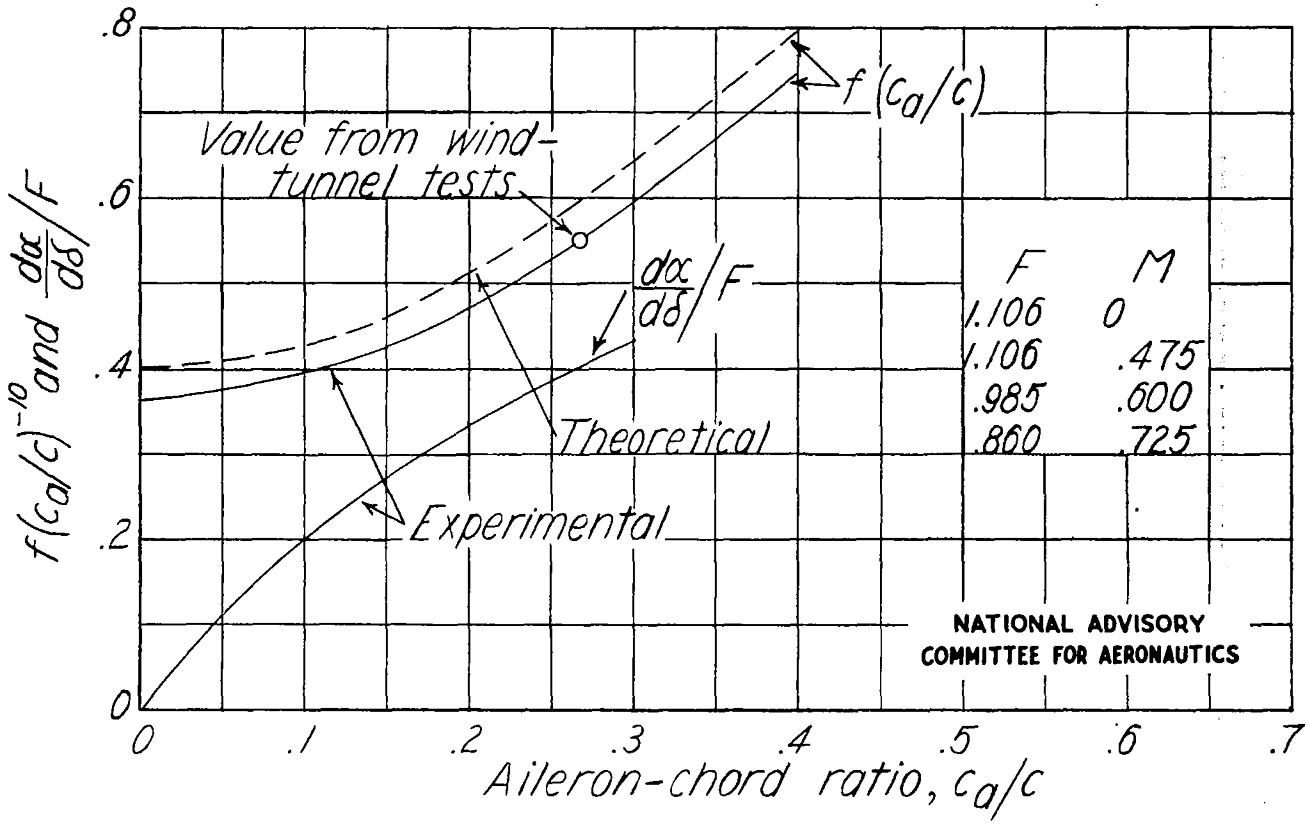

Figure 10.- Variation of section coefficients with aileron chord ratio. (Experimental curve for $\frac{d\alpha}{d\delta}/F$ from reference 1.)

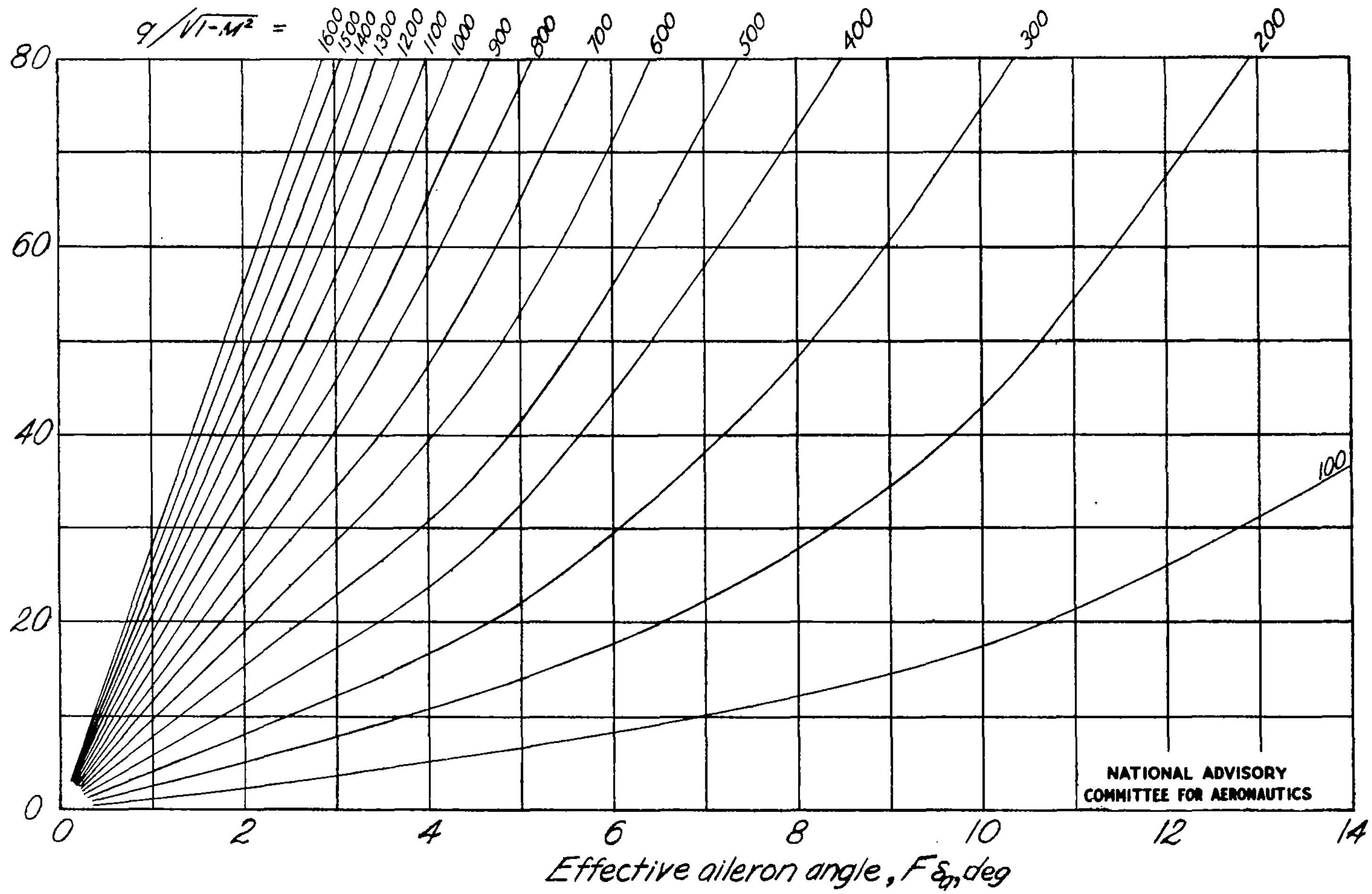

Figure 11.- Variation obtained in flight between stick force and $F\delta_a$ for various values of $q/\sqrt{1-M^2}$.

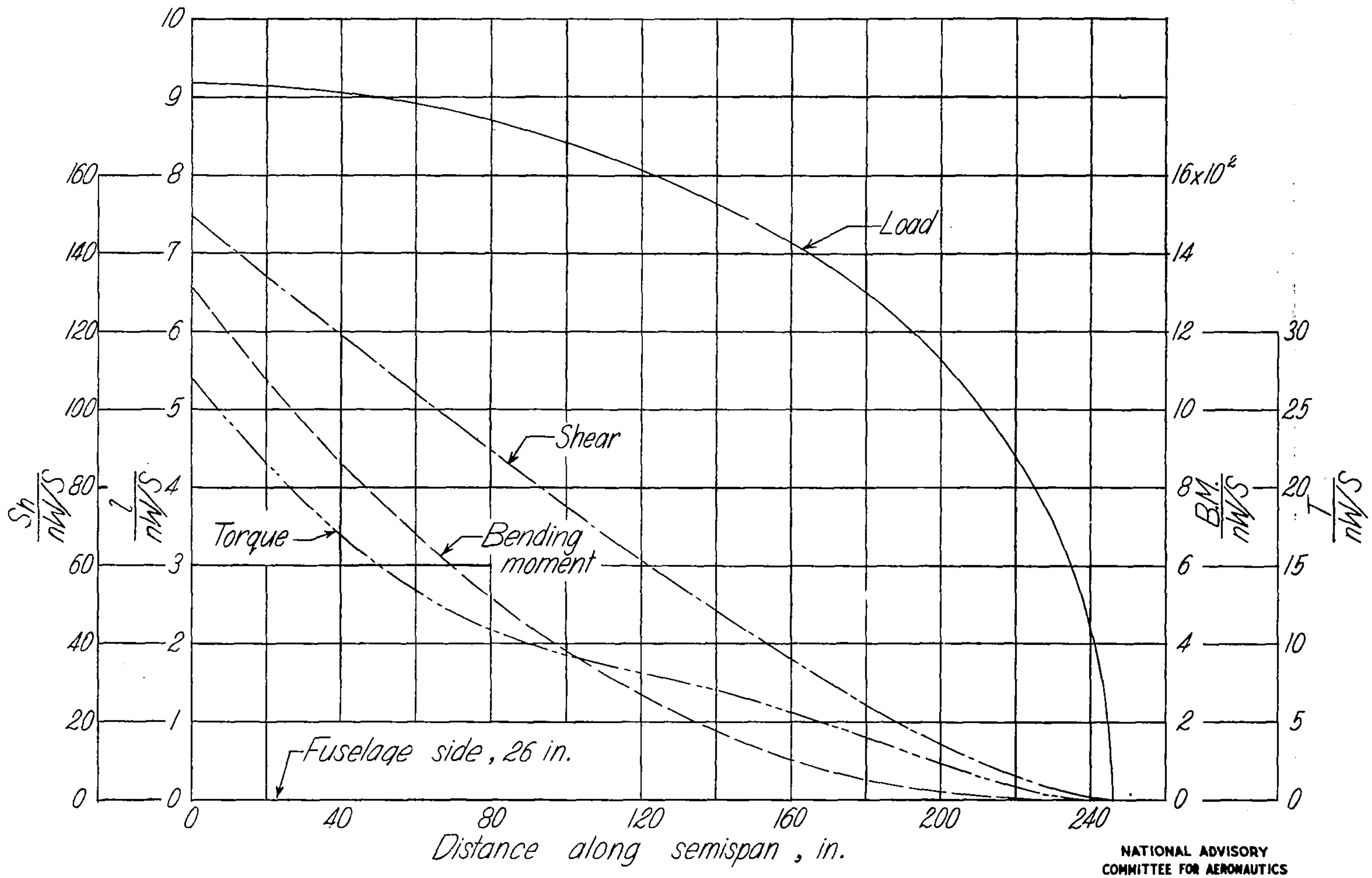

Figure 12.- Distribution of load, shear, bending moment, and torque for additional aerodynamic load.

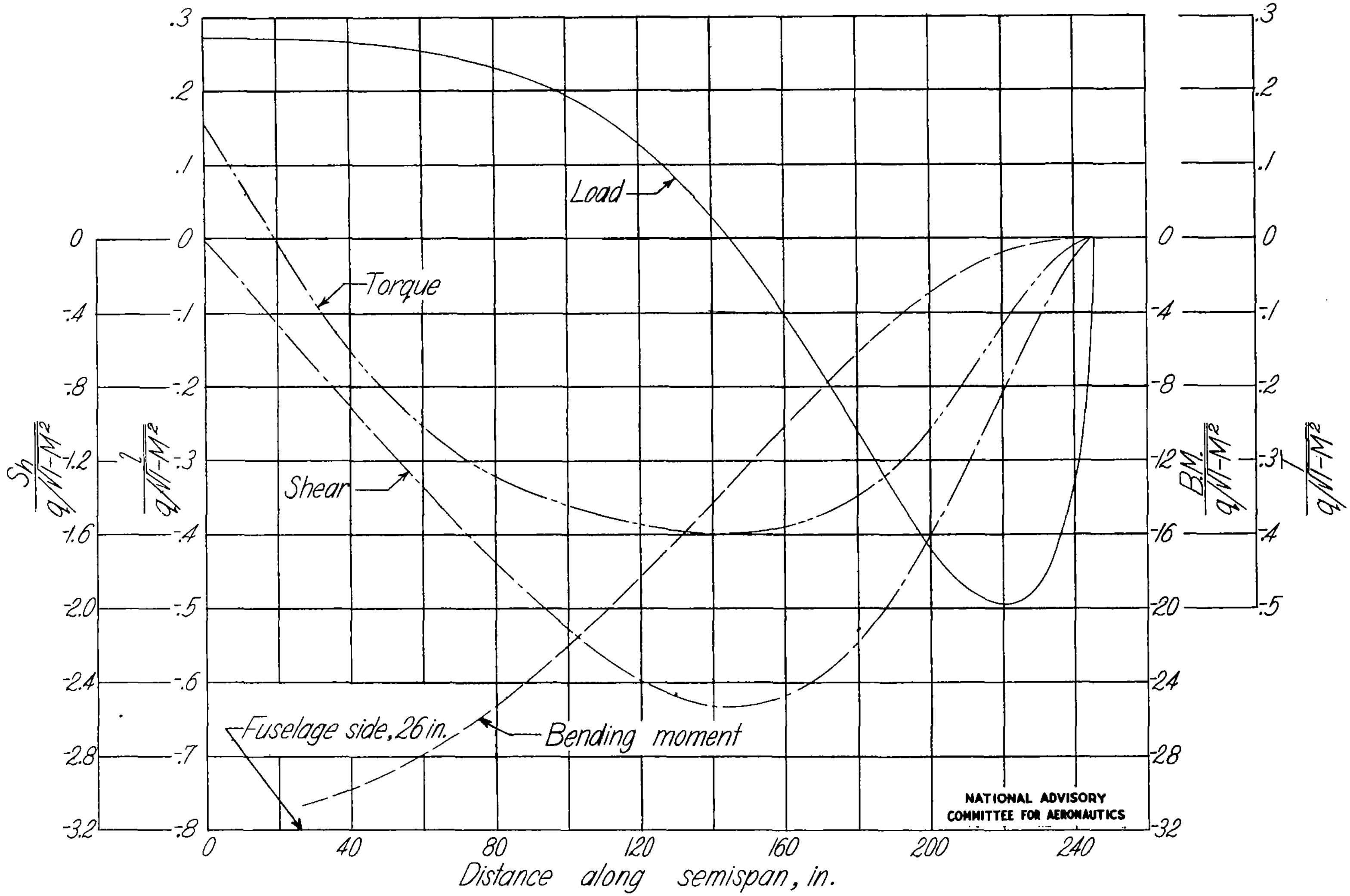

Figure 13.- Distribution of load, shear, bending moment, and torque for built-in-twist aerodynamic load.

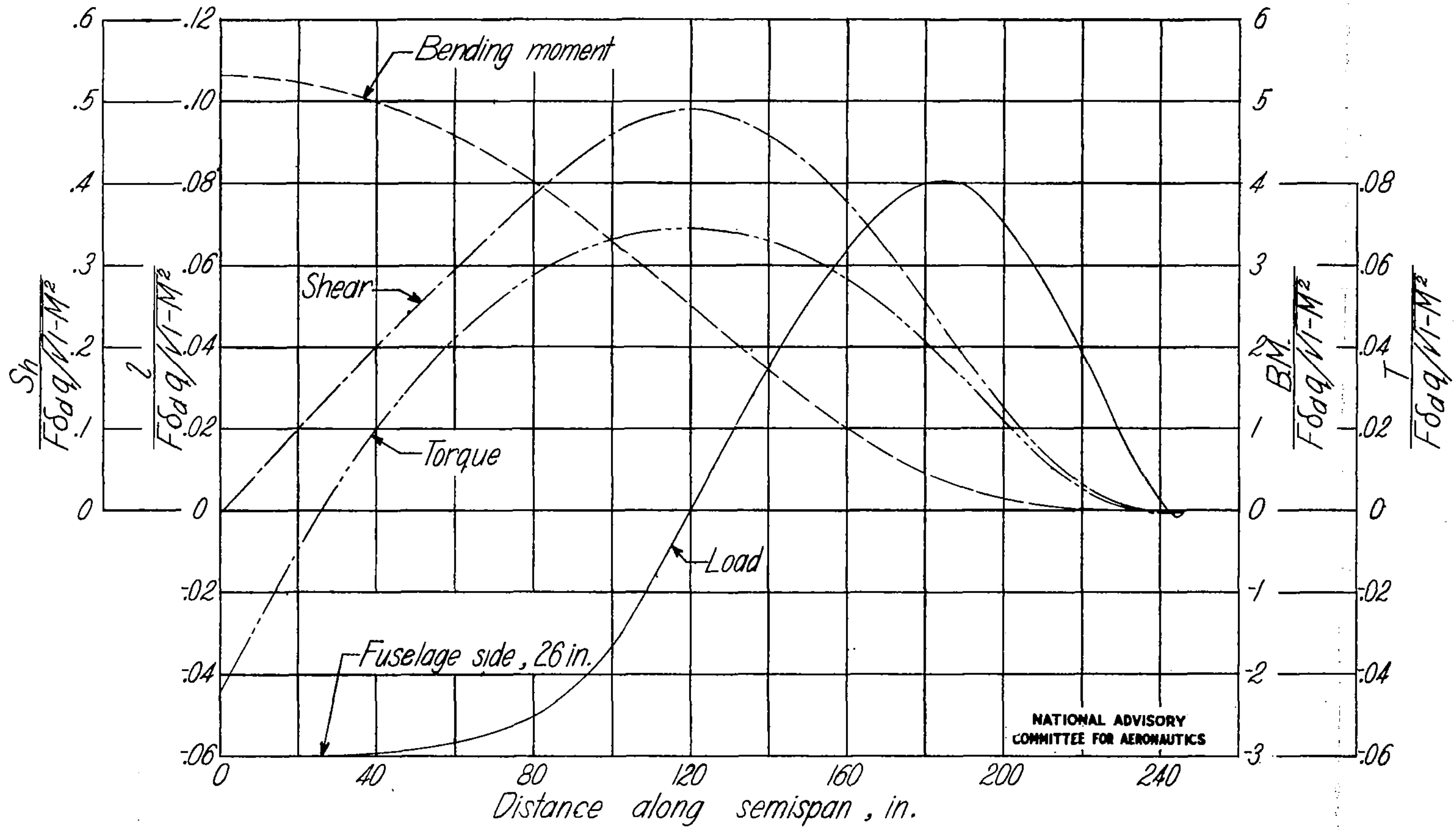

Figure 14.- Distribution of load, shear, bending moment, and torque for drooped-aileron aerodynamic load.

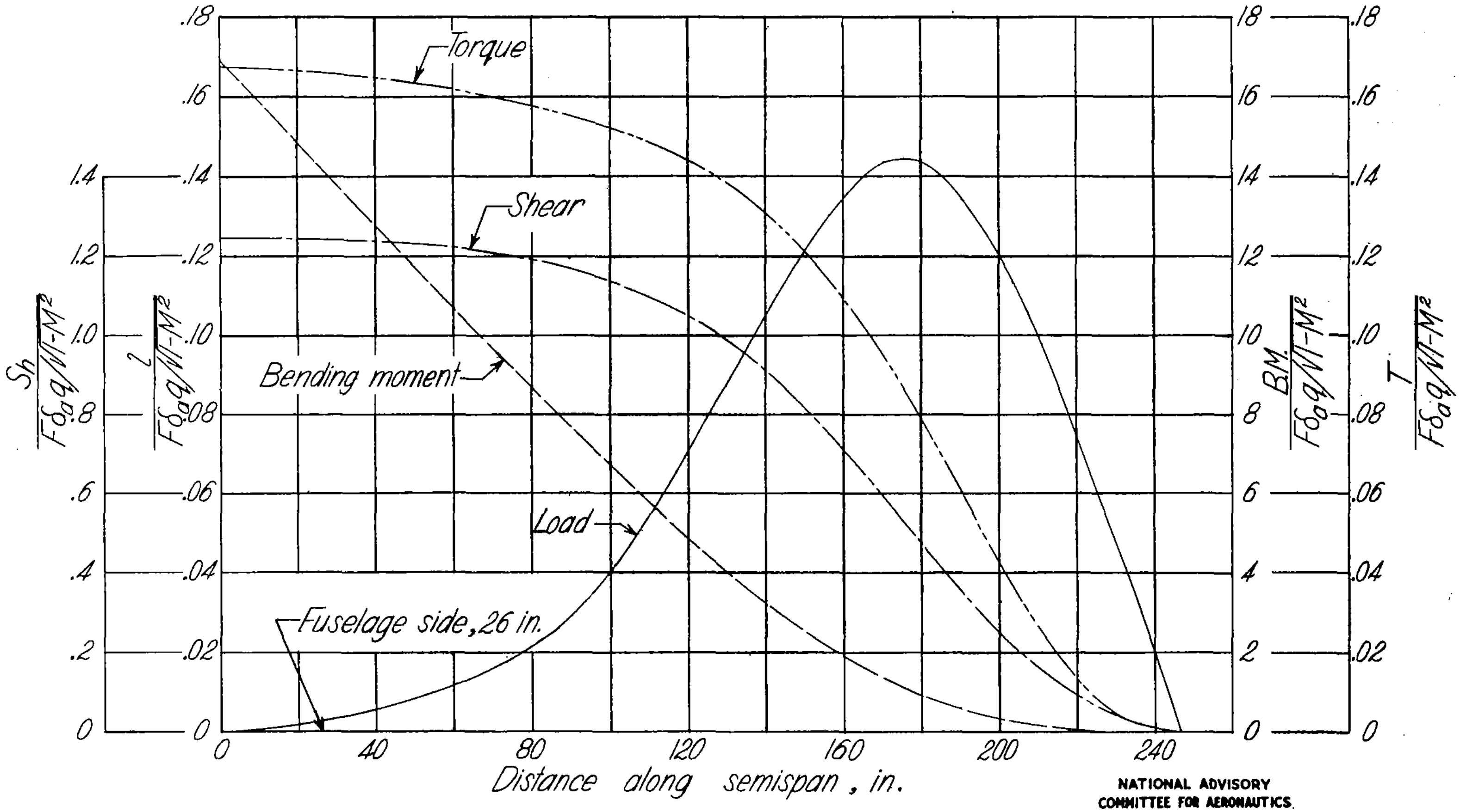

Figure 15.- Distribution of load, shear, bending moment, and torque for aerodynamic loads of ailerons deflected equally and oppositely.

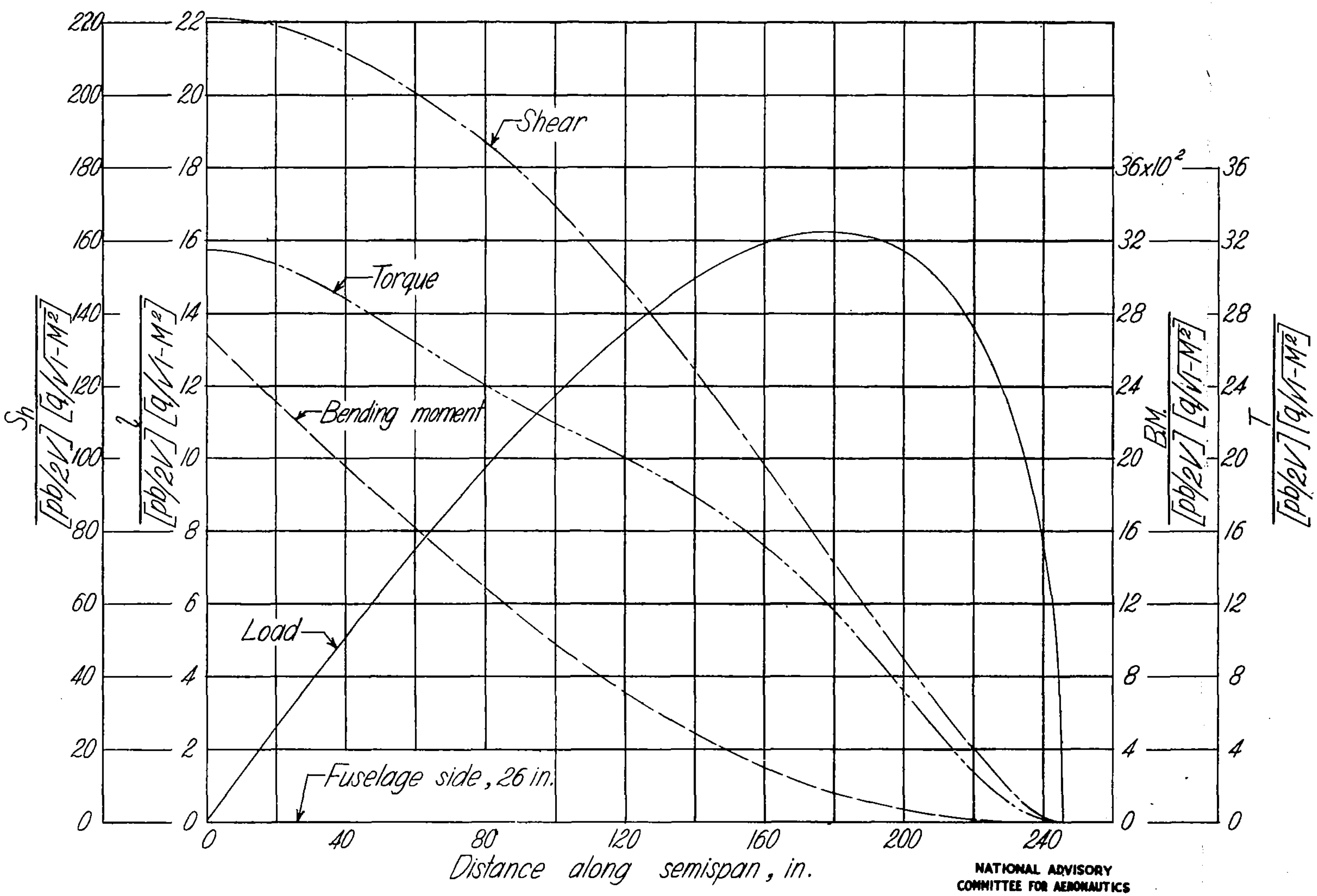

Figure 16.- Distribution of load, shear, bending moment, and torque for damping-in-roll aerodynamic load.

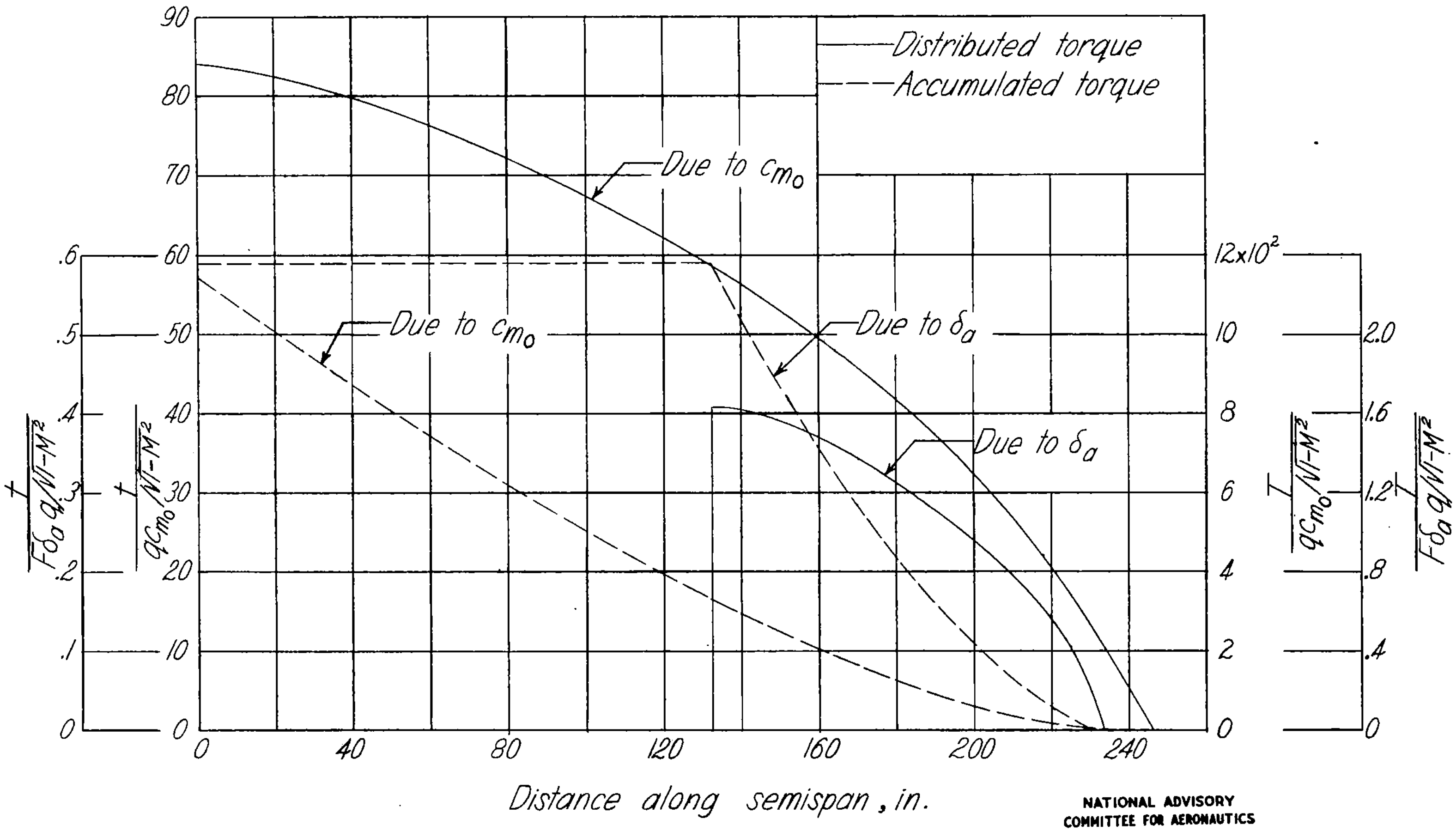

Figure 17.- Distributed and accumulated torque due to c_{m_0} and δ_a.

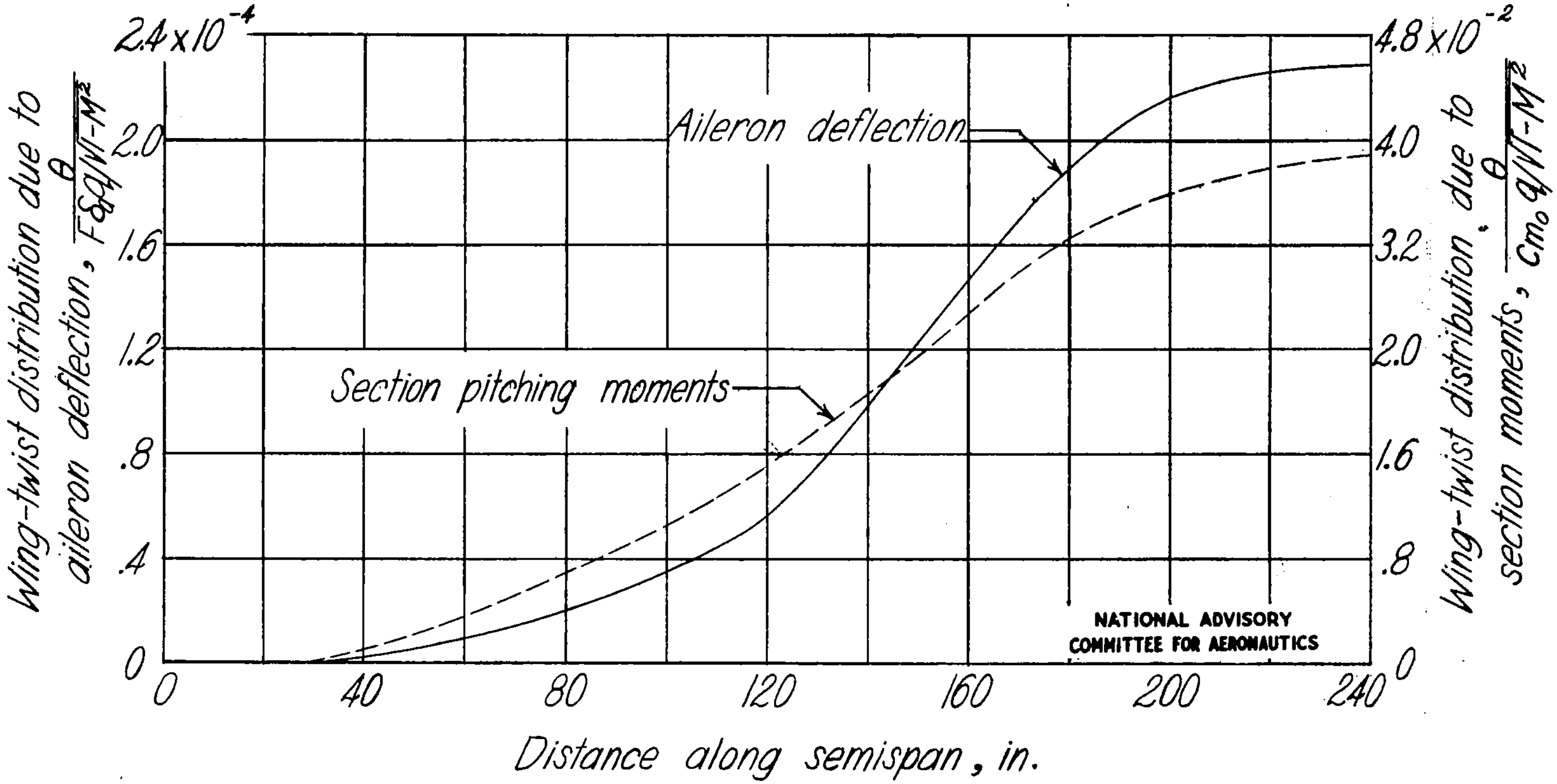

Figure 18.- Wing-twist distribution due to aileron deflection and section pitching moments.

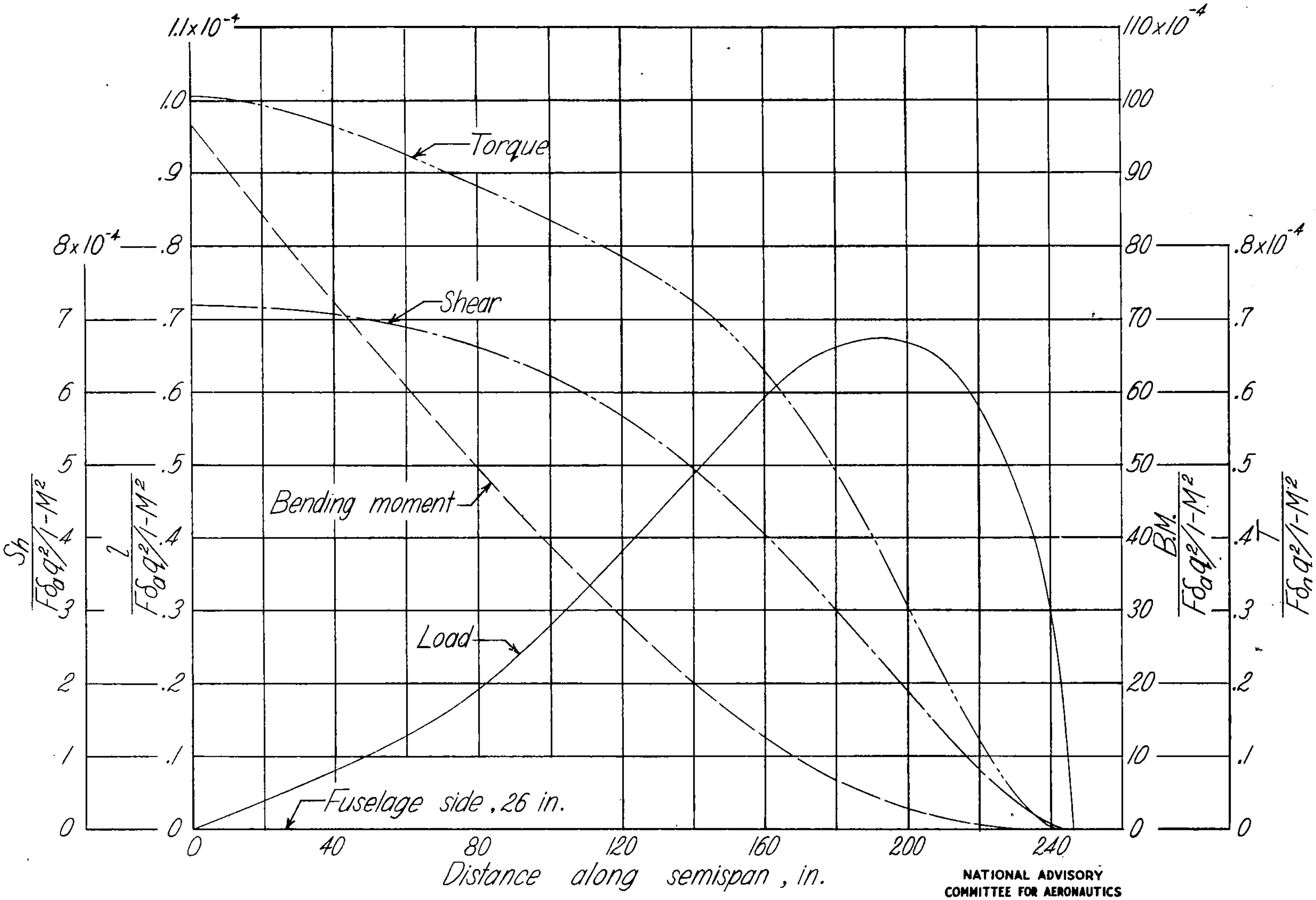

Figure 19.- Distribution of load, shear, bending moment, and torque due to wing-twist aerodynamic load.

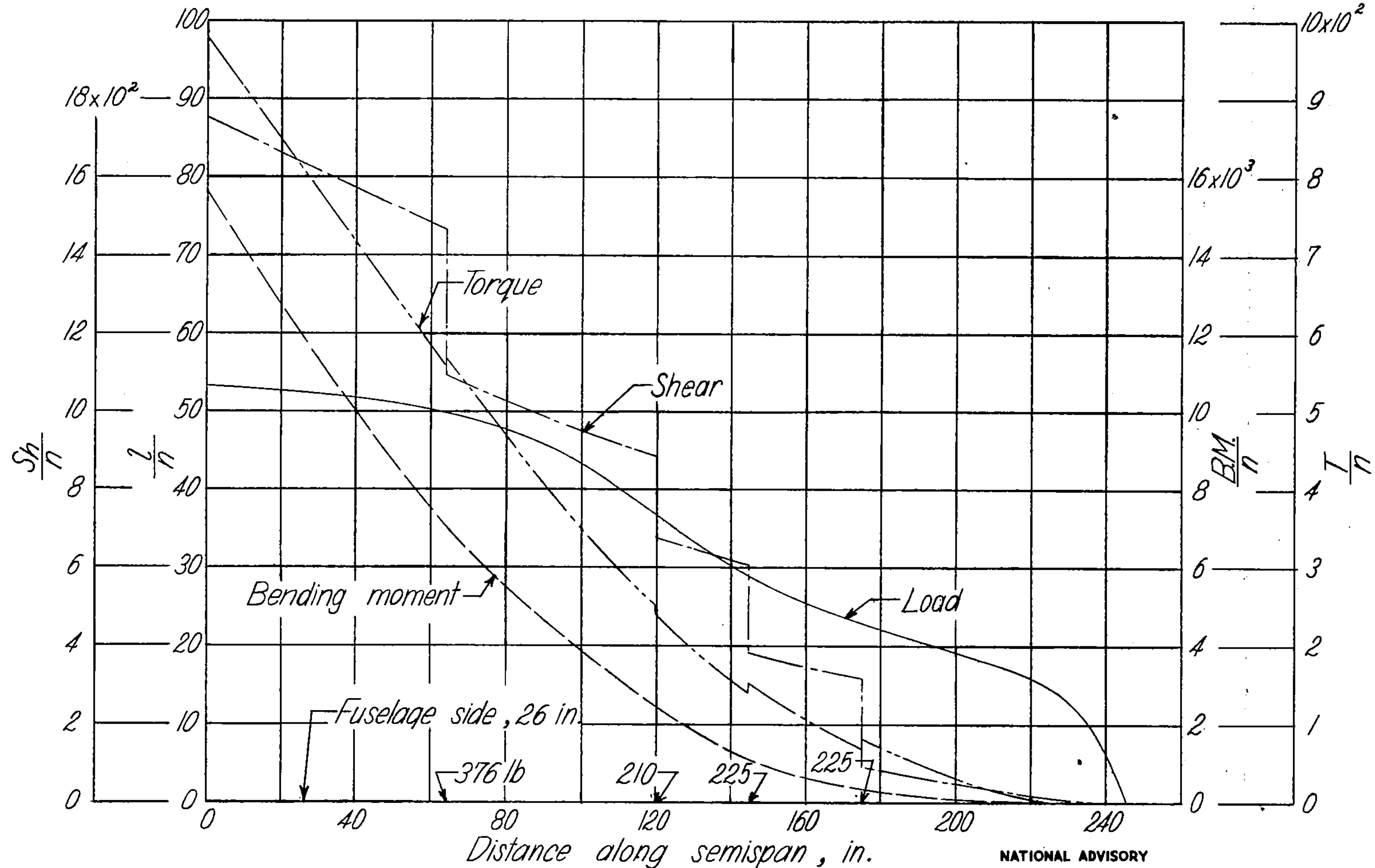

Figure 20.- Distribution of load, shear, bending moment, and torque for normal-inertia load.

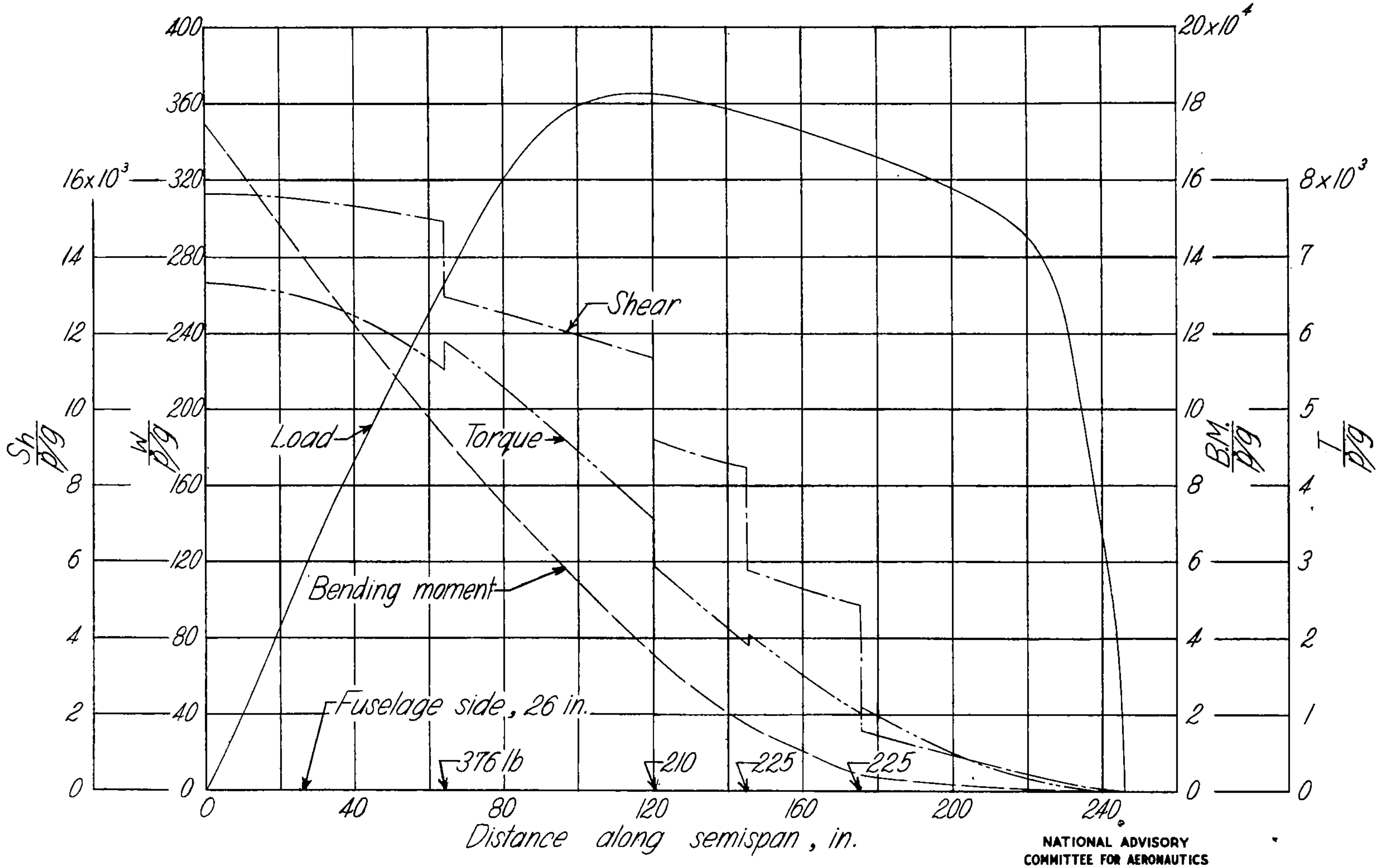

Figure 21.- Distribution of load, shear, bending moment, and torque for angular-inertia load.

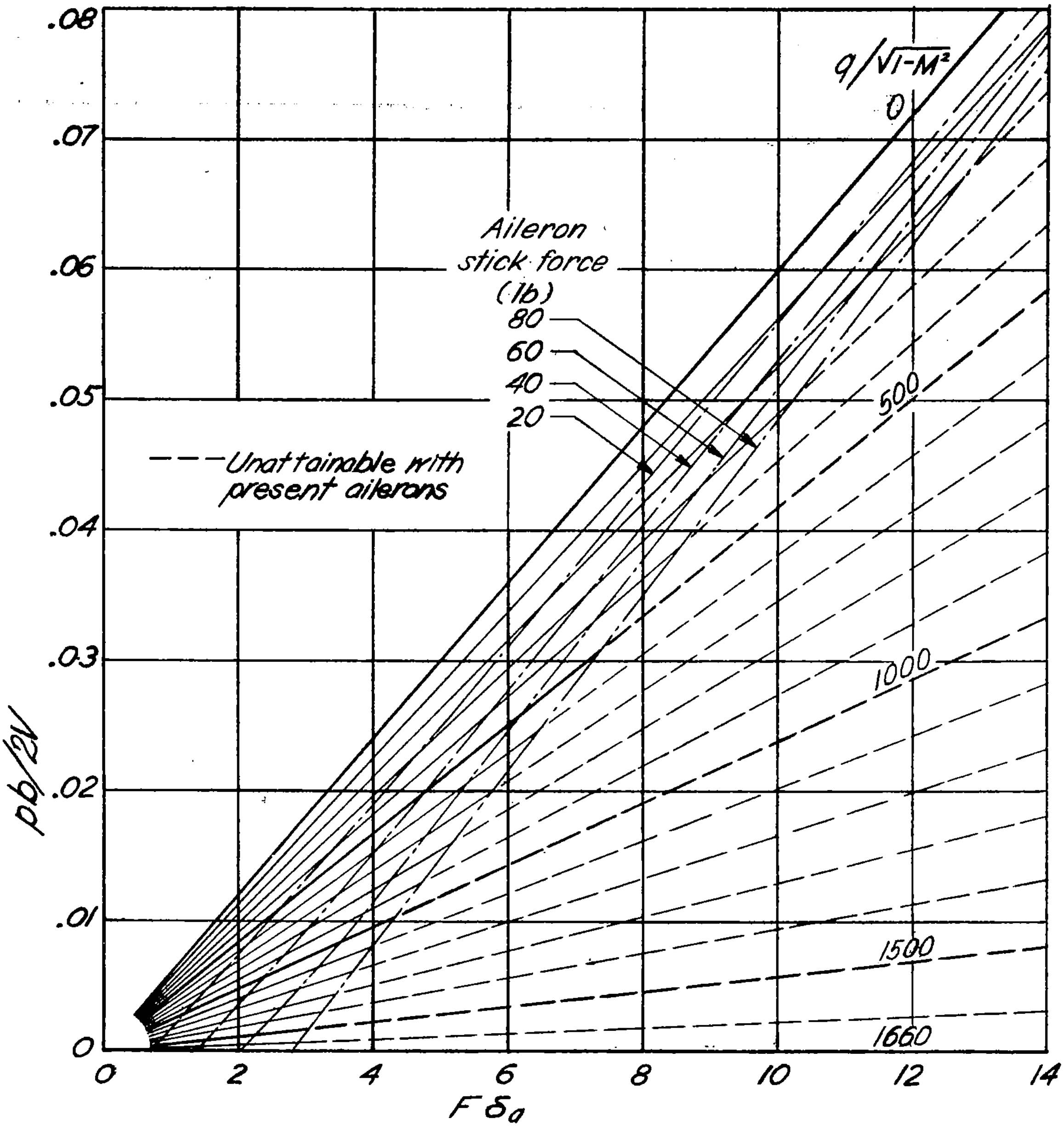

Figure 22.- Values of pb/2V for various values of $q/\sqrt{1-M^2}$ and stick force.

NATIONAL ADVISORY COMMITTEE FOR AERONAUTICS

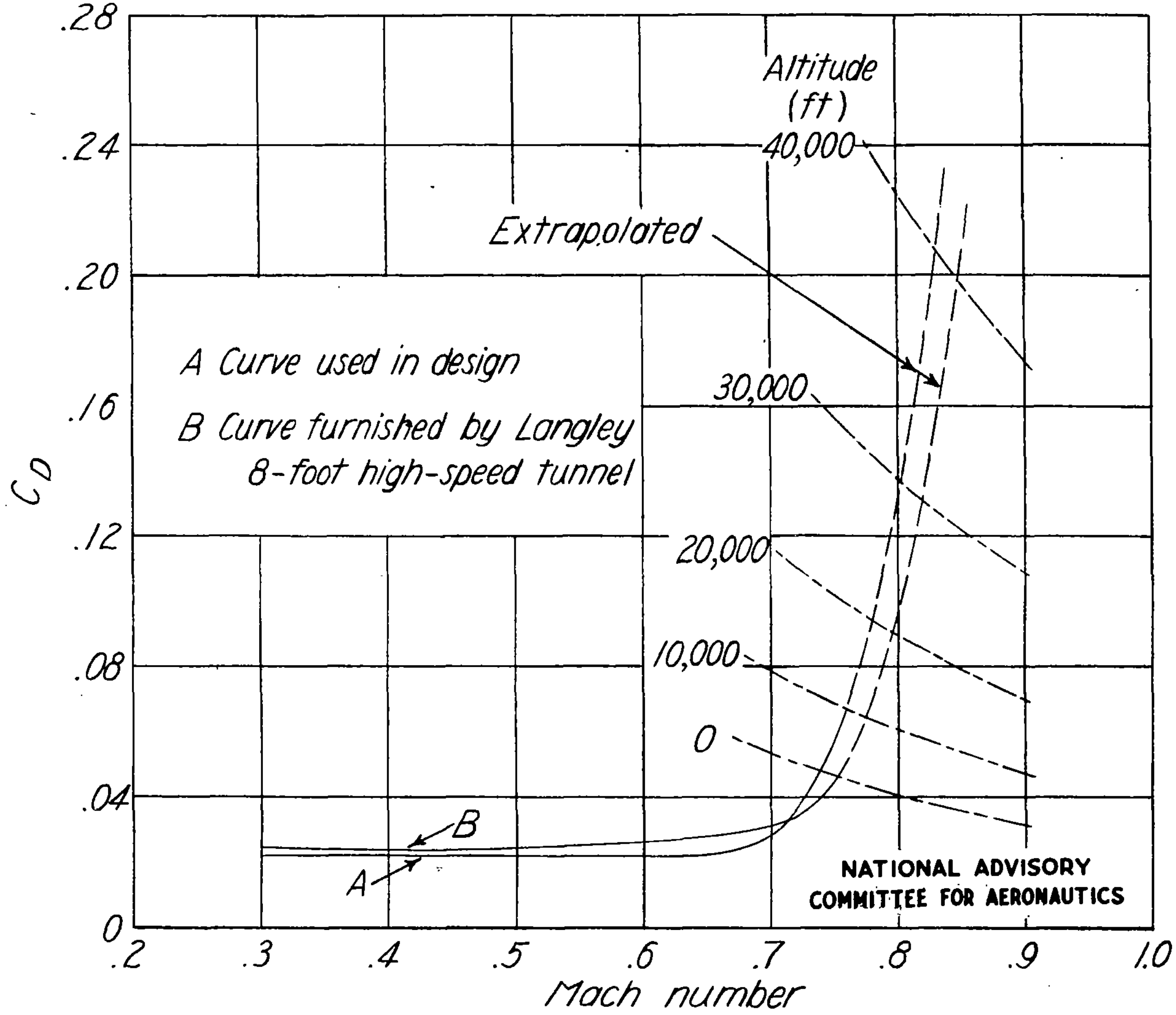

Figure 23.- Determination of terminal Mach number at various altitudes. $\frac{W}{S}$ = 40 pounds per square foot.

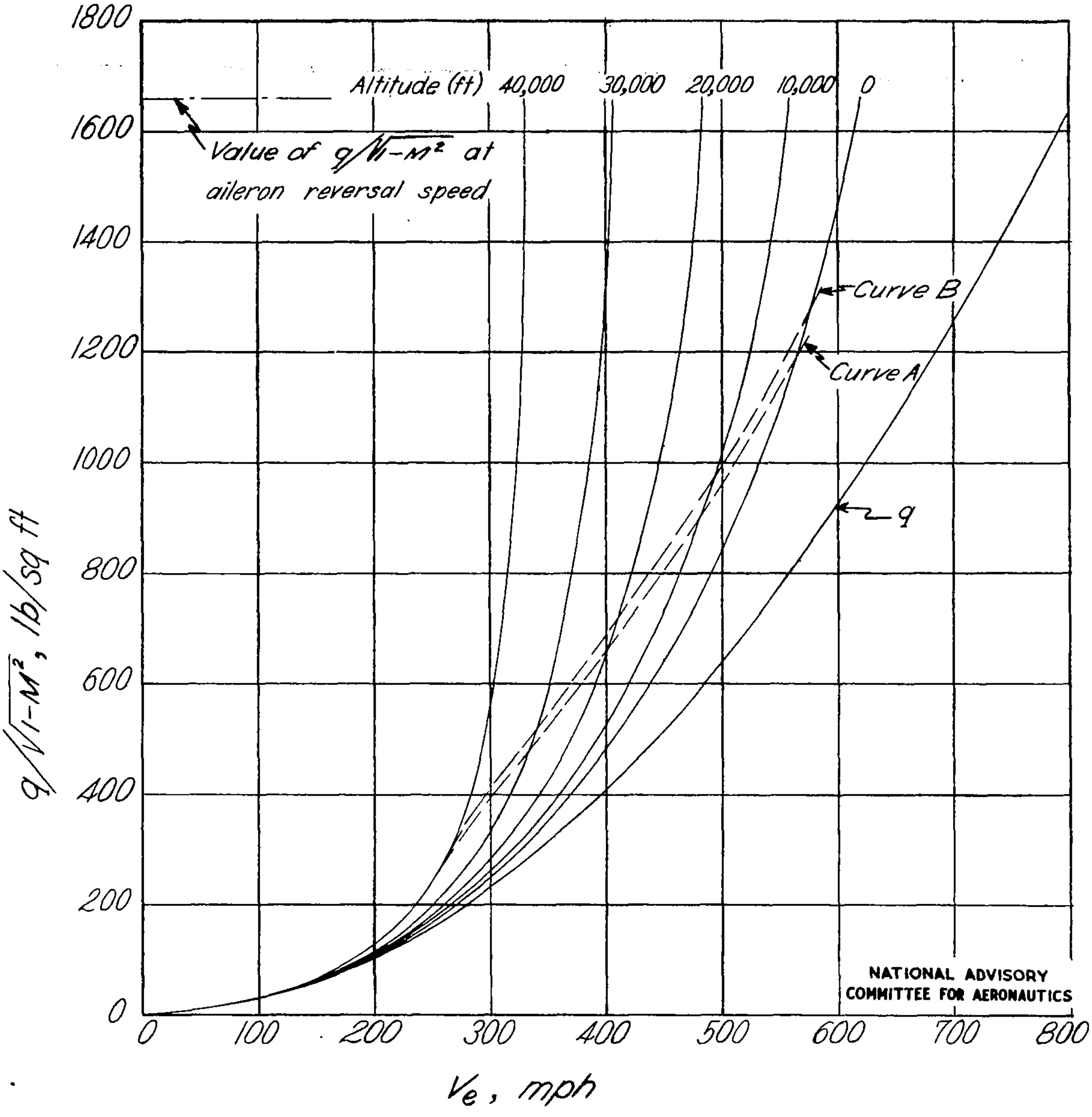

Figure 24.- Relations between V_e and $q/\sqrt{1-M^2}$ for various altitudes.

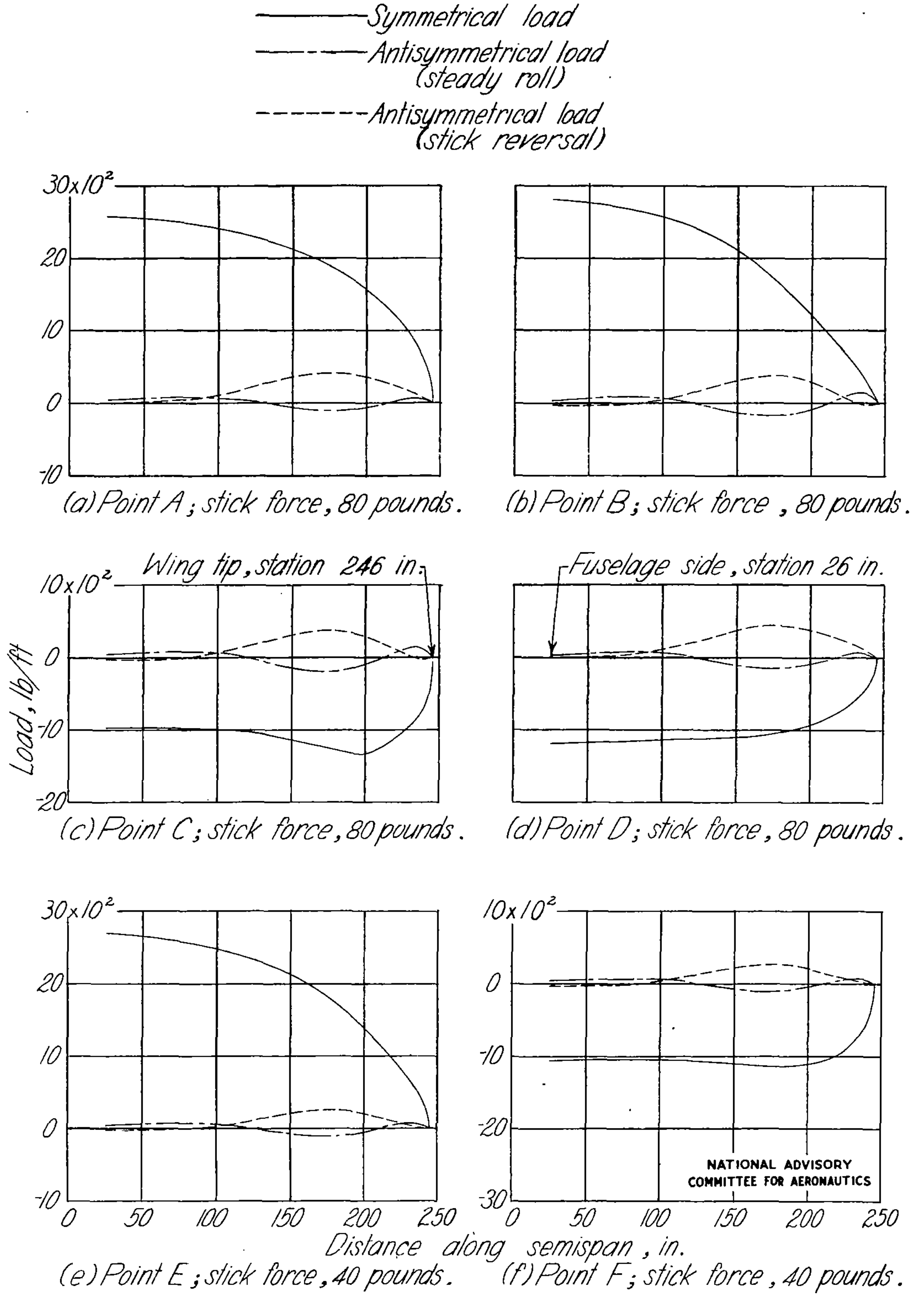

Figure 25.- Load distribution on right wing during right aileron roll for selected points on V-n diagram.

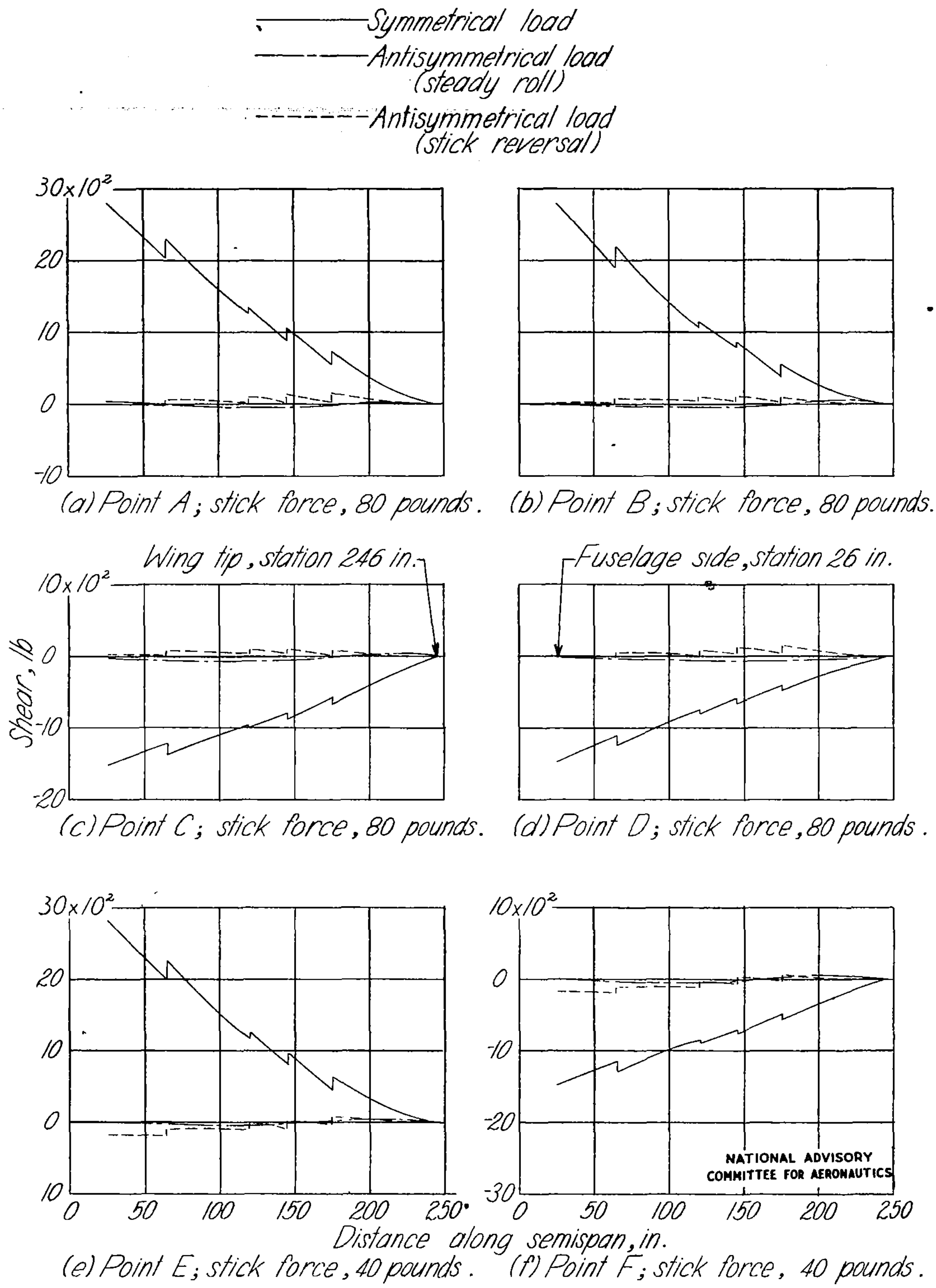

Figure 26.-Shear distribution on right wing during right aileron roll for selected points on V-n diagram.

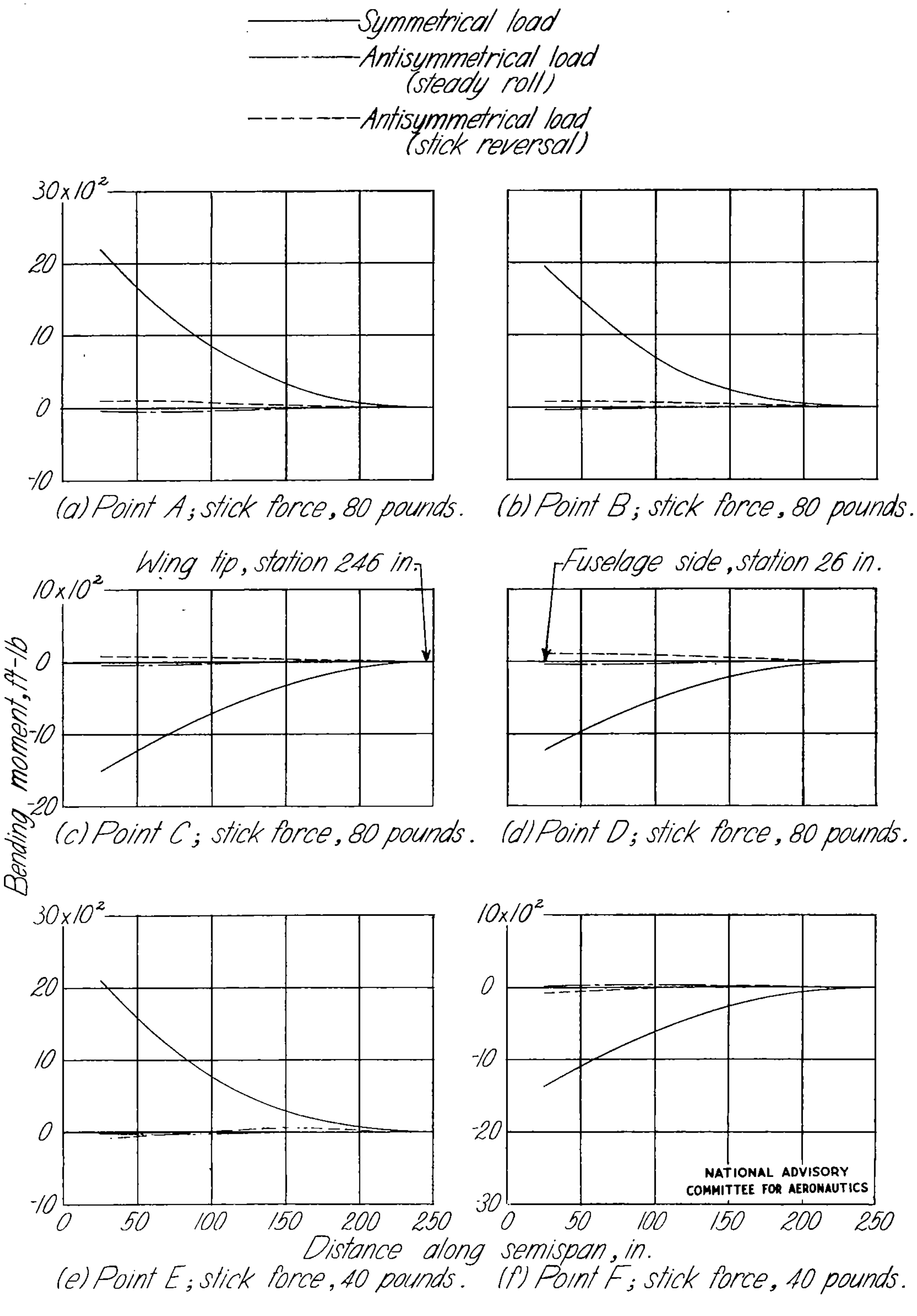

Figure 27.- Bending-moment distribution on right wing during right aileron roll for selected points on V-n diagram.

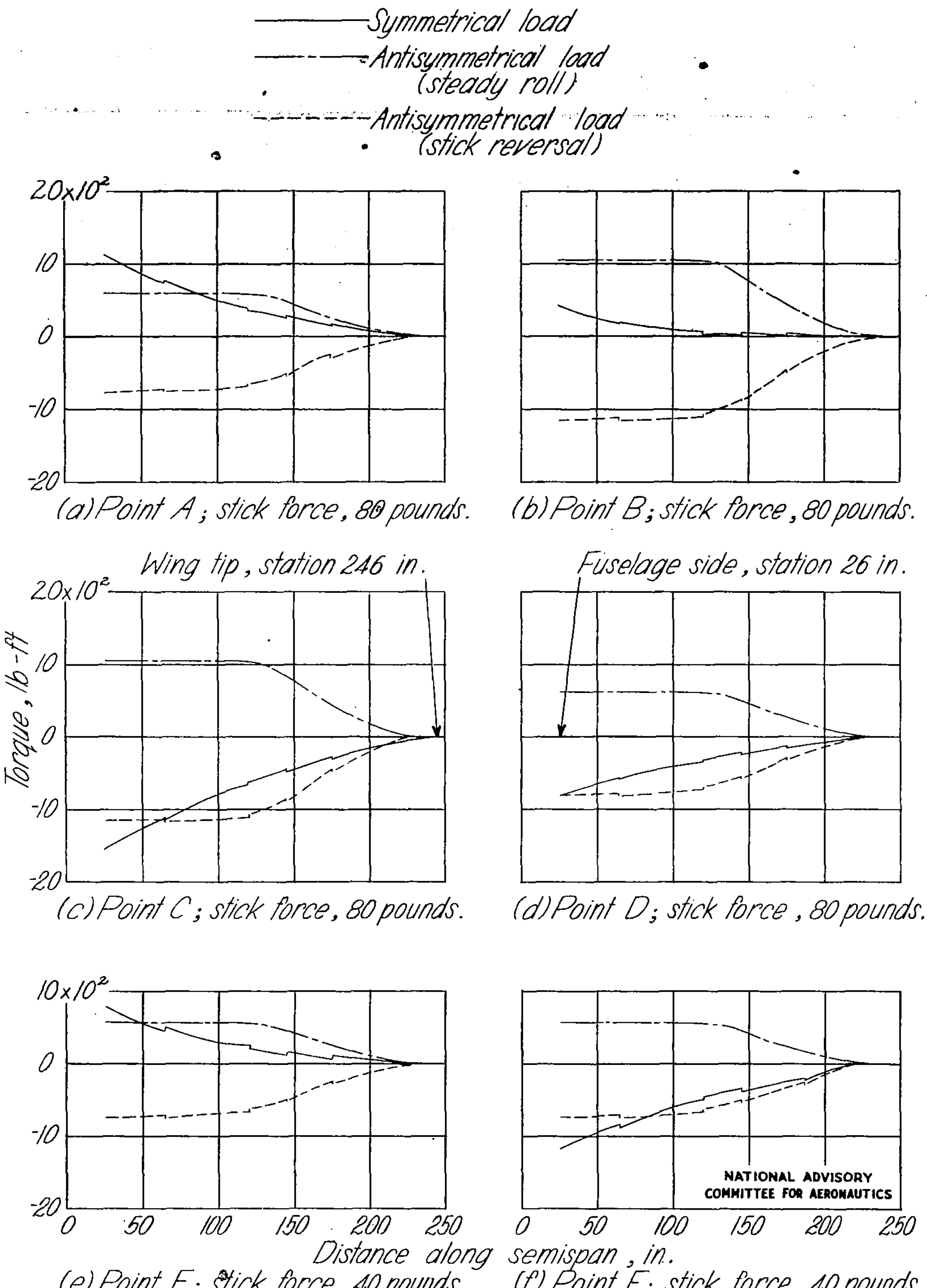

Figure 28.- Torque distribution on right wing during right aileron roll for selected points on V-n diagram.

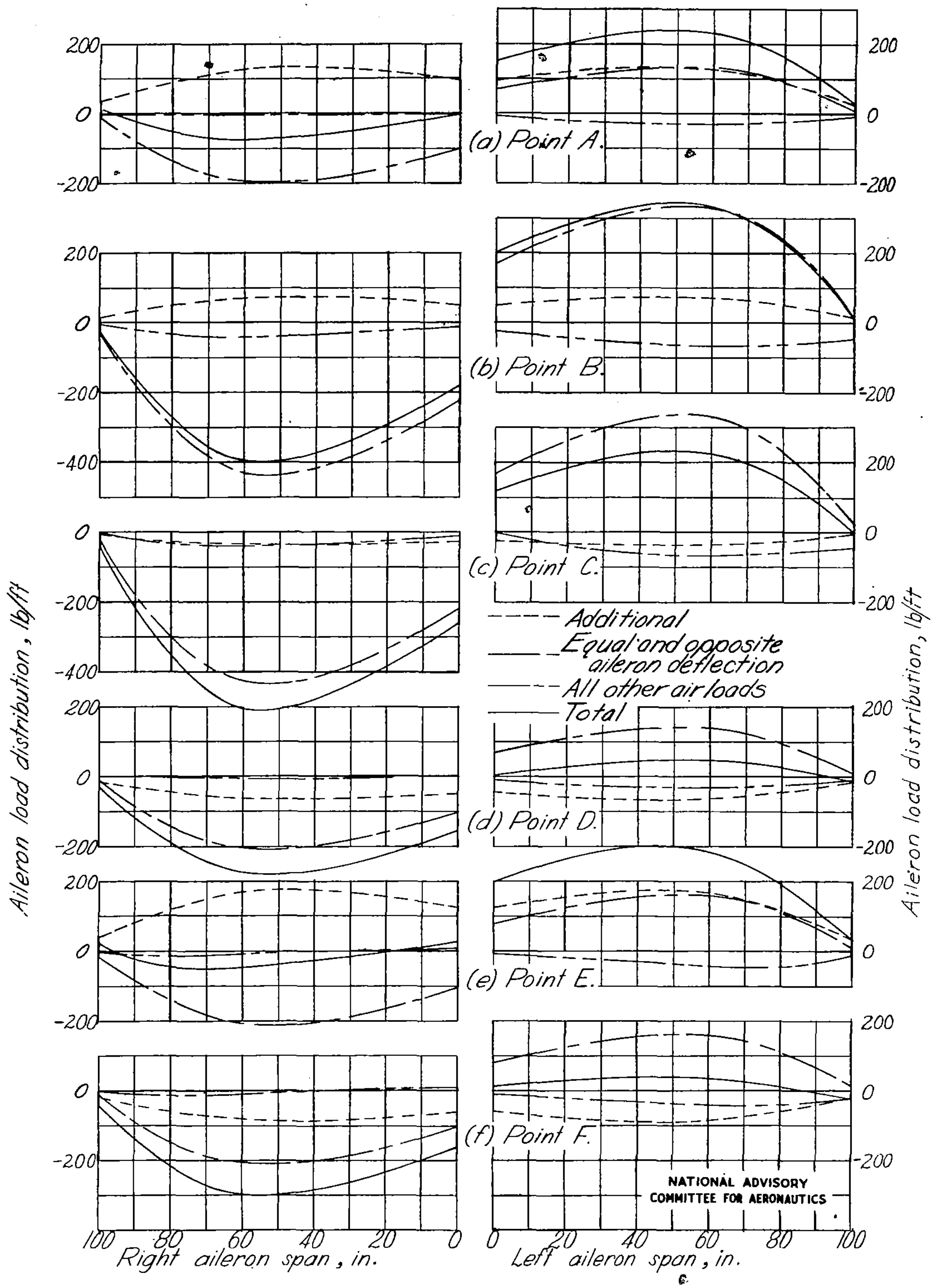

Figure 29.-Components of aileron aerodynamic-load distribution computed for selected points of V-n diagram with steady right roll.

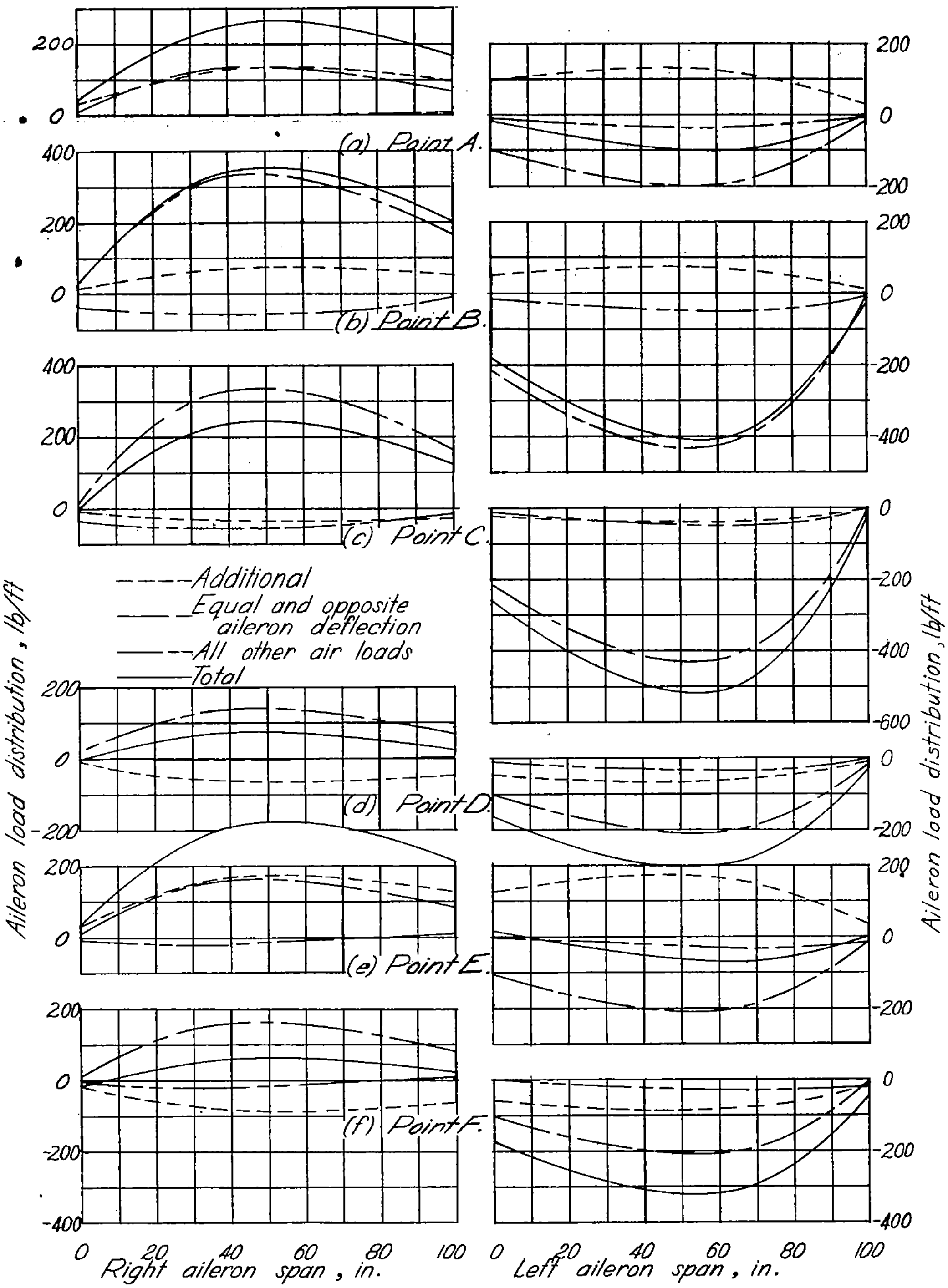

NATIONAL ADVISORY COMMITTEE FOR AERONAUTICS

Figure 30.- Components of aileron aerodynamic-load distribution computed for selected points of V-n diagram with aileron reversal during steady right roll.

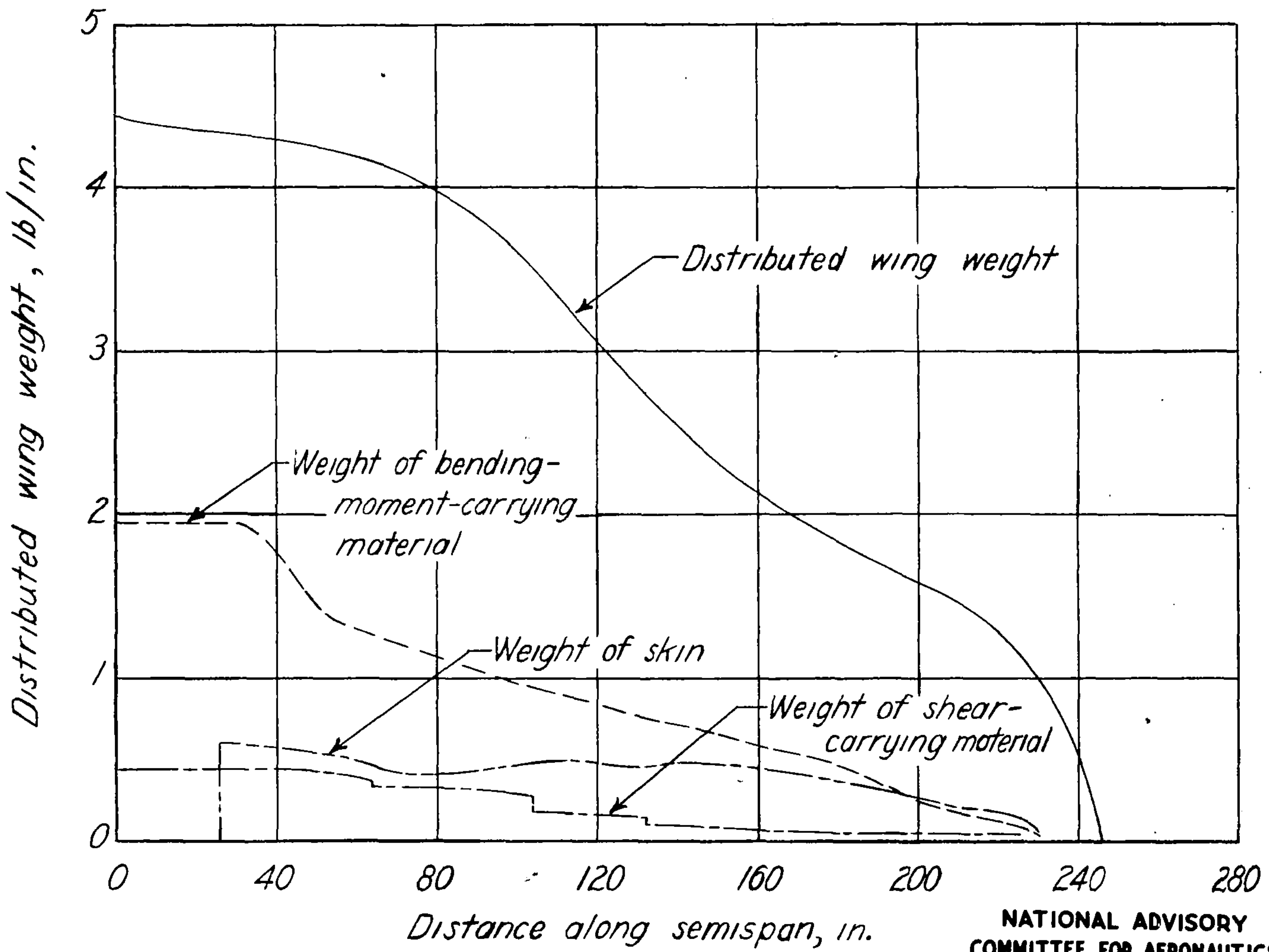

NATIONAL ADVISORY COMMITTEE FOR AERONAUTICS

Figure 31.- Breakdown of wing weight distribution.